Department of the Environment, Transport, Energy and Communications
Federal Office for the Environment (FOEN)

Seismic Risk for Existing Buildings
Framework for Risk Computation

20 March 2015

Commissioned by the Federal Office for the Environment (FOEN)

Risk&Safety AG
Ingenieure in Gemeinschaft

Bahnhofstrasse 92, Postfach 3605, 5000 Aarau
Telefon +41 61 823 78 37 / Fax +41 61 823 78 39 / www.risksafety.ch

Risk&Safety AG
Ingenieure in Gemeinschaft

Imprint

Commissioned by

Department of the Environment, Transport, Energy and Communications
Federal Office for the Environment (FOEN)
Coordination Center for Earthquake Mitigation
CH – 3003 Bern

Represented by Blaise Duvernay, dipl. ing. ETH
Phone: +41 58 464 17 34
E-mail: blaise.duvernay@bafu.admin.ch

Contractor

Risk&Safety AG
Hofstrasse 17
CH – 5073 Gipf-Oberfrick

Phone: +41 62 871 82 10
Fax: +41 62 871 82 86
www.risksafety.ch

Authors

Dr. Navid Jamali, Ehrfried Kölz

Review team

Blaise Duvernay (FOEN)
Dr. Pierino Lestuzzi (EPFL)
Dr. Clotaire Michel (SED)

Document

BE_BAFU_eqrisk2_20150320.docx
20 March 2015

Summary

Seismic examination of existing buildings in Switzerland is currently performed using the pre-standard SIA 2018 (2004) of the Swiss society of engineers and architects (SIA). In the seismic examination of existing buildings according to SIA 2018, a minimal acceptable safety level as well as the commensurability of retrofitting measures must be verified. The key element to do these verifications is the relationship between the degree of compliance of an existing building with the seismic safety requirements for new buildings and the risk to people inside the building. In SIA 2018, this relationship is presented as a curve with the so-called compliance factor of the building in abscissa and the annual casualty probability for people inside the building in ordinate. This curve was established based on risk calculations using empirical methods as well as on expert judgment to link empirical building vulnerability classes with plausible ranges of the compliance factor [Kölz et al., 2006].

In 2015 the pre-standard SIA 2018 will be replaced by the new building code SIA 269/8 ”Existing structures – Earthquake”. In this new building code the central concepts of minimal safety level and commensurability of measures of SIA 2018 will be kept and adapted to the current state of knowledge. For this, the curve linking the compliance factor with the risk to people in SIA 2018 must be verified. Furthermore, in order to extend the commensurability criterion to cope with damage to property, it is intended to propose a new curve linking the compliance factor with property damage.

As a support to the issuance of the new building code SIA 269/8 and in the interest of providing better tools for the probabilistic seismic risk computation for existing buildings in Switzerland, the Federal Office for the Environment (FOEN) initiated a research project in 2010 with the following objectives:

– Provide a consistent set of probabilistic hazard data in EMS-Intensity and spectral acceleration values for 3 to 5 sites covering the range of seismic hazard in Switzerland.
– Develop vulnerability functions for representative Swiss buildings, including uncertainties.
– Prepare a reusable documented computational framework for the probabilistic risk quantification.
– Obtain verification data for the risk curve for people in the pre-standard SIA 2018 and data for the risk curve for property in the new building SIA 269/8.

The partners of this project which was conducted by FOEN were the Swiss Seismological Service (SED), the Swiss Institute of Technology / applied computing and mechanics laboratory (IMAC) and Risk&Safety AG (R&S):

– SED provided the hazard data for the three locations Zurich, Basel, and Sion (two sites) as well as amplification factors considering local site effects. Hazard data was provided in 2 formats as a function of spectral acceleration and EMS-Intensity including percentile curves, which were demonstrating uncertainties of data.
– IMAC provided fragility curves for 5 benchmark buildings through nonlinear dynamic analysis. For two benchmark buildings fragility curves after retrofitting have also been provided. IMAC also computed the compliance factors for all the benchmarks using standard engineering procedures.
– R&S developed and documented a model to calculate risk combining the probabilistic hazard data and the fragility curves for both the mechanical and empirical approaches. The risk was then calculated for all the benchmark buildings.

The main focus of this report is to provide a computational framework for the risk assessment of typical buildings in Switzerland.

It is shown, that results of risk assessment based on the mechanical approach are reasonably comparable with those calculated according to the empirical approach. Results show that amplification factors considering local site effects are playing an important role in the final result of risk assessment.

It is shown, that generally risk values demonstrated as a function of force-based compliance factors are located below the curves given by SIA. Some exceptions are observed. They are discussed in detail in the report.

For risk values demonstrated as a function of the displacement-based compliance factor, however, there are several cases, in which the computed risk value lies above the SIA curves. Generally the compliance factors computed with the displacement-based method are two to three times larger than those computed with force-based method.

It is shown that the risk assessment with different models and assumptions results in a large amount of scatter in final risk values. The most important sources of this scatter are uncertainty associated with the seismic hazard, seismic fragility of the studied benchmarks and consequences of structural failure and/or damage.

SIA risk curves are intended to link “realistically” the compliance factor with the risk value. They are not intended to be too conservative. Because of this, it is accepted that that in reality for specific cases the risk values may be larger than those predicted by the curves. It is the task of the engineer to identify and handle such cases based on his/her “engineering judgment” with respect to the structural vulnerability and the possible seismic demand.

Table of Contents

Appendices

1 Introduction

1.1 Background

In 2004 the Swiss Society of Engineers and Architects (SIA) edited the Prestandard SIA 2018 in order to cover the problem of the seismic verification of existing buildings. The Prestandard sets minimal seismic safety requirements for existing buildings and proposes cost benefit criteria for their eventual retrofit. The seismic verification based on the Prestandard SIA 2018 results in a compliance factor which indicates the degree of compliance of an existing building compared to the requirements for new buildings. Below a minimal threshold value of the compliance factor, the safety of individuals is deemed unacceptable with an annual probability of death exceeding 1/100'000. Above this threshold, the safety of individuals is judged acceptable and the commensurability of possible measures must be evaluated. In this evaluation, life-saving costs, i.e. the ratio of safety costs to the reduction of the risk to people due to measures, must be determined.

For the definition of the minimal threshold value as well as for the assessment of the risk reduction – which is necessary for the assessment of the commensurability – a link between the compliance factor and the risk to people is given in form of a curve in the Prestandard SIA 2018. This curve was defined empirically.

It is planned to replace the Prestandard SIA 2018 by the new building code SIA 269/8 in 2015. This is an opportunity to verify several definitions contained in the Prestandard and to extend the risk-based approach to cope with other risks like the risk to property.

The aforementioned minimal accepted seismic safety must be verified based on casualty risk and property loss risk in case of structural damage or collapse.

1.2 Objective

The Swiss Federal Office for the Environment (FOEN) has initiated the project "*risque sismique des bâtiments existants*" with the objective to provide:

- A consistent set of probabilistic hazard data in EMS-Intensity and spectral acceleration for 3 to 5 sites covering the range of seismic hazard level in Switzerland
- Vulnerability functions for representative Swiss buildings, including uncertainties
- A reusable documented computational framework for the risk quantification
- A quantified dispersion of risk according to different available methodologies and relevant uncertainties
- Data for the verification of the risk curves in Prestandard SIA 2018.

The partners of this project which was conducted by FOEN, were the Swiss Seismological Service (SED), the Swiss Federal Institute of Technology, Lausanne (EPFL) / Applied Computing and Mechanics Laboratory (IMAC) and Risk&Safety AG (R&S):

- SED had to provide the hazard data for 3 locations Zurich, Basel, and Sion old town. Besides, amplification factors considering local site effects were to be delivered for the aforementioned locations and Sion Rhone valley as an extreme case. Hazard data was provided in 2 formats as a function of spectral acceleration and EMS-Intensity including percentile curves, which were demonstrating uncertainties of data.
- IMAC has provided fragility curves for 5 benchmarks through nonlinear dynamic analysis. For two benchmarks fragility curves after retrofitting have been provided, too. This has been documented in another report by IMAC [IMAC, 2014].

– R&S had to propose a model to calculate risk combining the given hazard data and the fragility curves analytically based on the mechanical approach. Moreover R&S had to define a model to calculate risk empirically based on EMS-Intensity data and fragility curves derived from the method proposed in the Risk-UE project. The risk should be calculated with both models and compared with each other as well as with the compliance factors of benchmark buildings.

With the objectives and tasks given above, five typical Swiss buildings have been studied and exposed to seismic hazard in 4 sites in Switzerland. Based on a probabilistic approach, casualty risk and property loss risk have been studied and compared with the values stated in the Prestandard SIA 2018.

1.3 Outline

Seismic risk assessment consists of three main parts (Figure 1):

– Evaluation of seismic hazard
– Evaluation of structural vulnerability
– Exposure

In chapter 2 probabilistic seismic hazard analysis done by SED is introduced. Hazard curves as a function of spectral acceleration and EMS-Intensity considering site effects are given in this chapter. In chapter 3 fragility curves of studied benchmarks (according to both analytical and empirical approaches) and the treatment of uncertainties are documented. In chapter 4 the consequences are introduced. The risk computation framework is introduced in chapter 5. Casualty risk and property loss risk values as well as compliance factors of studied benchmarks are summarized in chapter 6. Chapter 7 is devoted to the discussion of results. Conclusions are discussed in chapter 8. References are documented in chapter 9.

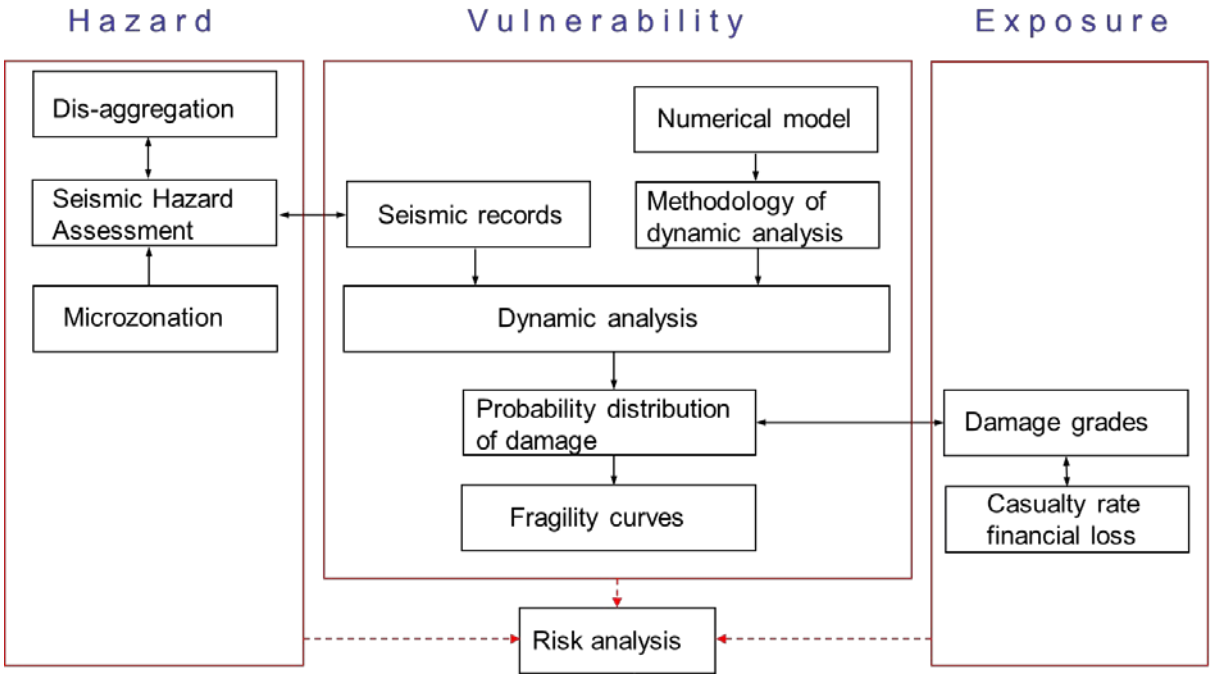

Figure 1: Elements of risk analysis

2 Seismic Hazard

2.1 Introduction

Swiss Seismological Service has done a Probabilistic Seismic Hazard Analysis (PSHA) to compute the seismic hazard in Switzerland [Wiemer et al., 2009 & Giardini et al., 2004].

The goal of probabilistic seismic hazard analysis is to quantify the rate (probability) of exceeding various ground motion levels at a given site taking into account all possible earthquakes. To quantify ground motions and relate it to the structural performance a ground motion Intensity Measure (IM) must be selected. The two following intensity measures are most common:

– Peak Ground Acceleration (PGA), which is the maximum ground acceleration of a recorded earthquake time history,
– Response spectral acceleration (Sa), which is the maximum acceleration experienced by a (normally 5%) damped single-degree-of-freedom oscillator at its natural period of vibration (1st mode).

Intensity scales, based on observable consequences of the ground motions, make it possible to qualify historical earthquakes. They are important in the interpretation of present earthquakes as well. The European Macroseismic Scale (EMS) is commonly used in Switzerland and is composed of 12 intensity degrees [EMS, 1998].

SED has delivered for this study hazard curves in terms of Sa and EMS-Intensity (EMS-I). In the following sections the hazard data will be firstly introduced and then some relevant factors affecting the hazard data for risk analysis (among them site effects) will be discussed.

2.2 Location of the calculated hazard data and comparison of results

Hazard data has been delivered for 3 sites Zurich, Basel and Sion [Wiemer, 2011] (also attached to this report in Attachment A). The coordinate of the sites are given below:

Zurich (ETHZ):	lat. 46.233°	long. 7.360°
Basel (Munster):	lat. 47.376°	long. 8.548°
Sion (old town):	lat. 47.554°	long. 7.590°

PSHA with Sa as IM has been done based on a Monte-Carlo approach [Wiemer et al., 2009], using a synthetic earthquake catalogue as input. This is the same set of data used for the current SIA code 261. The only change to the 2004 hazard model is the computation of 10th to 90th percentile hazard curves. Spectral values are provided at 0.5, 1, 2, 3, 5, 10 and 12 Hz.

The following figures depict the rock hazard with 10th to 90th percentiles for Zurich, Basel and Sion old town (hereafter abbreviated as Sion OT) at 1 and 5 Hz.

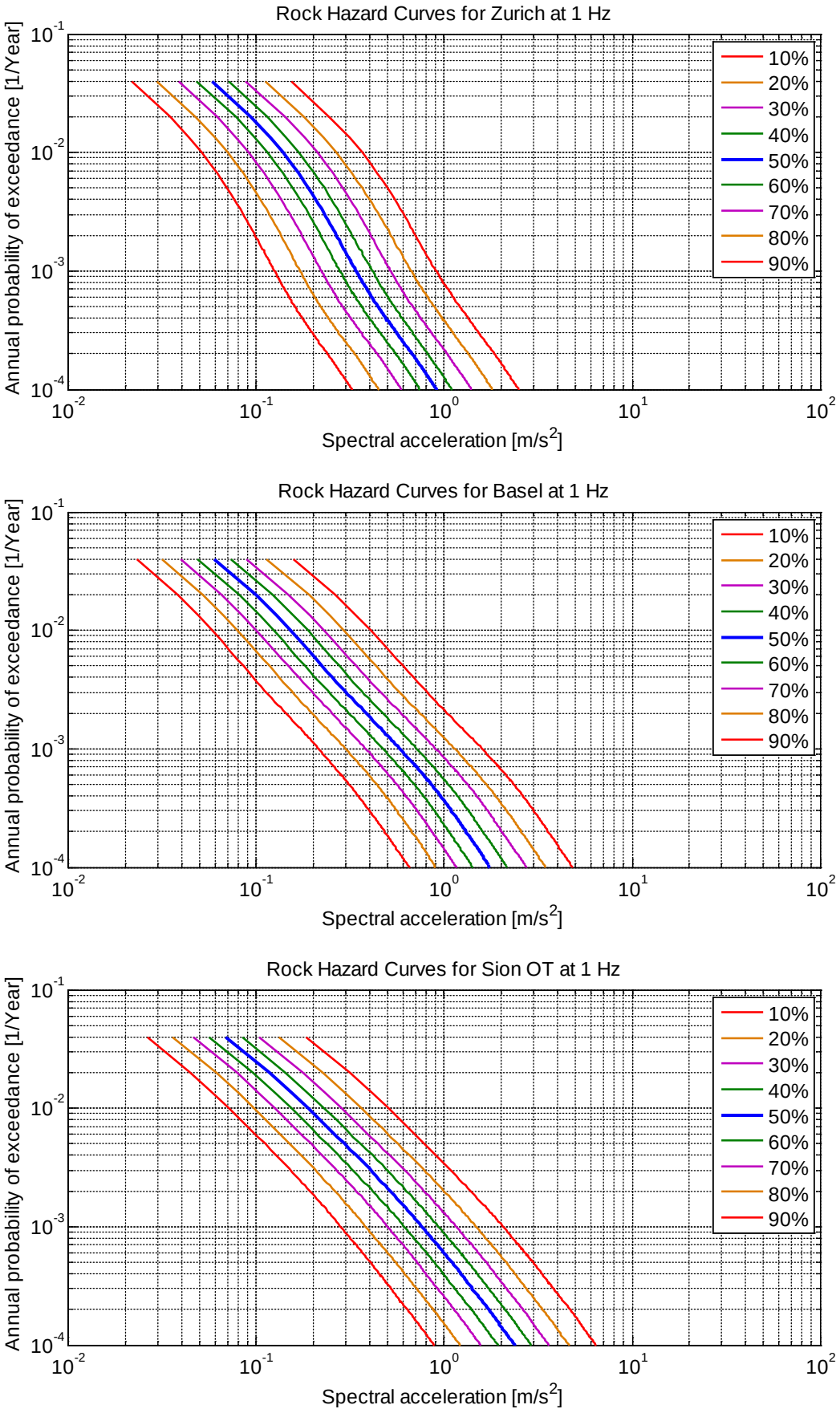

Figure 2: Rock hazard curves for Zurich (ETH), Basel and Sion OT at 1 Hz

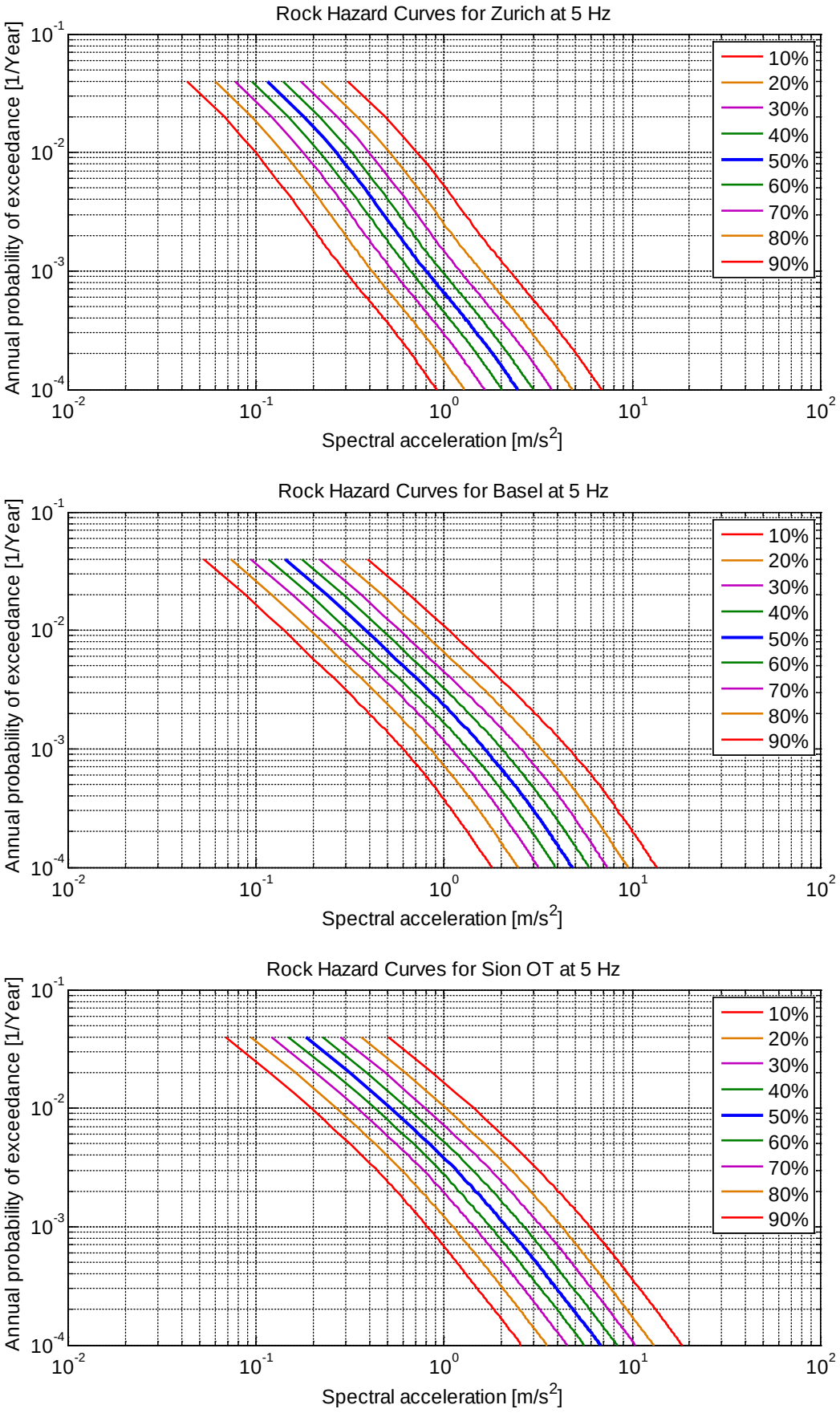

Figure 3: Rock hazard curves for Zurich (ETH), Basel and Sion OT at 5 Hz

2.3 Hazard spectra

Rock hazard in each site is given for several periods (Figure 4). Generally it can be seen that as the frequency increases, the spectral acceleration increases too (for frequencies between 0.5 Hz and 12 Hz, see Figure 5).

Uniform hazard spectrum (UHS) for an annual probability of exceedance of 2E-3 (10% exceedance probability in 50 years, i.e. a return period of 500 years), 4E-4 (2% exceedance probability in 50 years, i.e. a return period of 2'500 years) and 1E-4 (0.5% exceedance probability in 50 years, i.e. a return period of 10'000 years) are given in Figure 5.

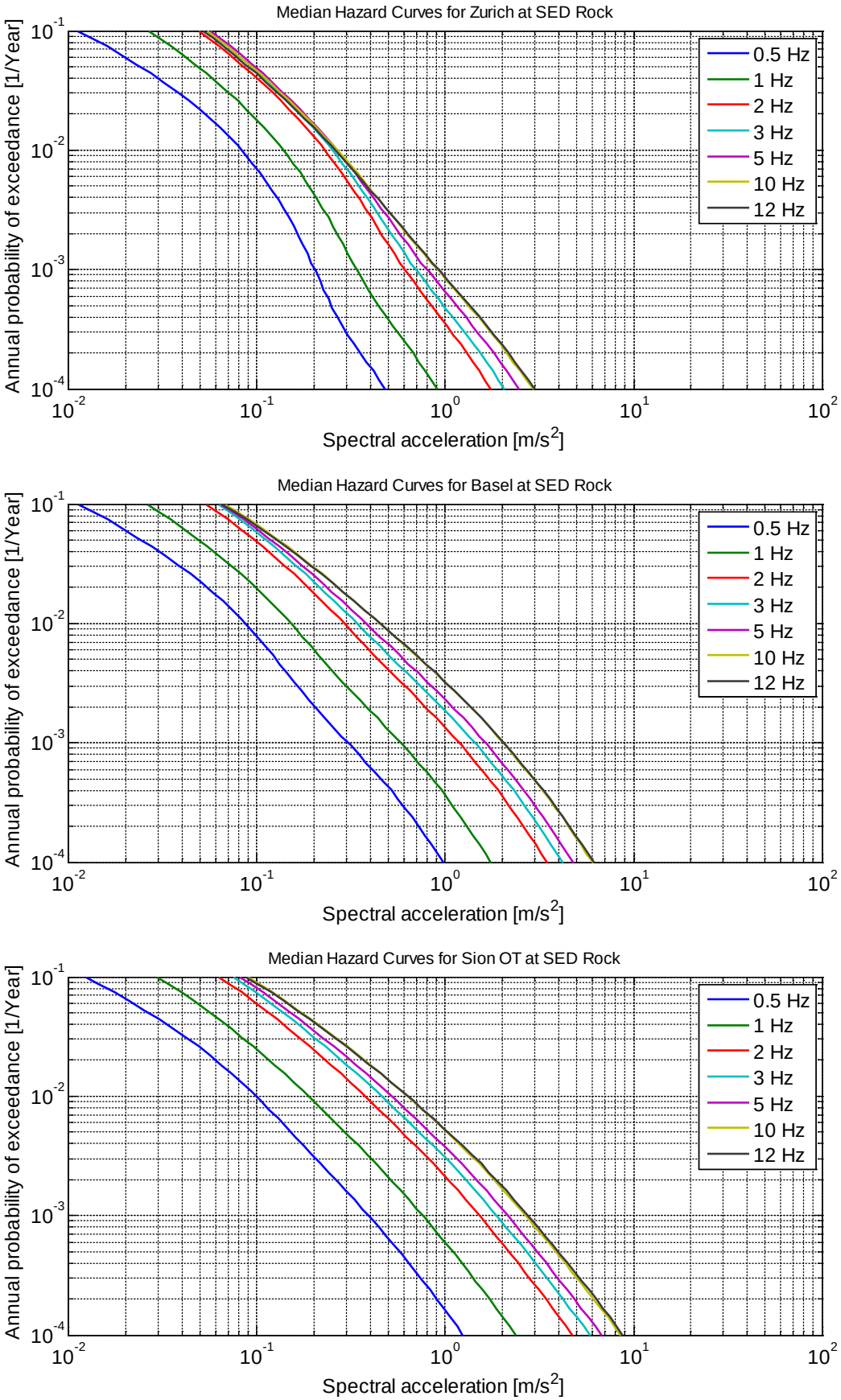

Figure 4: Rock hazard as a function of frequency for Zurich (ETH), Basel and Sion OT

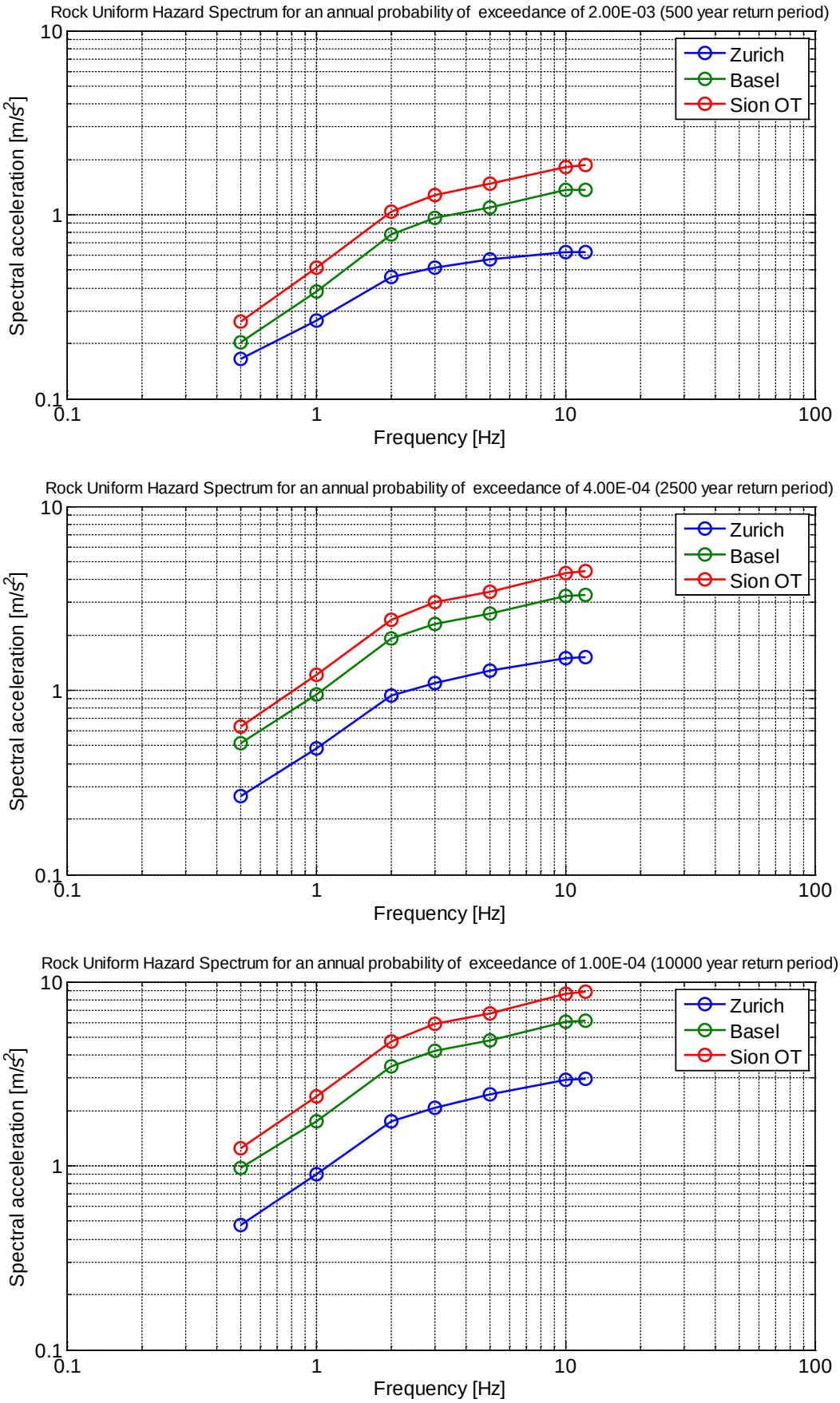

Figure 5: Rock uniform hazard spectrum for a return period of 500, 2'500 and 10'000 years

2.4 Site effects

Probabilistic seismic hazard analysis (PSHA) has been done to compute the rock hazard. To consider site effects, for each site an amplification factor has been provided (Figure 6). Beside the aforementioned three sites an amplification factor is provided for an extra location with deep unconsolidated deposits in the Rhone valley (hereafter called Sion TE).

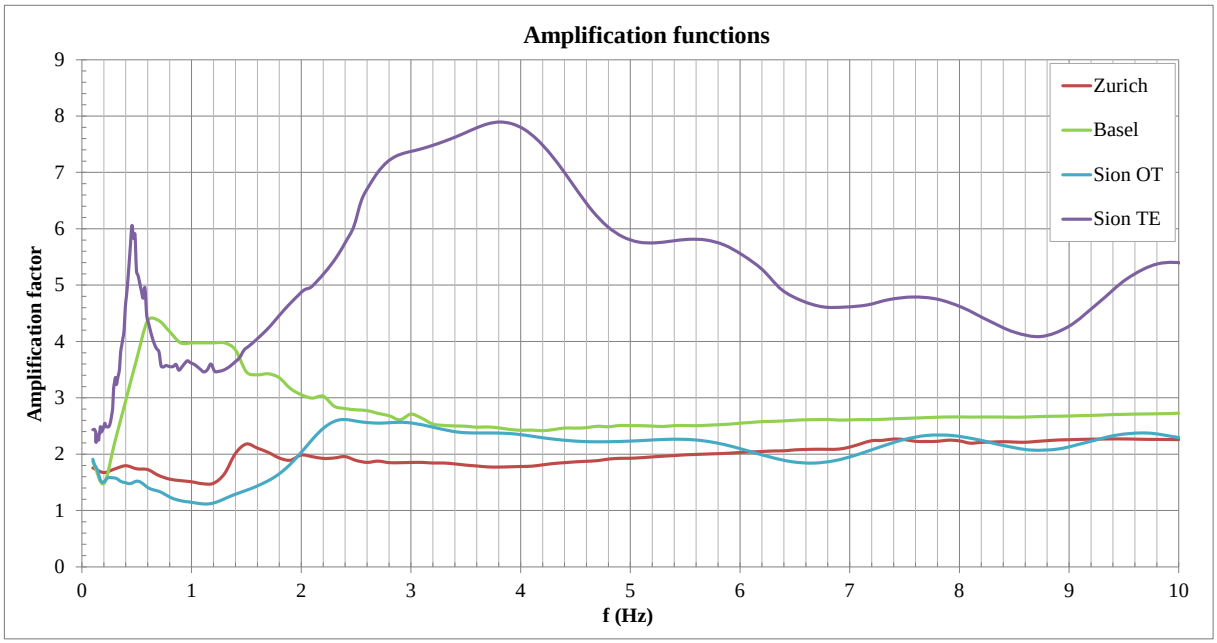

Figure 6: Amplification factors (C_{amp}) for frequencies between 0.1 and 10 Hz

It must be taken into consideration that the provided amplification factors are computed for low acceleration levels. Nonlinearities have not been considered in computing them. Applying a constant amplification factor over the whole range of spectral acceleration leads to an overestimation of the expected accelerations (and displacements) at the surface. To avoid unrealistic ground motions, the nonlinear response of the sites has been considered.

To this end some de-amplification factors (C_{deamp}) are calculated based on [ASCE 41-06, 2007]. They are documented in Table 1. Note that two series of factors are given. For risk assessment of benchmarks with periods of vibration shorter than 1 second (short period), de-amplification factors from the upper table are used. For benchmarks with long period of vibration (larger than 1 second) the factors from the lower table are used.

Table 1: De-amplification factors ($C_{de\text{-}amp}$) for short and long periods of vibration

Short period

	Site class		Sa(5 Hz, SED) [m/s^2]				
eqrisk site	ASCE	sia 261	< 1.25	2.50	3.75	5.00	> 6.25
			Ss(5 Hz, ASCE) [m/s2]				
			< 2.50	5.00	7.50	10.00	> 12.50
	A		1.0	1.0	1.0	1.0	1.0
Zürich	B	A	1.0	1.0	1.0	1.0	1.0
SION OT	C	B	1.0	1.0	0.9	0.8	0.8
Basel	D	C, E	1.0	0.9	0.8	0.7	0.6
SION TE	E	D	1.0	0.7	0.5	0.4	0.4

Long period

	Site class		Sa(1 Hz, SED) [m/s^2]				
eqrisk site	ASCE	sia 261	< 0.5	1.0	1.5	2.0	> 2.5
			S1(1 Hz, ASCE) [m/s2]				
			< 1.0	2.0	3.0	4.0	> 5.0
	A		1.0	1.0	1.0	1.0	1.0
Zürich	B	A	1.0	1.0	1.0	1.0	1.0
SION OT	C	B	1.0	0.9	0.9	0.8	0.8
Basel	D	C, E	1.0	0.8	0.8	0.7	0.6
SION TE	E	D	1.0	0.9	0.8	0.7	0.7

2.5 Soil hazard

Rock hazard for the main frequency of vibration of benchmarks is computed with logarithmic interpolation of SED rock hazard between 0.5 Hz and 10 Hz. Applying the amplification (Figure 6) and de-amplification factors (Table 1) to it the soil hazard curves are computed. Median soil hazard curves as a function of frequency for four locations Zurich, Basel, Sion OT and Sion TE are given in Figure 7.

Uniform hazard spectra (UHS) for a return period of 500, 2'500 and 10'000 years are given in Figure 8.

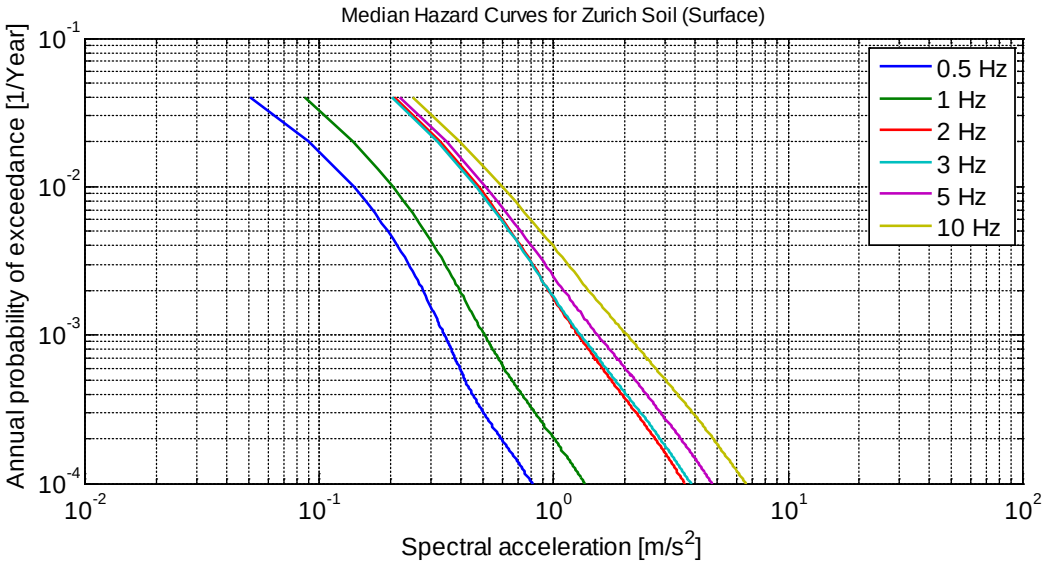

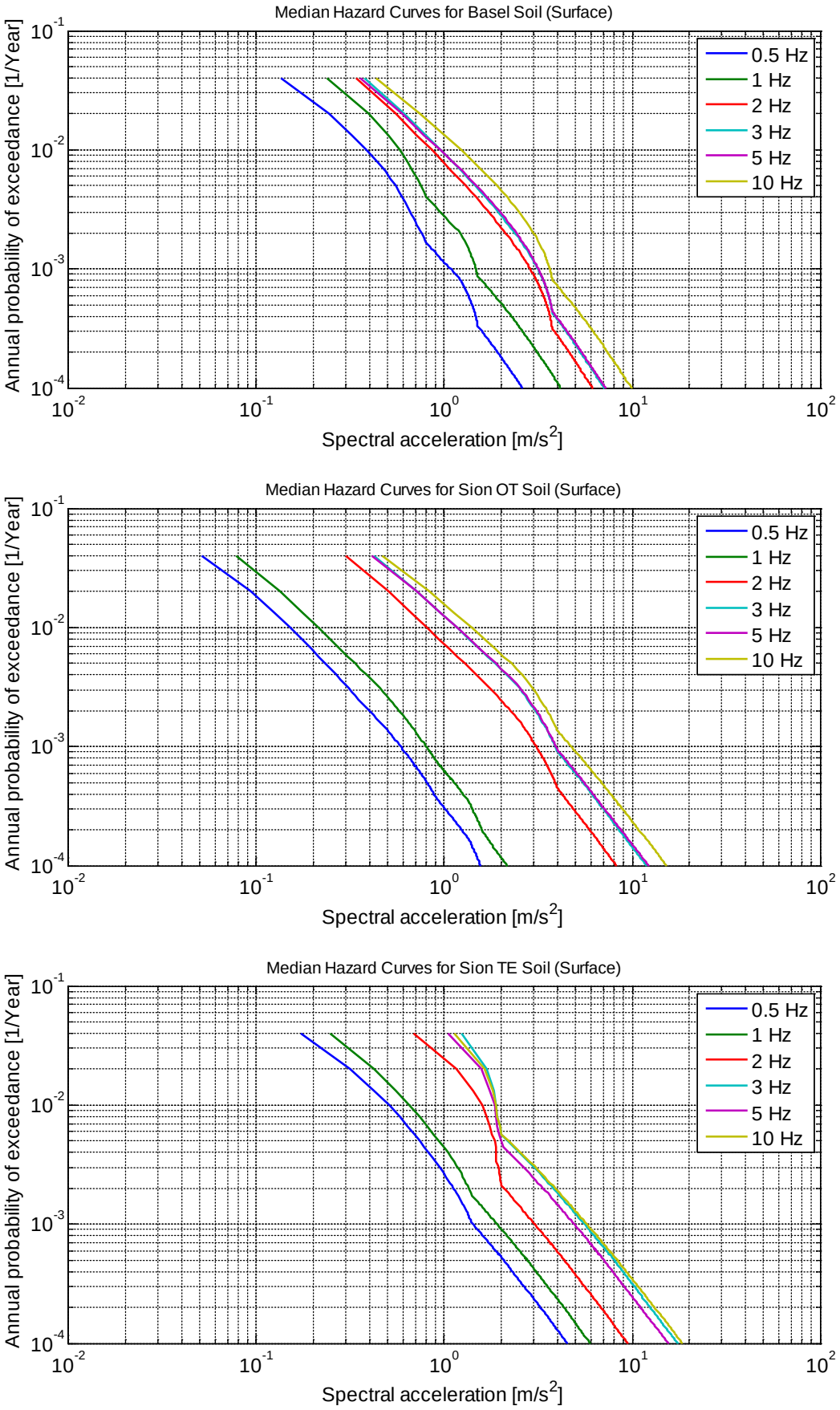

Figure 7: Soil hazard as a function of frequency for Zurich (ETH), Basel, Sion OT and Sion TE

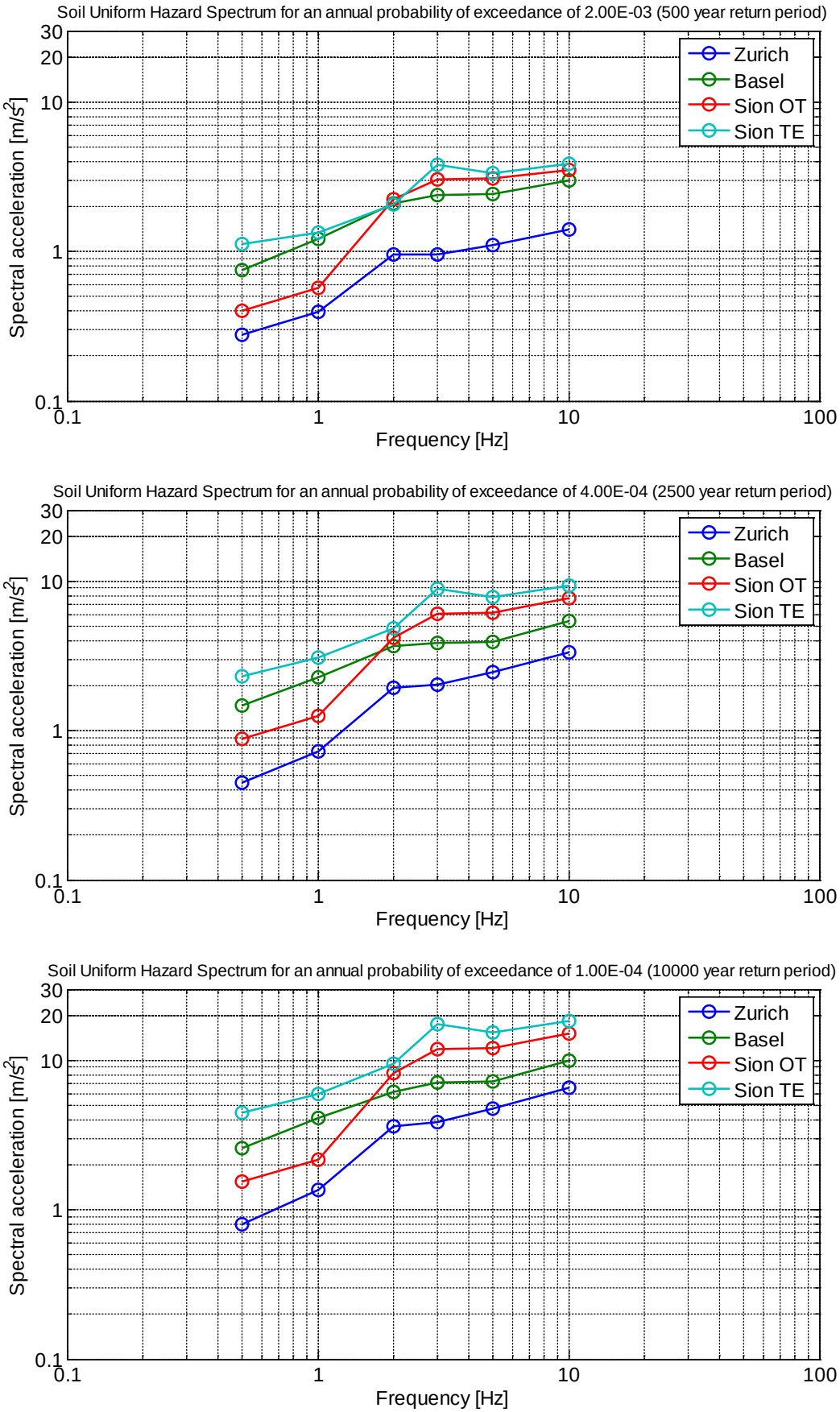

Figure 8: Soil uniform hazard spectrum for a return period of 500, 2'500 and 10'000 years

2.6 EMS-Intensity Hazard

Hazard assessment with EMS-Intensity [EMS, 1998] has not been done within the 2004 Swiss hazard study. Two approaches have been applied in order to receive the desired hazard based on EMS-Intensity:

– Direct intensity prediction (IPE) [Cua et al., 2010, Fäh et al., 2003]

– Ground motion to intensity conversion equations (GMICE) [Faenza and Michelini, 2010]. The following functional form is adopted from [Faenza and Michelini, 2010]:
$I = [(1.01 + 2.56log_{10}\mathrm{Sa}(3\mathrm{Hz})) + (3.02 + 2.1log_{10}\mathrm{Sa}(1\mathrm{Hz}))]/2$
in which $\mathrm{Sa}(3\mathrm{Hz})$ and $\mathrm{Sa}(1\mathrm{Hz})$ are spectral acceleration at 3 and 1 Hz, respectively, in cm/s^2 and I is the EMS-Intensity (for more details see Attachment A).

SED has delivered for each location two sets of hazard curves in terms of EMS-I. For Basel and Sion OT both sets are similar to each other. Hence only the one according to the first approach has been used. Note that the computed EMS-Intensity hazard set corresponds to the soil hazard and no further modification factor has been applied.

To consider the strong amplification of seismic waves because of deep unconsolidated deposits in Rhone valley (Sion TE), one degree of intensity has been added to hazard data at this location (only applied to this site).

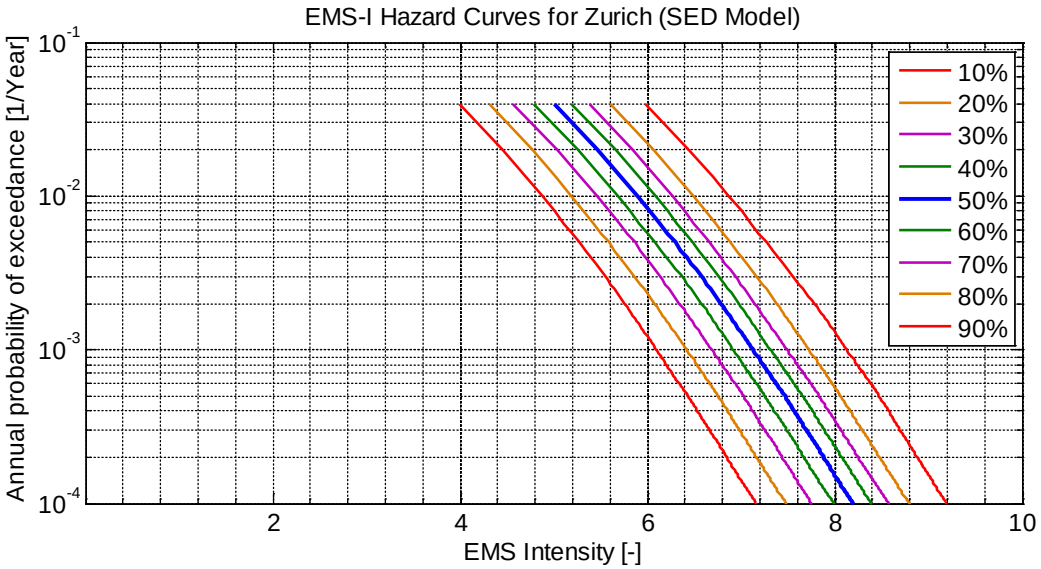
EMS-I Hazard Curves for Zurich (SED Model)
Annual probability of exceedance [1/Year]
EMS Intensity [-]
10%
20%
30%
40%
50%
60%
70%
80%
90%

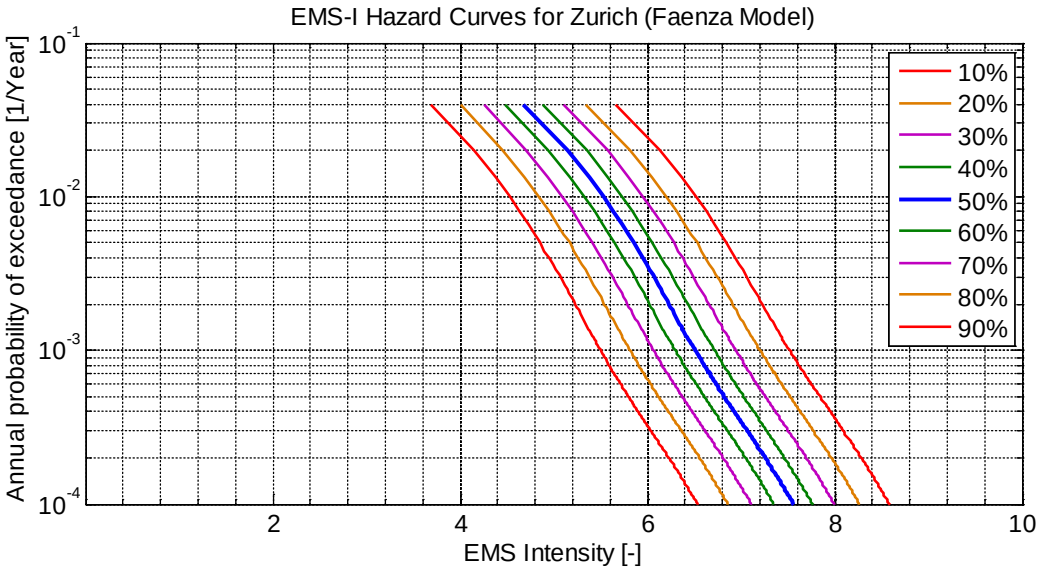
EMS-I Hazard Curves for Zurich (Faenza Model)
Annual probability of exceedance [1/Year]
EMS Intensity [-]
10%
20%
30%
40%
50%
60%
70%
80%
90%

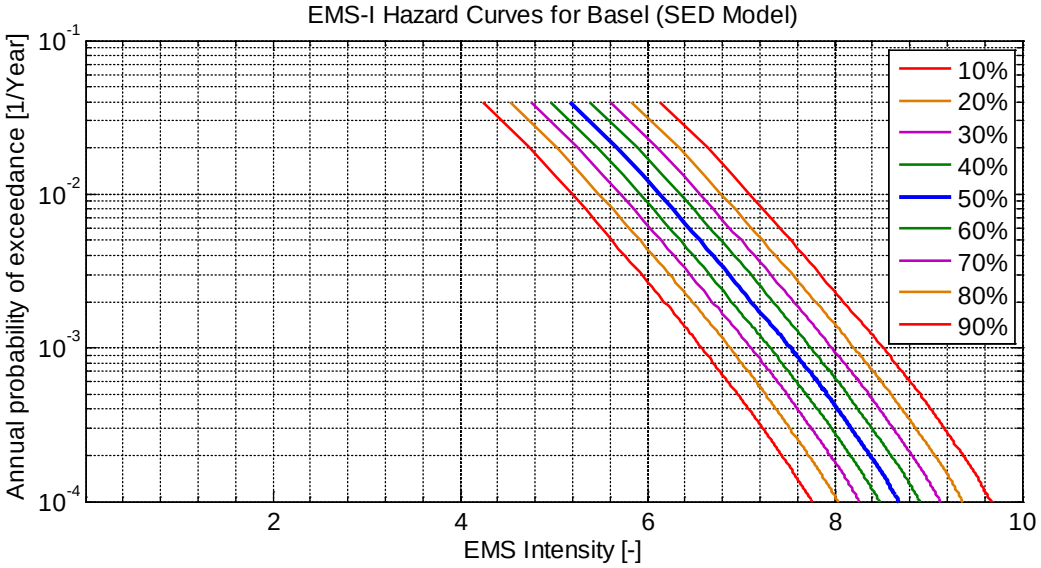
EMS-I Hazard Curves for Basel (SED Model)
Annual probability of exceedance [1/Year]
EMS Intensity [-]
10%
20%
30%
40%
50%
60%
70%
80%
90%

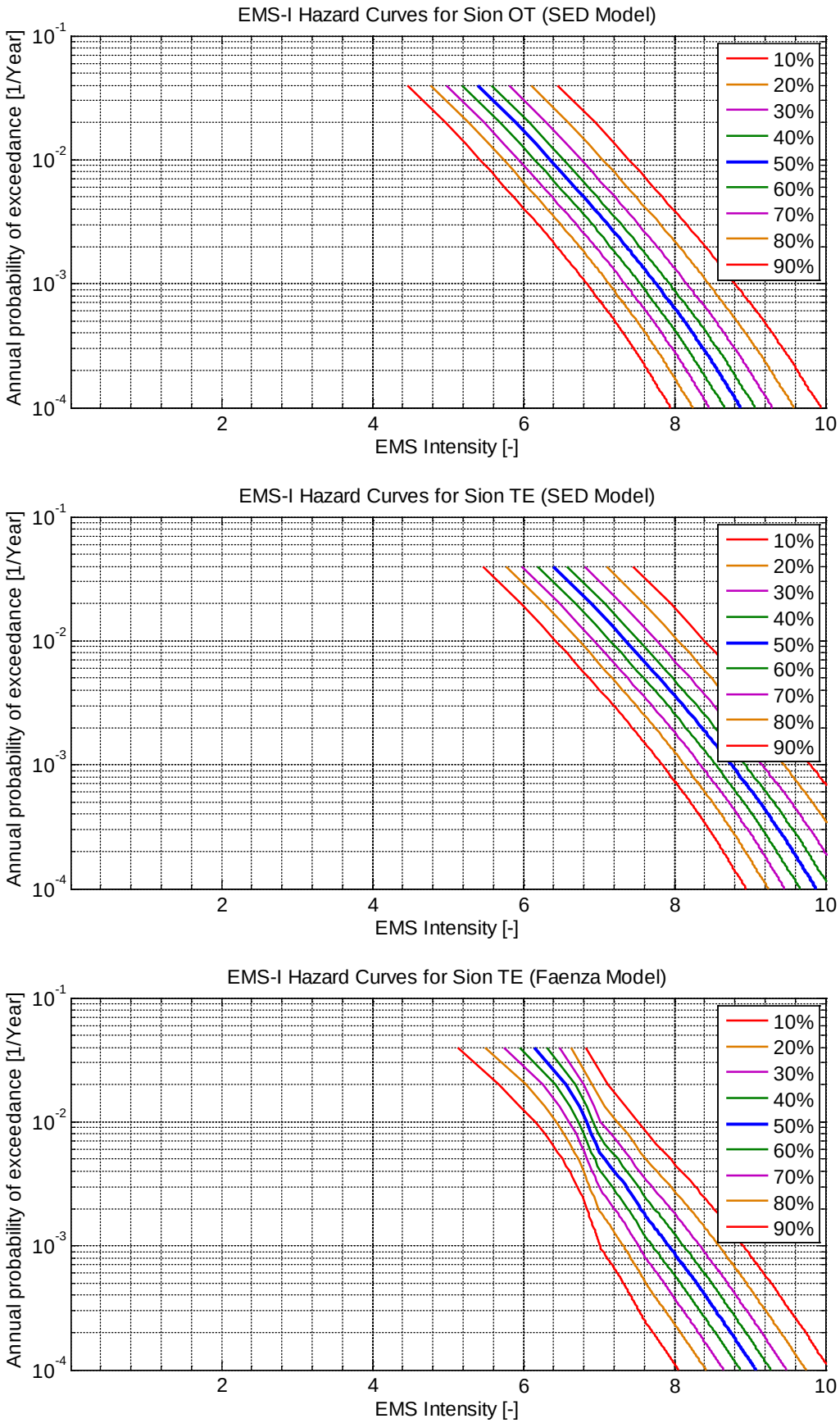

Figure 9: EMS-I hazard curves for Zurich (SED and Faenza models), Basel (SED model), Sion OT (SED model) and Sion TE (SED and Faenza models)

3 Seismic Fragility

3.1 Introduction

In the evaluation of the seismic risk, the fragility curves are giving the probability of exceedance a certain limit state (in this project damage grade) as a function of the applied ground motion intensity measure. In this study two sets of fragility curves based on spectral acceleration and EMS-Intensity measures are derived:

– Fragility curves based on spectral acceleration, which are computed through the nonlinear dynamic analysis of the structure. IMAC has provided this type of fragility curves for this study. Applied Element Method (AEM) has been used to model the seismic behaviour of masonry buildings. To model reinforced concrete structures Finite Element Method (FEM) has been applied. Expected values (mean) of structural properties have been used. Details on the selection of ground motion records, dynamic analysis of the structural system and definition of damage grades are presented in another report prepared by IMAC [IMAC, 2014]. Results are summarized in section 3.5.
– Fragility curves based on EMS-Intensity, which are derived based on Risk-UE project [Risk-UE, 2003 & Lagomarsino and Giovinazzi, 2006]. Results are summarized in section 3.6.

Numerical assessment of existing buildings for seismic loads is done in Switzerland according to Prestandard SIA 2018 and SIA 269/8 Existing structures – Earthquakes (currently in the closing stages of discussion). In the seismic assessment of existing buildings a minimal acceptable seismic safety must be verified. The result of the assessment is given in terms of the so-called compliance factor. The compliance factor is that factor by which the seismic load has to be multiplied in order to just fulfil the earthquake verification. In the simplest case, the compliance factor is the ratio of the seismic load which can be verified to the seismic load which should be verified. In this study several analysis methods have been used to compute the compliance factor of the studied benchmarks. They are summarized in Table 2.

Table 2: Different analysis methods applied in this study to compute the compliance factor

Notation	Analysis method
$\alpha_{force,\ I}$	Force-based method, in which forces are distributed according to the moment of inertia of bearing walls
$\alpha_{force,\ R}$	Force-based method, in which forces are distributed according to the strength of the bearing walls
$\alpha_{def,EC8}$	Displacement-based method according to EC8 assumptions for strength and displacement capacity
$\alpha_{def,SIAD0237}$	Displacement-based method according to SIA D0237 assumptions for strength and displacement capacity

To compute compliance factors, besides spectral acceleration provided by SED for this study [Wiemer, 2011], spectral acceleration according to several other sources have been considered too. These sources are summarized in Table 3.

Table 3: Different studies for the computation of the spectral acceleration at specified sites

Notation	Study source
SED 2011	Spectral acceleration considering site effects as described in section 2.4, based on SED hazard curves for rock [Wiemer, 2011]
SED Micro.	Spectral acceleration based on microzonation studies conducted by SED in Basel and Zürich
Rés Micro.	Spectral acceleration based on microzonation studies conducted by Résonance in Sion OT and Sion TE
SIA 261 BGK X	Spectral acceleration according to SIA 261 (2003) for soil type X (A to E)

Five buildings have been studied. Two of them have been studied both in their original configuration and after retrofitting.

3.2 Damage grades

Within the context of this report, the assessment of vulnerability and risk is based upon the classification of damage contained in the European Macroseismic Scale [EMS, 1998]. The EMS distinguishes between five damage grades (Table 4). For the sake of completeness damage grade 0 (no damage) is added.

Table 4: Damage classification [EMS, 1998]

Classification of damage	Masonry buildings	Reinforced concrete buildings
Damage grade 0: No damage	-	-
Damage grade 1: Negligible to slight damage (no structural damage, slight non-structural damage)	Hair-line cracks in very few walls. Fall of small pieces of plaster only. Fall of loose stones from upper parts of buildings in very few cases.	Fine cracks in plaster over frame members or in walls at the base. Fine cracks in partitions and infills.
Damage grade 2: Moderate damage (slight structural damage, moderate non-structural damage)	Cracks in many walls. Fall of fairly large pieces of plaster. Partial collapse of chimneys.	Cracks in columns and beams of frames and in structural walls. Cracks in partition and infill walls; fall of brittle cladding and plaster. Falling mortar from the joints of wall panels.
Damage grade 3: Substantial to heavy damage (moderate structural damage, heavy non-structural damage)	Large and extensive cracks in most walls. Roof tiles detach. Chimneys fracture at the roof line; failure of individual non-structural elements (partitions, gable walls).	Cracks in columns and beam column joints of frames at the base and at joints of coupled walls. Spalling of concrete cover, buckling of reinforced rods. Large cracks in partition and infill walls, failure of individual infill panels.
Damage grade 4: Very heavy damage (heavy structural damage, very heavy non-structural damage)	Serious failure of walls; partial structural failure of roofs and floors.	Large cracks in structural elements with compression failure of concrete and fracture of rebars; bond failure of beam reinforced bars; tilting of columns. Collapse of a few columns or of a single upper floor.
Damage grade 5: Destruction (very heavy structural damage)	Total or near total collapse.	Collapse of ground floor or parts (e. g. wings) of buildings.

3.3 Development of the Fragility curves

To develop fragility curves the following steps have been done (details are documented in IMAC report [IMAC, 2014]):

– Selection of the ground motion records for the nonlinear dynamic analysis of the benchmarks. Records are selected from the European strong motion database, Italian database and several registered records from the Christchurch earthquake. Records are chosen so, that they have spectral acceleration values close to the spectral acceleration values provided by the Swiss Seismological Service for different cities in Switzerland. Each record is represented by the value of its spectral acceleration at a period T. Period T is computed as the geometrical mean of the periods in two horizontal directions. To consider structural damages and their effect on the period, the periods are computed in damage grade 2.

– Nonlinear dynamic analysis of benchmarks. In each run of analysis based on the description of the damage grades for buildings according to [EMS, 1998] and engineering judgment the damage grade of the structure is determined.
– Distribution fitting. After completion of all dynamic analyses for each benchmark there are several records, which bring the structure to a certain damage grade. For each set of data (for a damage grade) a lognormal distribution is fitted, which is considered to be the fragility curve for that damage grade (Figure 10).

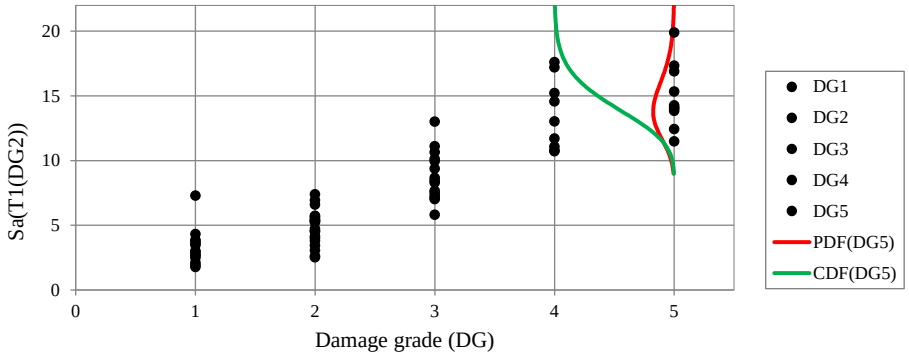

Figure 10: Benchmark YVR14, distribution of spectral acceleration values for damage grade 5

In some cases fragility curves intersect each other. As this is physically not possible, in such cases the fragility curves are considered to be equal (only for the problematic region, see e.g. Figure 11).

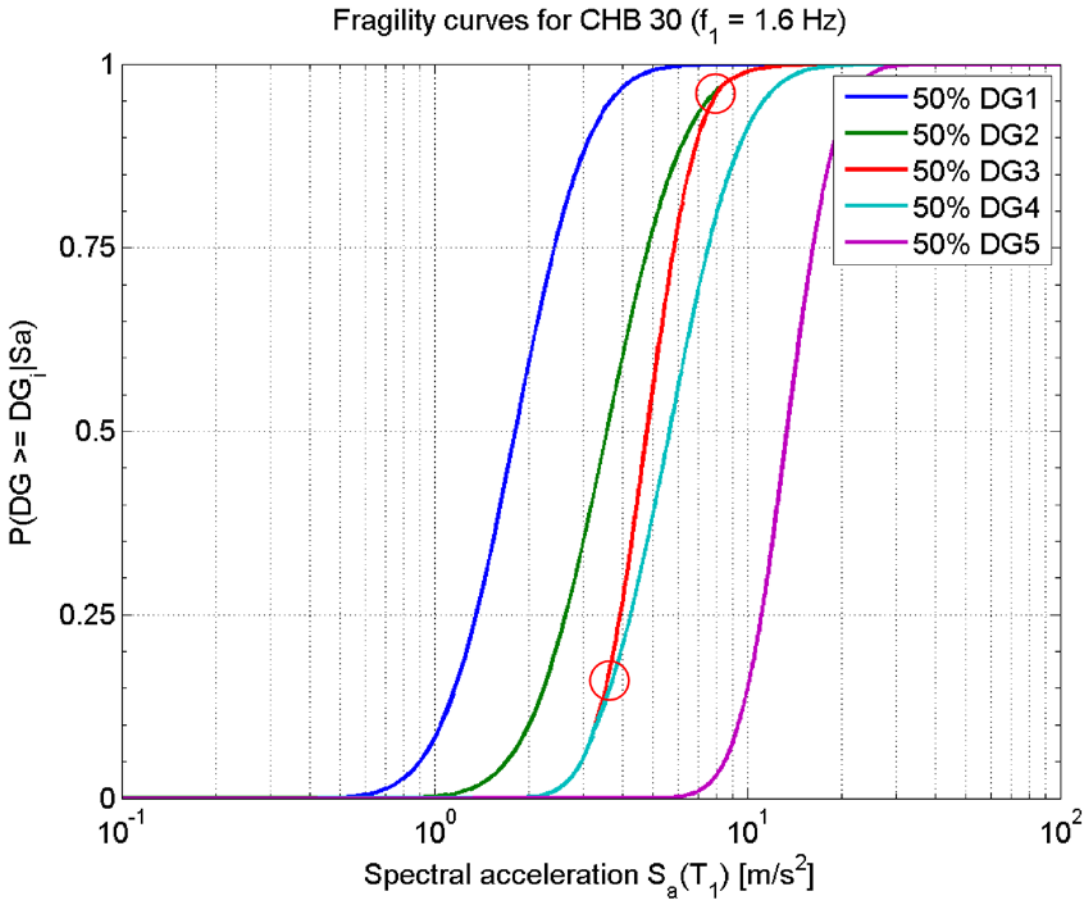

Figure 11: An example for intersecting fragility curves and its solution

3.4 Treatment of the model uncertainty

While there can be many sources of uncertainty, in the context of modelling, it is convenient to categorize the character of uncertainties as either aleatory or epistemic [Kiureghian, 2007]. Aleatory uncertainty (usually called randomness) is presumed to be the intrinsic randomness of a phenomenon, for example because of the record-to-record randomness. By considering a set of time histories corresponding to the relevant scenarios, this type of uncertainty is assumed to be covered. There remains yet the epistemic uncertainty associated to the question, to which extend the used records are able to represent the seismicity in Switzerland.

Epistemic uncertainty is presumed to be caused by lack of knowledge (or data). The epistemic uncertainty can be considered as a measure for the ability of a model to predict the reality. It is theoretically possible to reduce the model uncertainty by gathering more information and knowledge and developing better models. Basically to capture this kind of uncertainty either experimental tests must be done or several numerical models must be studied. Such information was not available.

The fragility curves are considered to disperse around the numerically produced fragility curves following a lognormal distribution with parameters mean of 1 and with β_U (sometimes called σ_{LN}) of 0.3.

Figure 12 shows the fragility curve of the benchmark YVR14 for DG5. The figure illustrates how record-to-record and model uncertainties are modelled.

Uncertainty because of material properties (of random nature) is not considered.

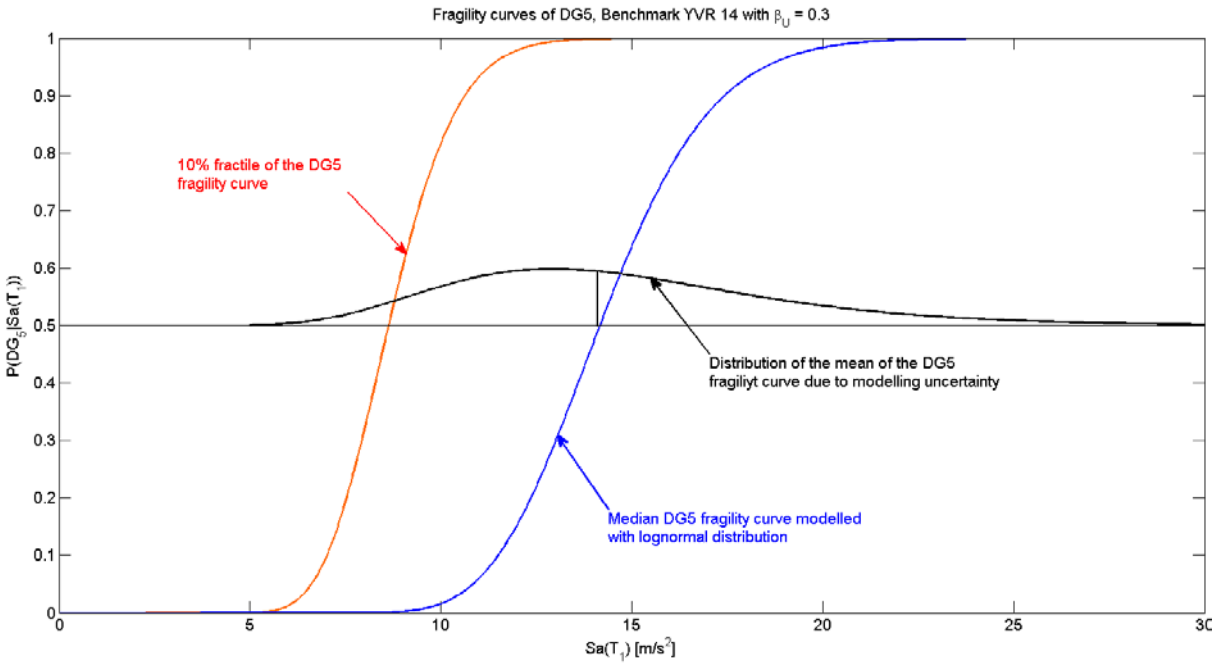

Figure 12: Fragility curve for Benchmark YVR14 DG5 with its 10th percentile curve

3.5 Structural fragility function in terms of spectral acceleration

3.5.1 Benchmark YVR14

The building YVR14 (Figure 13 and Table 5) is a 4-story brick masonry structure with RC slabs from ca. 1955. The building is 30 m long and 12 m wide. The story height is 2.7 m.

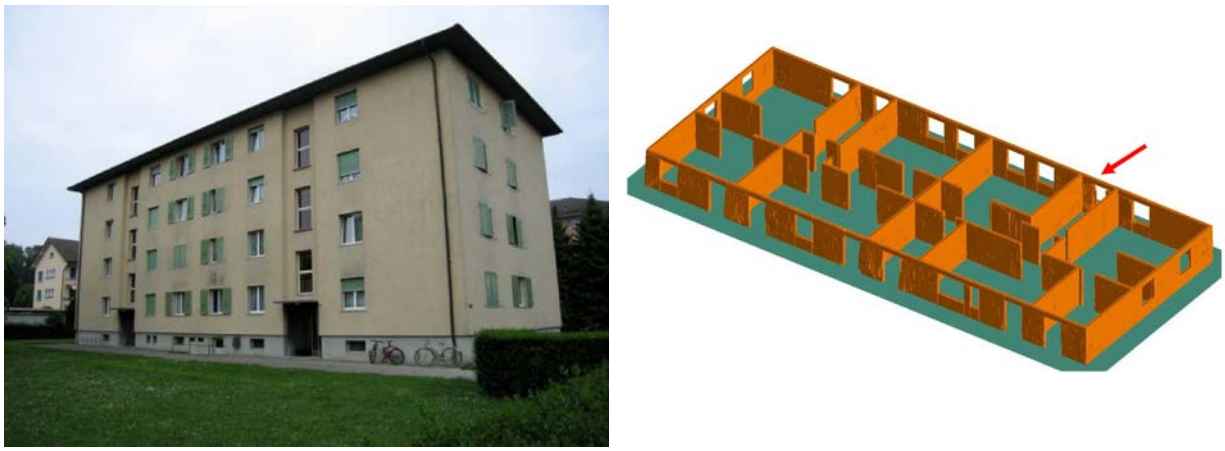

Figure 13: Benchmark YVR14, right: section view of the first floor [IMAC, 2014]

Table 5: Structural characteristics of the benchmark YVR14

1st mode frequency (transverse) FE-model*	3.5 Hz (0.29 s)
1st mode frequency engineering model	3.7 Hz (0.27 s)
Masonry compressive strength (normal to bed joints)	10.5 N/mm^2
Masonry compressive strength (normal to head joints)	6.3 N/mm^2
Masonry tensile strength	1 N/mm^2
Wall thickness at first floor	15 - 18 cm
Thickness of RC slabs	20 cm
Number of stories	4

* Used for the risk analysis

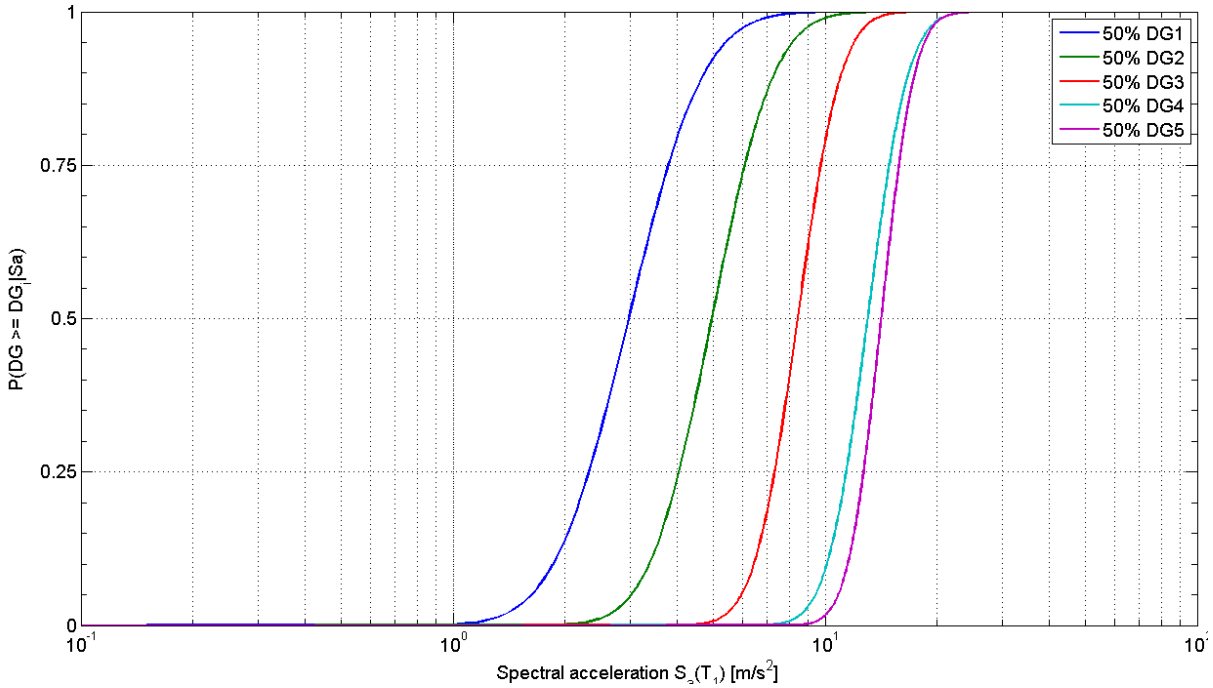

Figure 14: Benchmark YVR14 fragility curves of DG1 to DG5 (median curves)

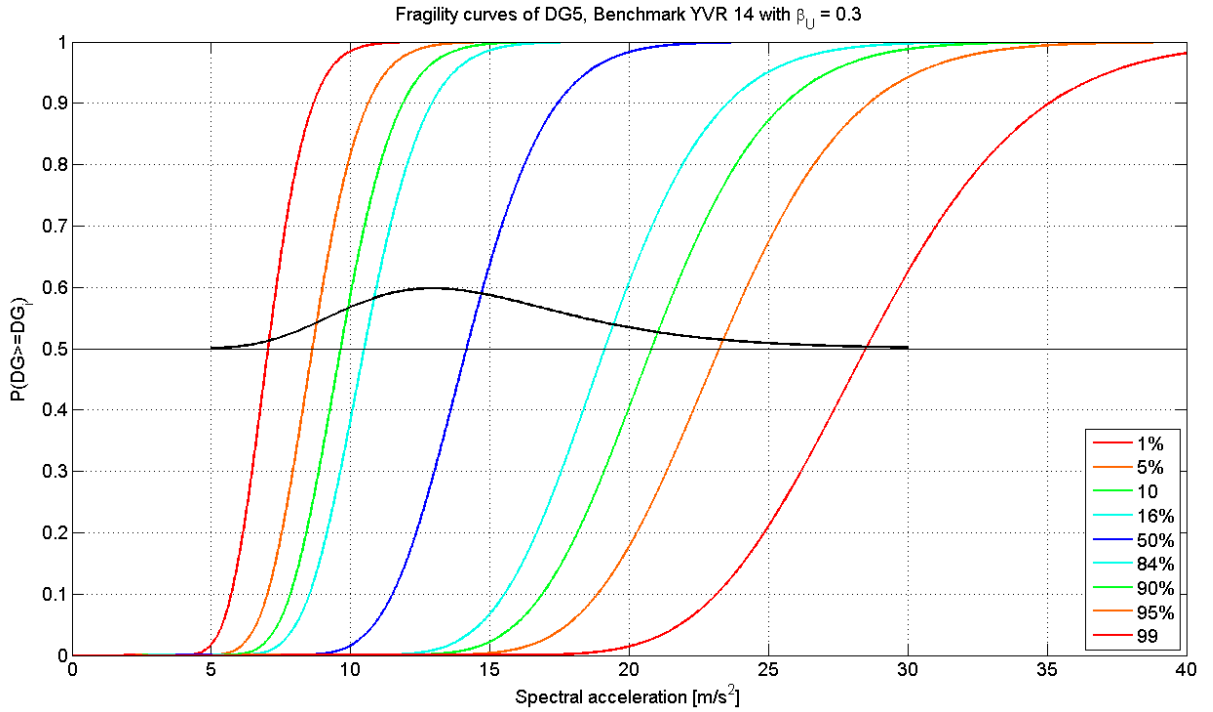

Figure 15: 1st to 99th percentile fragility curves of DG5 for YVR14 (assuming a model uncertainty of 0.3, for more details see chapter 3.4)

Table 6: Compliance factors for YVR14

YVR14	**Sa (3.7 Hz) [m/s^2]**	**$\alpha_{def,EC8}$**	**$\alpha_{def,SIAD0237}$**	**$\alpha_{force,\ I}$**	**T_c [s]**	**$\alpha_{force,\ R}$**
Basel SED 2011	2.36					
Basel SED Micro.	3.35	1.25	1.60	0.31	0.60	0.96
Basel SIA 261 BGK C	3.74	1.04	1.37	0.28	0.60	0.86
Sion OT SED 2011	2.12					
Sion OT Rés Micro.	5.40	0.60	0.84	0.19	0.60	0.60
Sion OT SIA 261 BGK C	4.60	0.75	1.04	0.23	0.60	0.70
Sion TE SED 2011	3.26					
Sion TE Rés Micro.	4.60	0.62	0.83	0.23	0.80	0.70
Sion TE SIA 261 BGK D	5.40	0.49	0.67	0.19	0.80	0.60
Zurich SED 2011	1.08					
Zurich SED Micro.	1.35	4.00	6.14	0.77	0.40	2.39
Zurich SIA 261 BGK A	1.50	3.60	5.53	0.70	0.40	2.15

3.5.2 Benchmark CHB30

The building CHB30 (Figure 16 and Table 7) is a 6-story stone masonry structure retrofitted with RC slabs (originally timber slabs). The building is 14 m long and 12 m wide. The story height is ca. 3.0 m.

Fragility curves are given in Figure 17. Note that numerically computed fragility curves (based on the assumption that they can be modelled with log normal distribution) may intersect each other. In such cases the fragility curve for the higher damage grade is modified so that both intersecting curves from the intersection point have the same value (e.g. Figure 17 fragility curves of DG2, DG3 and DG4).

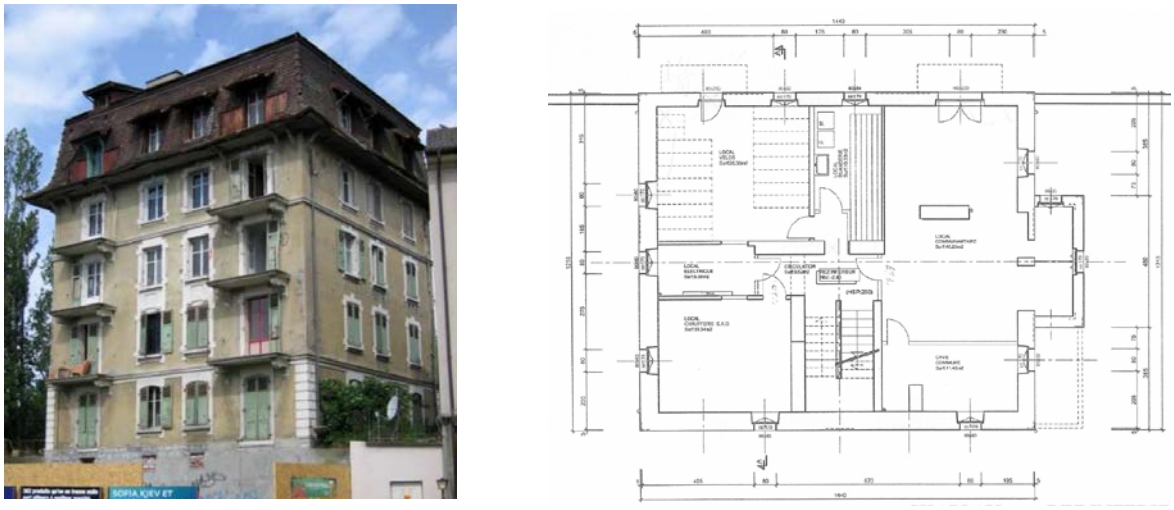

Figure 16: Benchmark CHB30, right: first floor plan [IMAC, 2014]

Table 7: Structural characteristics of the benchmark CHB30

1st mode frequency FE-model (longitudinal)*	1.6 Hz (0.63 s)
1st mode frequency engineering model	2.4 Hz (0.42 s)
Masonry compressive strength (normal to bed joints)	10 N/mm^2
Masonry compressive strength (normal to head joints)	2.7 N/mm^2
Masonry tensile strength	0.75 N/mm^2
Wall thickness in first floor	up to 60 cm

* Used for the risk analysis

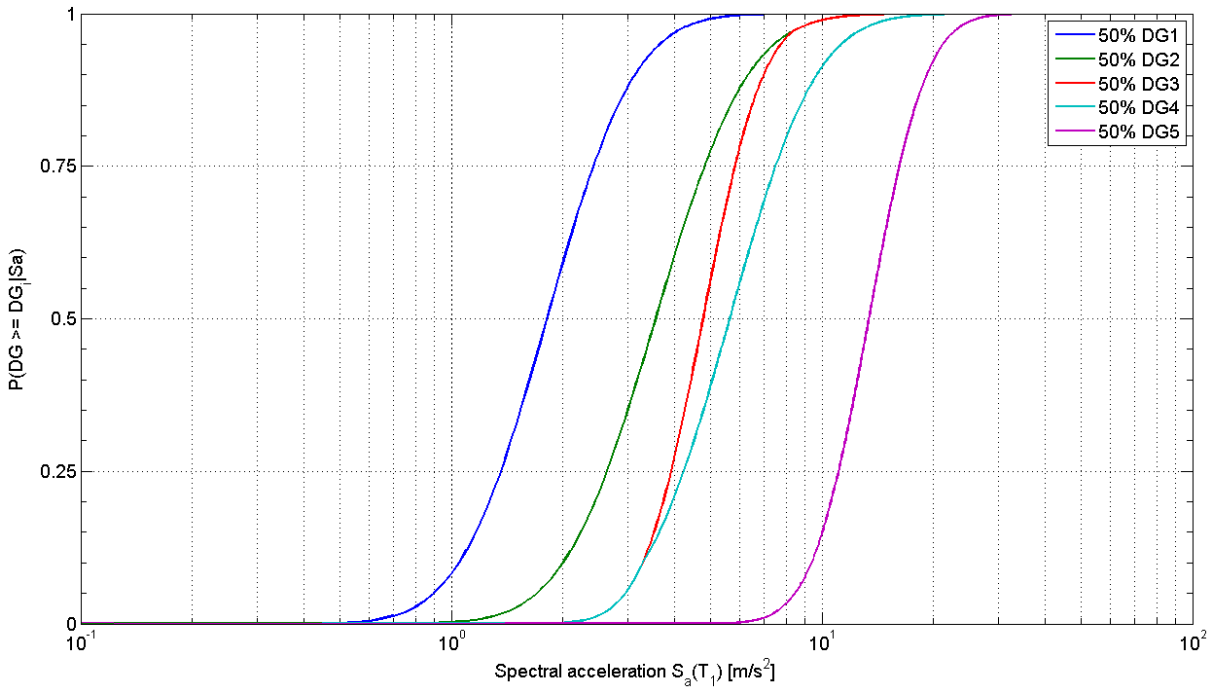

Figure 17: Benchmark CHB30 fragility curves of DG1 to DG5 (median curves)

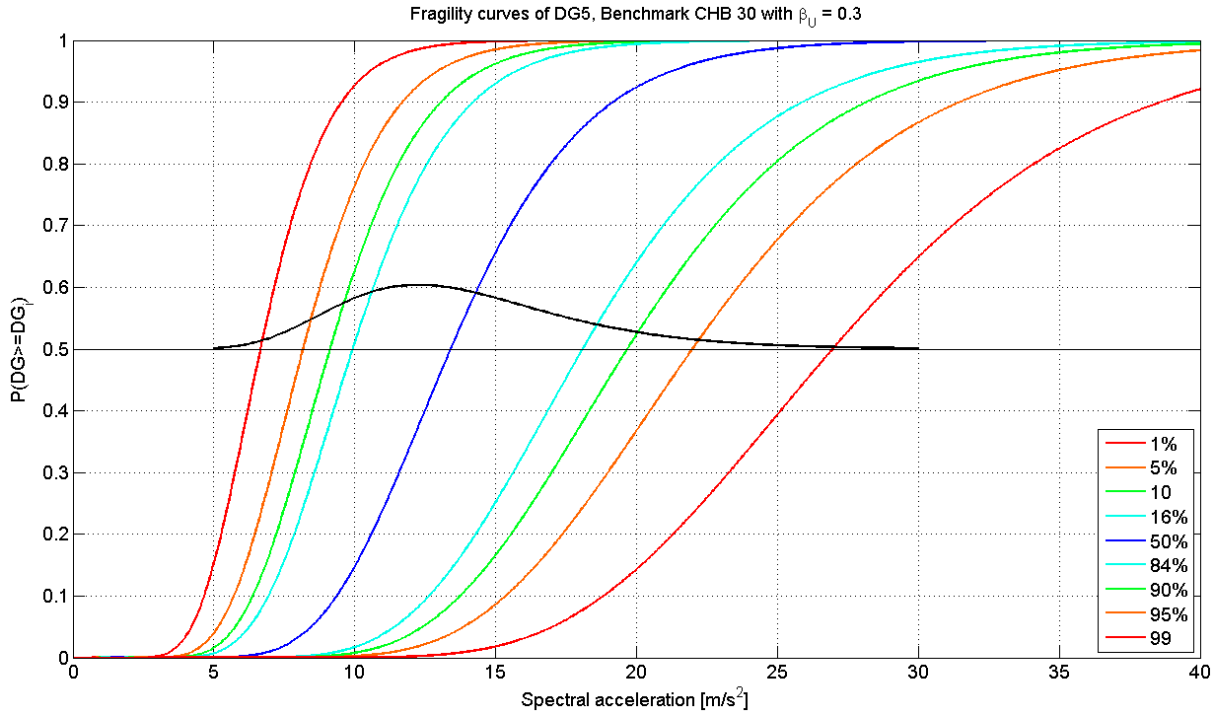

Figure 18: 1st to 99th percentile fragility curves of DG5 for CHB30 (assuming a model uncertainty of 0.3)

Table 8: Compliance factors for CHB30

CHB30	**Sa (2.4 Hz) [m/s^2]**	**$\alpha_{def,EC8}$**	**$\alpha_{def,SIAD0237}$**	**$\alpha_{force,\ I}$**	**T_c [s]**	**$\alpha_{force,\ R}$**
Basel SED 2011	2.42					
Basel SED Micro.	3.30	0.90		0.24	0.60	
Basel SIA 261 BGK C	3.74	0.78		0.21	0.60	
Sion OT SED 2011	1.38					
Sion OT Rés Micro.	5.40	0.53		0.14	0.60	
Sion OT SIA 261 BGK C	4.60	0.62		0.17	0.60	
Sion TE SED 2011	3.24					
Sion TE Rés Micro.	4.60	0.49		0.17	0.80	
Sion TE SIA 261 BGK D	5.40	0.41		0.14	0.80	
Zurich SED 2011	0.95					
Zurich SED Micro.	1.15	3.35		0.68	0.40	
Zurich SIA 261 BGK A	1.50	2.57		0.52	0.40	

3.5.3 Benchmark CHB30 ORG

This benchmark is the same as benchmark CHB30 (chapter 3.5.2) but with floors in their original condition (timber slabs, Figure 19).

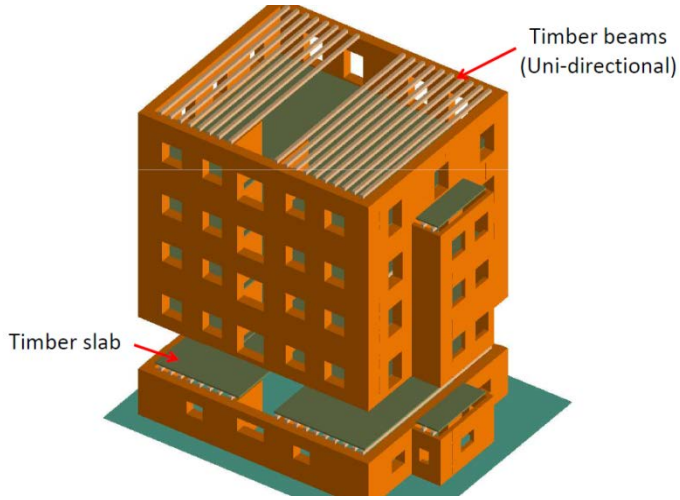

Figure 19: Benchmark CHB30 ORG computer model [IMAC, 2014]

Table 9: Structural characteristics of the benchmark CHB30 ORG (material properties are the same as benchmark CHB30)

1st mode frequency (longitudinal) FE-model*	1.8 Hz (0.56 s)
1st mode frequency engineering model	Not available

* Used for the risk analysis

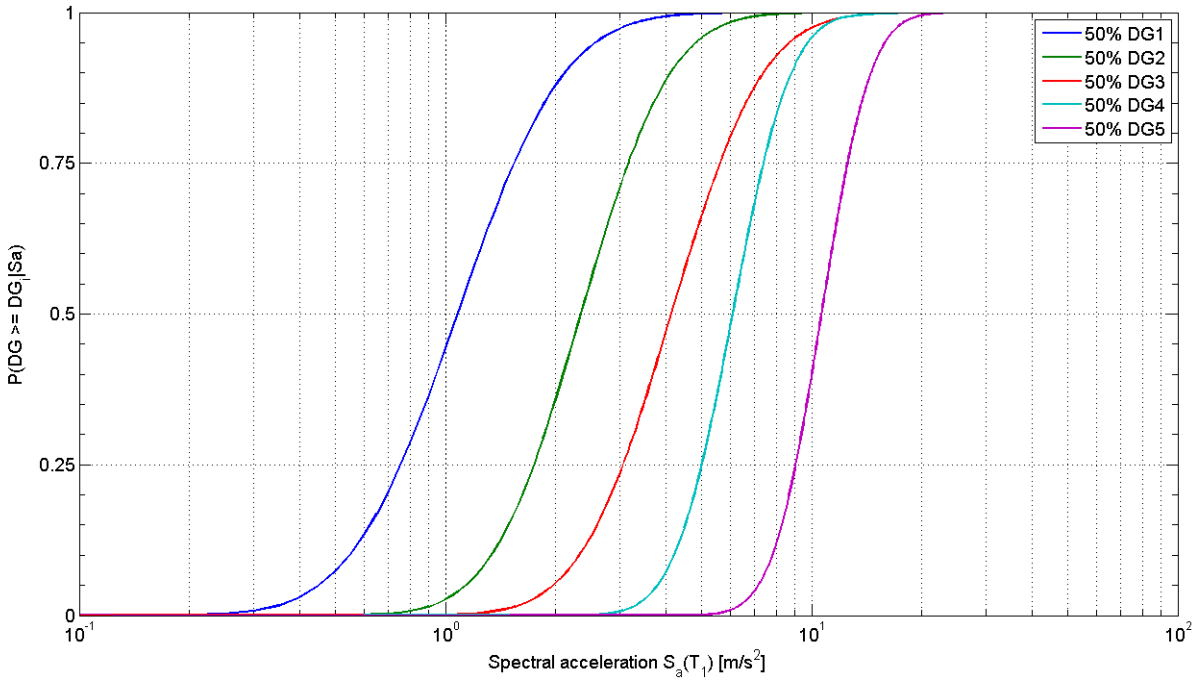

Figure 20: Benchmark CHB30 ORG fragility curves of DG1 to DG5 (median curves)

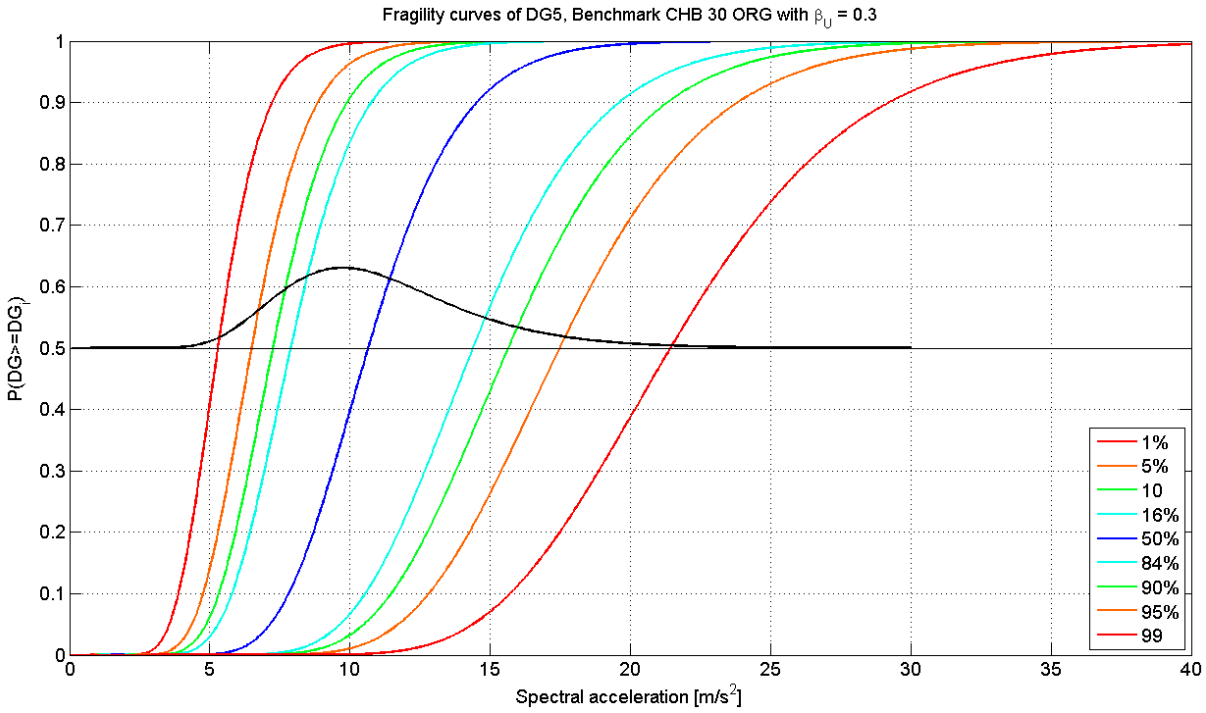

Figure 21: 1st to 99th percentile fragility curves of DG5 for CHB30 ORG (assuming a model uncertainty of 0.3)

Table 10: Compliance factors for CHB30 ORG

CHB30 ORG	**Sa $_{max}$ [m/s^2]**	**$\alpha_{def,EC8}$**	**$\alpha_{def,SIAD0237}$**	**$\alpha_{force,\ I}$**	**T_c [s]**	**$\alpha_{force,\ R}$**
Basel SED 2011	2.42					
Basel SED Micro.	3.30			0.16	0.60	
Basel SIA 261 BGK C	3.74			0.14	0.60	
Sion OT SED 2011	1.38					
Sion OT Rés Micro.	5.40			0.10	0.60	
Sion OT SIA 261 BGK C	4.60			0.11	0.60	
Sion TE SED 2011	3.24					
Sion TE Rés Micro.	4.60			0.11	0.80	
Sion TE SIA 261 BGK D	5.40			0.10	0.80	
Zurich SED 2011	0.95					
Zurich SED Micro.	1.15			0.45	0.40	
Zurich SIA 261 BGK A	1.50			0.35	0.40	

3.5.4 Benchmark SECH7

The building SECH7 is a 7-story brick masonry structure with RC slabs with a thickness of 18 cm from ca. 1960. The building is 21 m long and 11 m wide. The story height is 2.8 m. The building has several masonry walls in its transvers direction. In the other direction, however, there are only some very short walls (Figure 22).

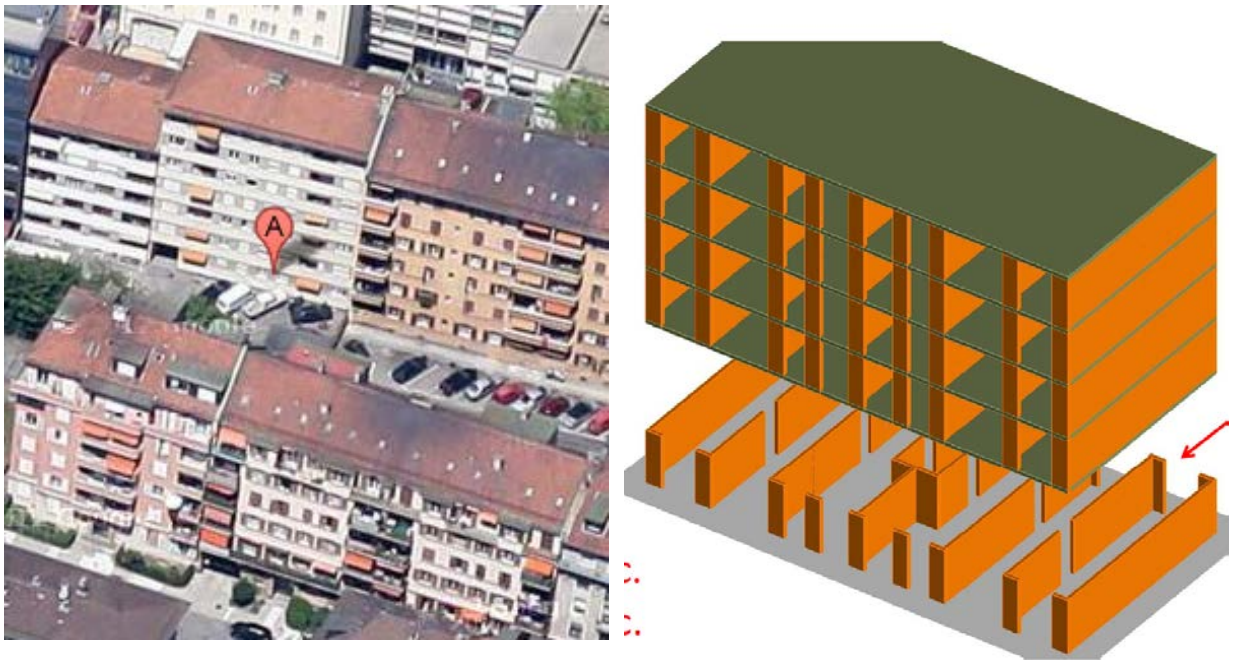

Figure 22: Benchmark SECH7, right: computer model [IMAC, 2014]

Table 11: Structural characteristics of the benchmark SECH7

1st mode frequency (longitudinal) FE-model*	0.9 Hz (1.16 s)
1st mode frequency engineering model	0.5 Hz (2.00 s)
Masonry compressive strength (normal to bed joints)	10 N/mm^2
Masonry tensile strength	1 N/mm^2
Wall thickness in first floor	18 cm

* Used for the risk analysis

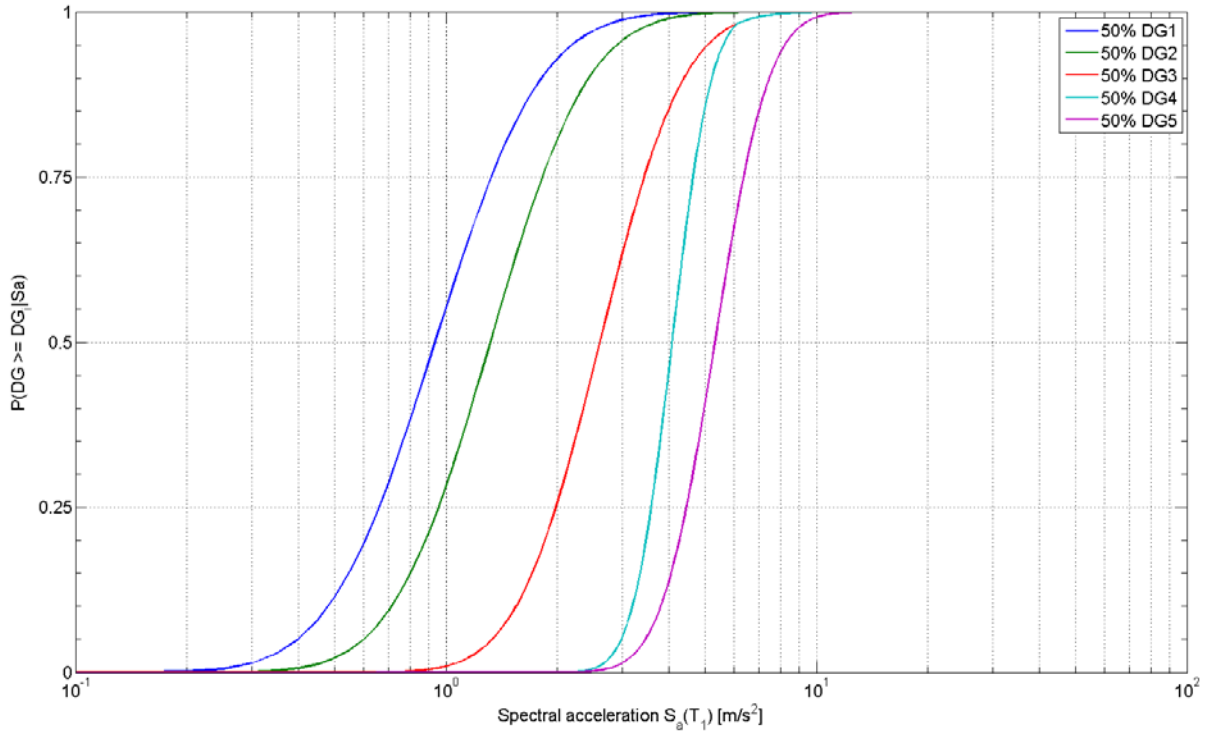

Figure 23: Benchmark SECH7 fragility curves of DG1 to DG5 (median curves)

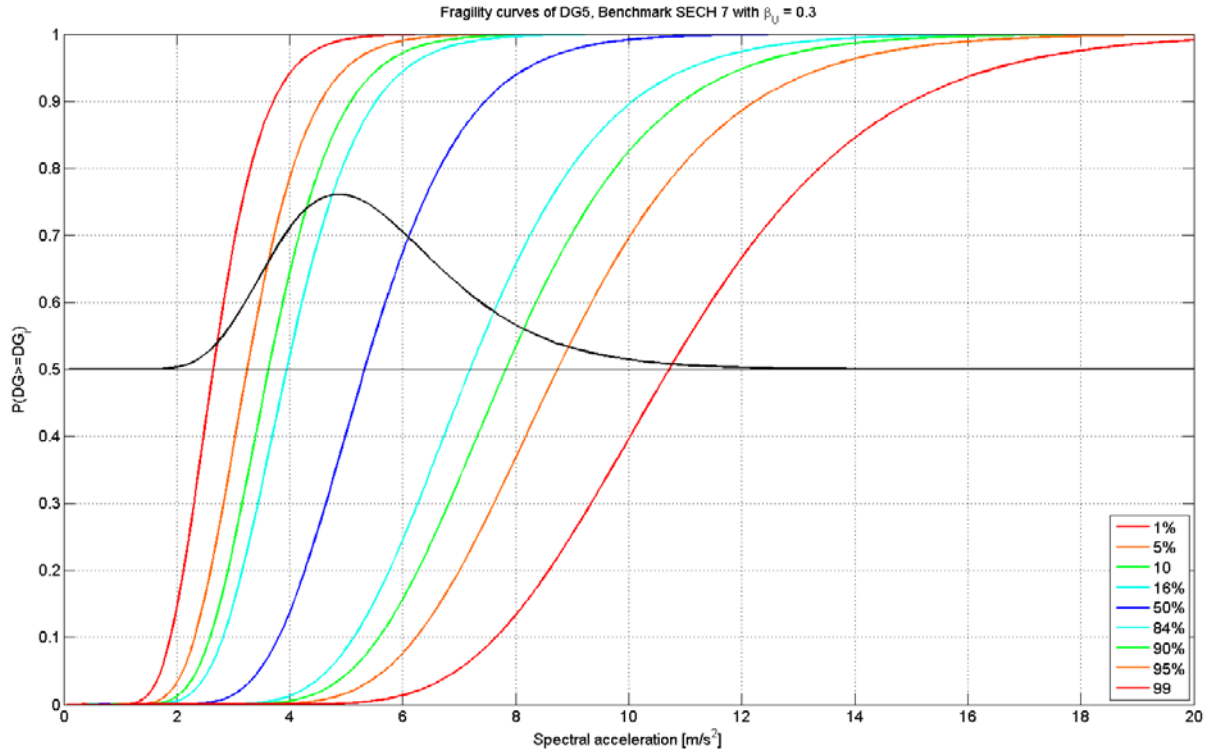

Figure 24: 1st to 99th percentile fragility curves of DG5 for SECH7 (assuming a model uncertainty of 0.3)

Table 12: Compliance factors for SECH7

SECH7	**Sa(0.5 Hz) [m/s^2]**	**$\alpha_{def,EC8}$**	**$\alpha_{def,SIAD0237}$**	**$\alpha_{force,\ I}$**	**T_c [s]**	**$\alpha_{force,\ R}$**
Basel SED 2011	0.62	0.38		0.45		
Basel SED Micro.						
Basel SIA 261 BGK C	1.12	0.21		0.25		
Sion OT SED 2011	0.28	0.83		0.99		
Sion OT Rés Micro.						
Sion OT SIA 261 BGK C	1.38	0.17		0.20		
Sion TE SED 2011	0.67	0.35		0.41		
Sion TE Rés Micro.						
Sion TE SIA 261 BGK D	2.16	0.11		0.13		
Zurich SED 2011	0.20	1.17		1.39		
Zurich SED Micro.						
Zurich SIA 261 BGK A	0.30	0.78		0.92		

3.5.5 Benchmark SUVA

The SUVA building is an 11-story RC structure with RC slabs from ca. 1967. The building is 33 m long and 15 m wide. The story height is 3 m (first two floors 4 m). The first and the fifth floors are considerably softer than other floors (Figure 25).

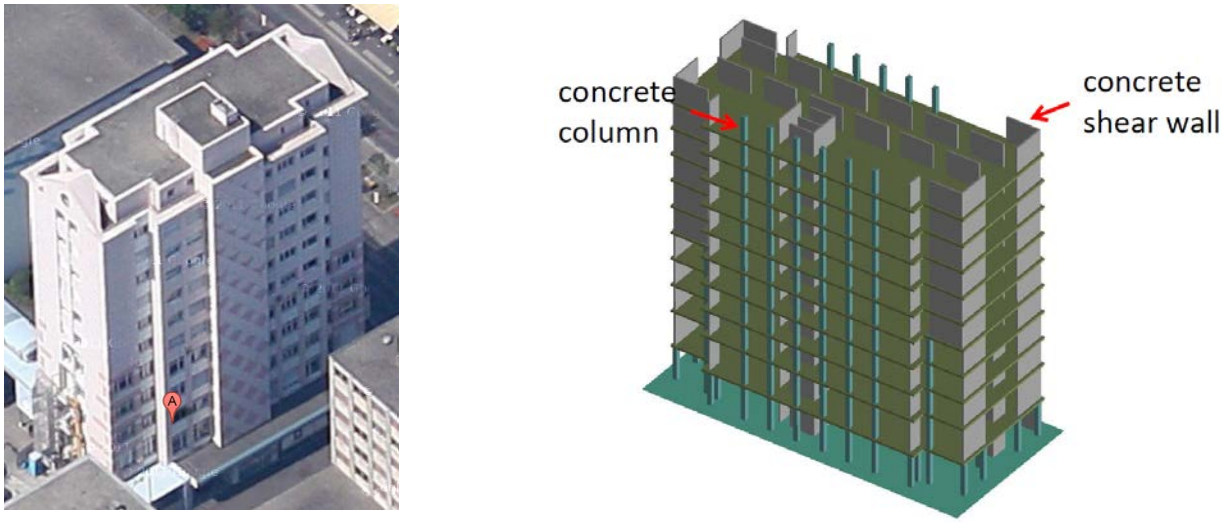

Figure 25: Benchmark SUVA, right: computer model [IMAC, 2014]

Table 13: Structural characteristics of the benchmark SUVA

1st mode frequency (transverse) FE-model*	0.8 Hz (1.27 s)
1st mode frequency engineering model	1.0 Hz (1.0 s)
Concrete compressive strength	33 N/mm^2
Concrete tensile strength	3 N/mm^2

* Used for the risk analysis

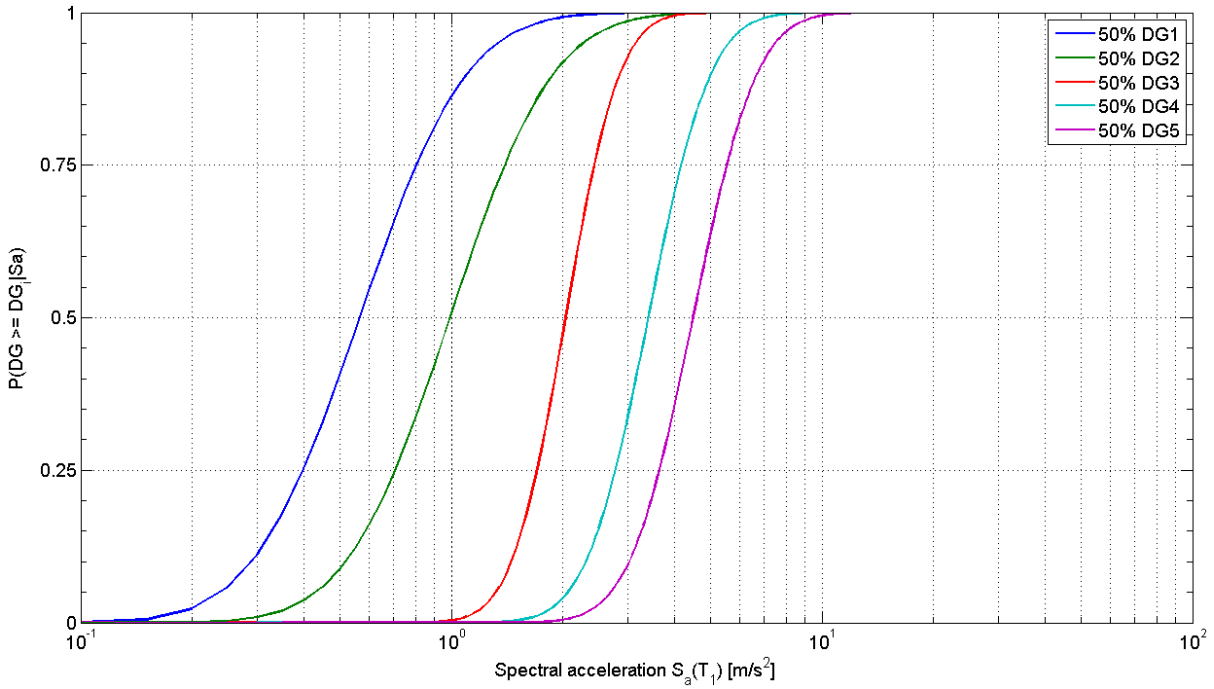

Figure 26: Benchmark SUVA fragility curves of DG1 to DG5 (median curves)

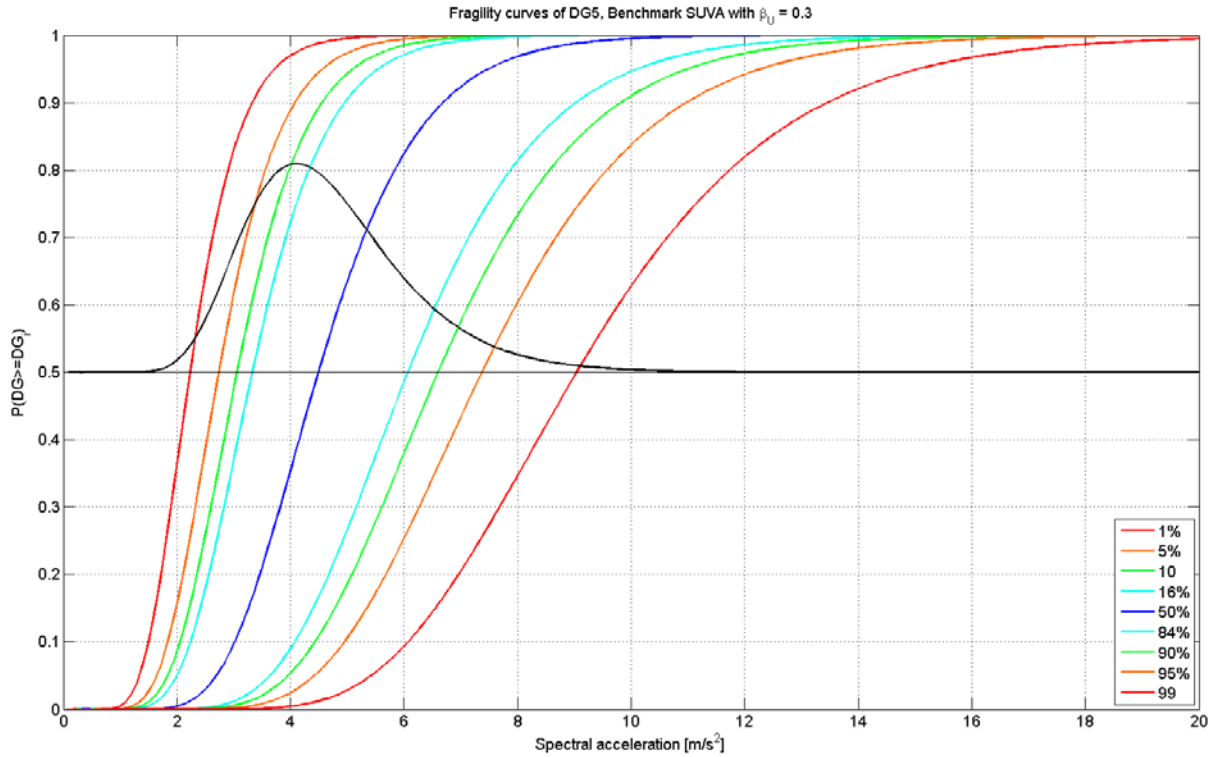

Figure 27: 1st to 99th percentile fragility curves of DG5 for SUVA (assuming a model uncertainty of 0.3)

Table 14: Compliance factors for SUVA

SUVA	**Sa(1 Hz) [m/s^2]**	**$\alpha_{def,EC8}$**	**$\alpha_{def,SIAD0237}$**	**$\alpha_{force,\ I}$**	**T_c [s]**	**$\alpha_{force,\ R}$**
Basel SED 2011	1.20					
Basel SED Micro.					0.60	
Basel SIA 261 BGK C	2.24	0.59		0.11	0.60	
Sion OT SED 2011	0.60					
Sion OT Rés Micro.	3.88	0.34		0.06	0.80	
Sion OT SIA 261 BGK C	2.76	0.48		0.09	0.60	
Sion TE SED 2011	1.35					
Sion TE Rés Micro.	3.69	0.36		0.07	0.75	
Sion TE SIA 261 BGK D	4.32	0.31		0.06	0.80	
Zurich SED 2011	0.40					
Zurich SED Micro.					0.40	
Zurich SIA 261 BGK A	0.60	2.21		0.41	0.40	

3.5.6 Benchmark STD40 ORG

The STD40 building is a 6-story structure with several masonry walls, two RC shear walls (one very short) and several concrete columns. The concrete and masonry walls in the façade are missing in first floor. Decks are RC slabs. The building is ca. 20 m long, 14 m wide and 25 m high. The first floor is considerably softer than other floors (Figure 28).

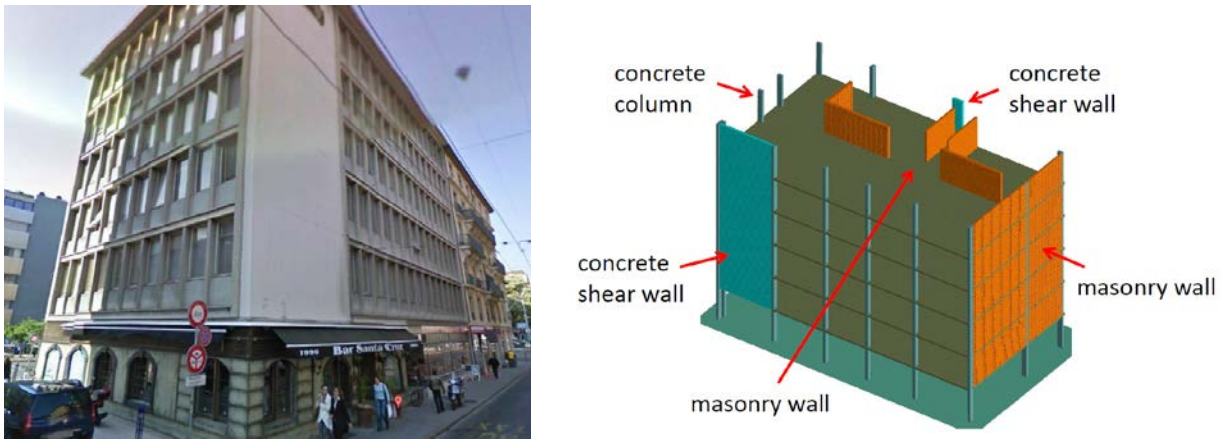

Figure 28: Benchmark STD40 ORG, left: google map street view, right: computer model [IMAC, 2014]

Table 15: Structural characteristics of the benchmark STD40 ORG

1st mode frequency FE-model (transverse)*	0.8 Hz (1.29 s)
1st mode frequency engineering model	1.4 Hz (0.7 s)
Masonry compressive strength (normal to bed joints)	10 N/mm^2
Masonry tensile strength	1.0 N/mm^2
Concrete compressive strength	30 N/mm^2

* Used for the risk analysis

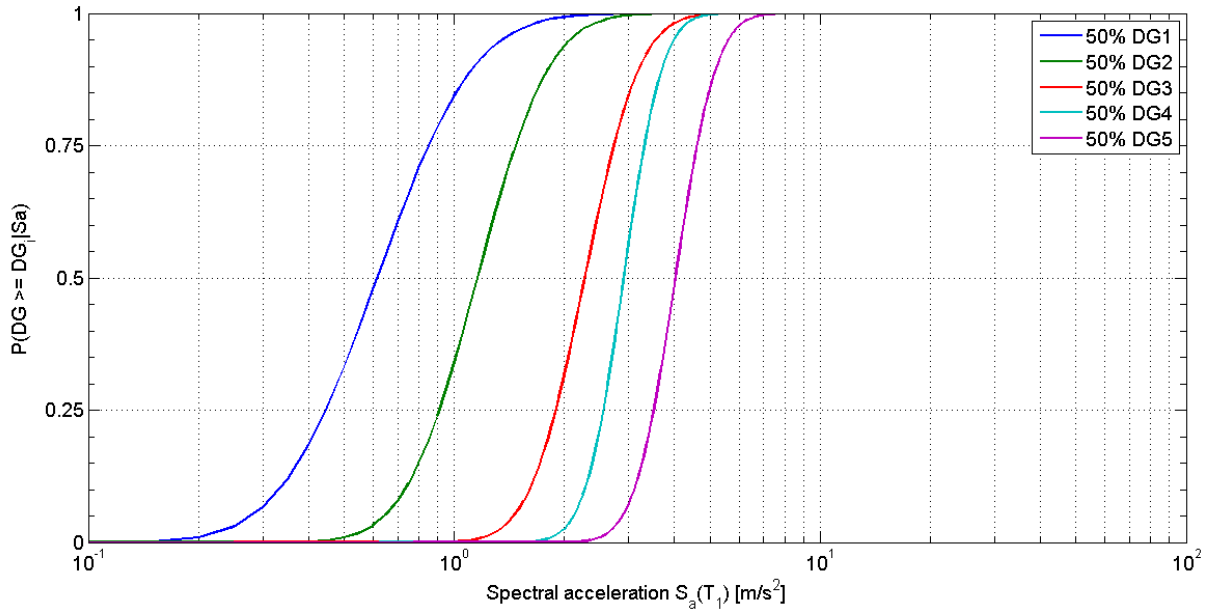

Figure 29: Benchmark STD40 ORG fragility curves of DG1 to DG5 (median curves)

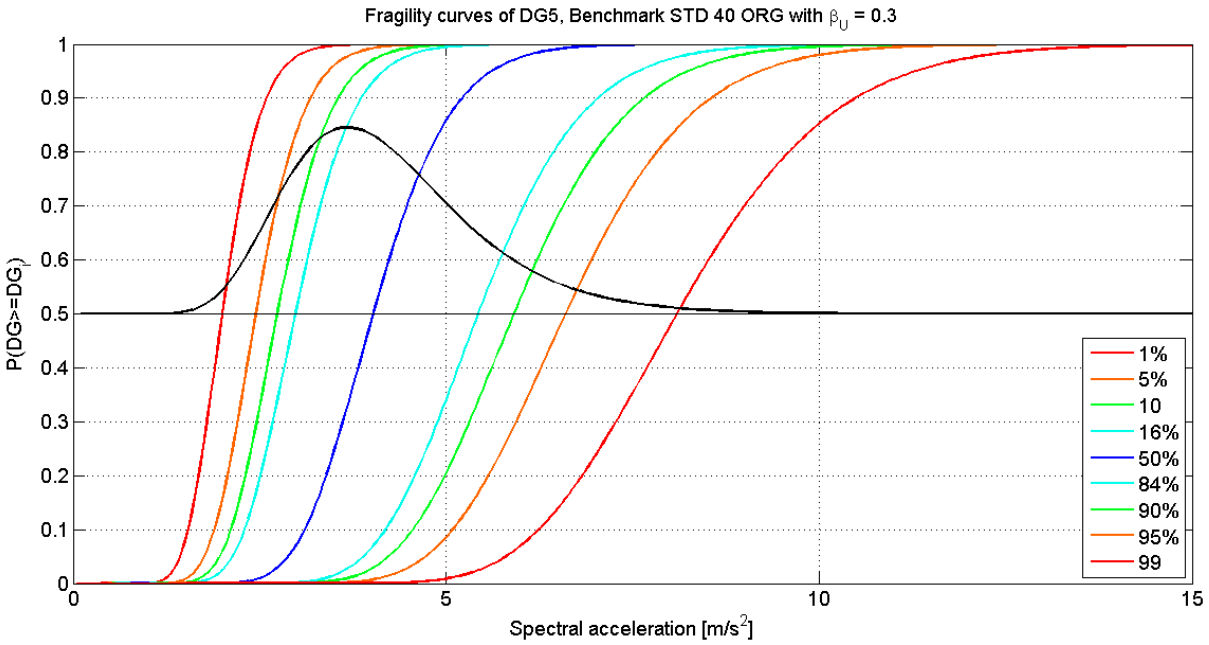

Figure 30: 1st to 99th percentile fragility curves of DG5 for STD40 ORG (assuming a model uncertainty of 0.3)

Table 16: Compliance factors for STD40 ORG

STD40 ORG	**Sa(1.4 Hz) [m/s^2]**	**$\alpha_{def,EC8}$**	**$\alpha_{def,SIAD0237}$**	**$\alpha_{force,\ I}$**	**T_c [s]**	**$\alpha_{force,\ R}$**
Basel SED 2011	1.66					
Basel SED Micro.					0.60	
Basel SIA 261 BGK C	3.14	0.34		0.37	0.60	
Sion OT SED 2011	0.78	1.26		1.50	0.60	
Sion OT Rés Micro.	5.40	0.18		0.22	0.80	
Sion OT SIA 261 BGK C	3.86	0.28		0.30	0.60	
Sion TE SED 2011	1.86	0.77		0.63	0.80	
Sion TE Rés Micro.	4.60	0.23		0.25	0.75	
Sion TE SIA 261 BGK D	5.40	0.18		0.22	0.80	
Zurich SED 2011	0.55	1.69		2.13	0.40	
Zurich SED Micro.					0.40	
Zurich SIA 261 BGK A	0.84	1.18		1.39	0.40	

3.5.7 Benchmark STD40

This benchmark is the retrofitted benchmark STD40 ORG with concrete and masonry walls, all continuing in the first floor (fictive retrofit).

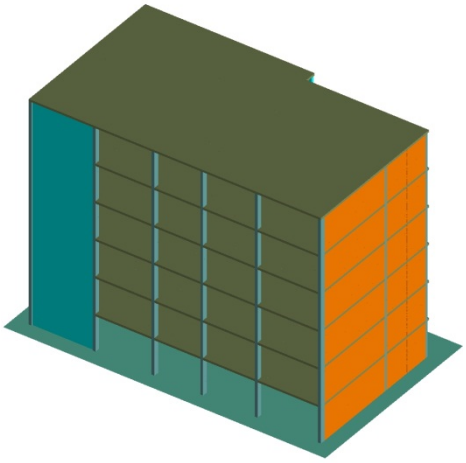

Figure 31: Benchmark STD40 computer model [IMAC, 2014]

Table 17: Structural characteristics of the benchmark STD40

1st mode frequency (transvers) FE-model*	0.7 Hz (1.37 s)
1st mode frequency engineering model	2.0 Hz (0.5 s)
Masonry compressive strength (normal to bed joints)	10 N/mm^2
Masonry tensile strength	1.0 N/mm^2
Concrete compressive strength	30 N/mm^2

* Used for the risk analysis

Table 18: Compliance factors for STD40

STD40	**Sa(2 Hz) [m/s^2]**	$\alpha_{def,EC8}$	$\alpha_{def,SIAD0237}$	$\alpha_{force,\ I}$	T_c **[s]**	$\alpha_{force,\ R}$
Basel SED 2011	2.06					
Basel SED Micro.						
Basel SIA 261 BGK C	3.74	0.63		0.47		
Sion OT SED 2011	2.19					
Sion OT Rés Micro.	5.40	0.36		0.27	0.80	
Sion OT SIA 261 BGK C	4.60	0.51		0.38		
Sion TE SED 2011	2.01					
Sion TE Rés Micro.	4.60	0.38		0.28	0.75	
Sion TE SIA 261 BGK D	5.40	0.33		0.24		
Zurich SED 2011	0.93					
Zurich SED Micro.						
Zurich SIA 261 BGK A	1.00	2.35		1.75		

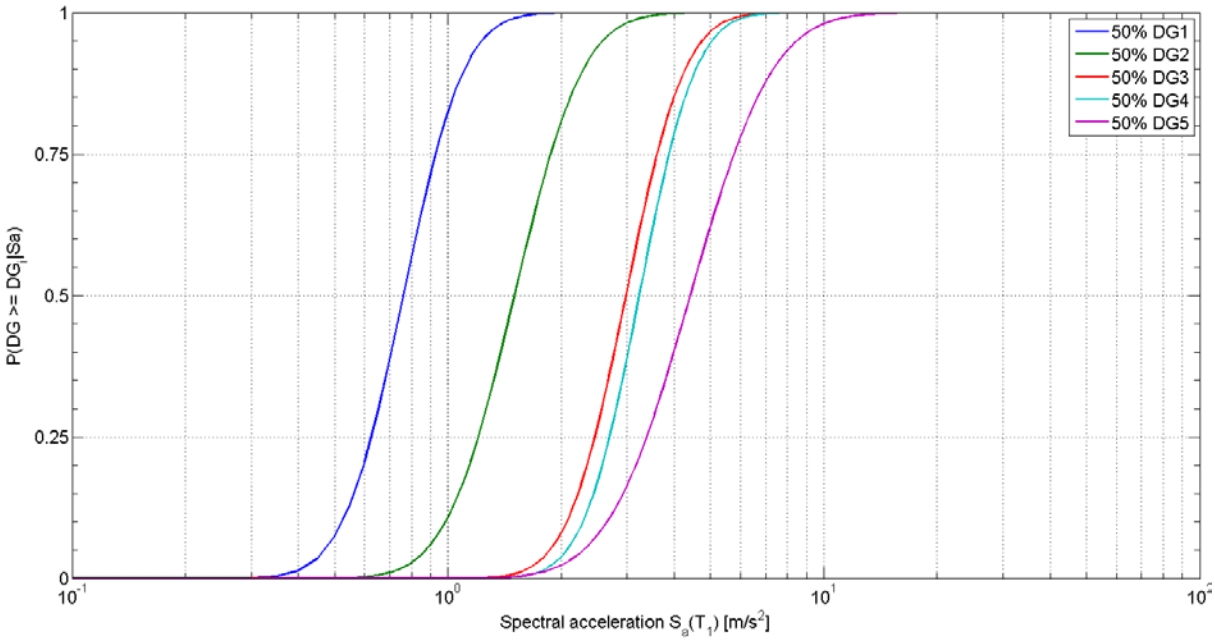

Figure 32: Benchmark STD40 fragility curves of DG1 to DG5 (median curves)

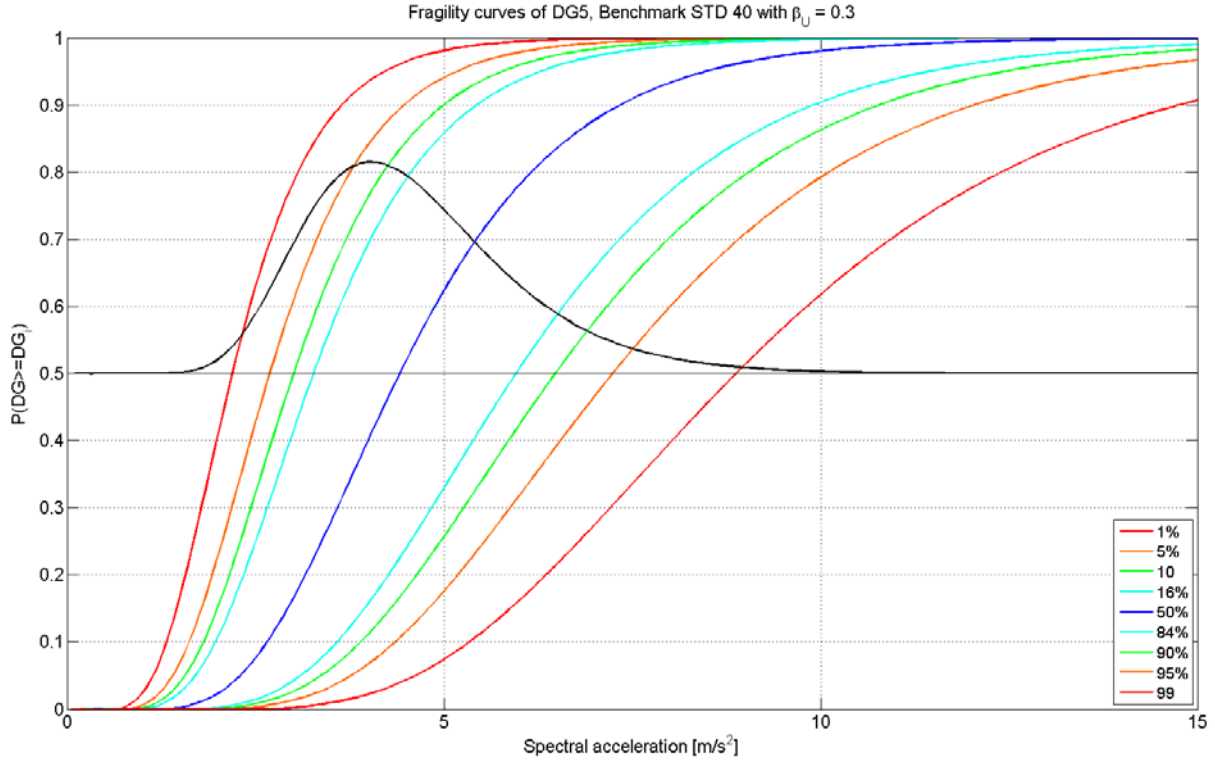

Figure 33: 1st to 99th percentile fragility curves of DG5 for STD40 (assuming a model uncertainty of 0.3)

3.6 Structural fragility function in terms of EMS-Intensity

Fragility curves based on EMS-Intensity are proposed in the Risk-UE project [Risk-UE, 2003 & Lagomarsino and Giovinazzi, 2006]. To compute fragility curves a binomial distribution function has been used [Koelz and Buerge, 2001] instead of the continuous beta distribution function suggested in Risk-UE project. Fragility curves are computed in 3 steps:

– Selection of an appropriate vulnerability class based on [EMS-98] documentation. Through considering behaviour modifiers (ΔV_m) the vulnerability index is modified.
– Calculation of the mean damage ratio as a function of EMS-Intensity and vulnerability index.
– Calculation of damage grades for the selected intensity range assuming a binomial distribution function:

$$PDF(i) = \frac{5!}{k!\,(5-k)!}\left(\frac{\mu_D(I)}{5}\right)^k\left(1-\frac{\mu_D(I)}{5}\right)^{5-k}$$

$$\mu_D = 2.5\left[1+\tanh\left(\frac{I+6.25\bar{V}_I-13.1}{2.3}\right)\right]$$

where μ_D is the mean damage grade, k is the damage grade and I is the EMS-Intensity.

3.6.1 Benchmark YVR14

Structural characteristics of the benchmark YVR14 are already documented in Table 5. The benchmark can be best categorized in class M6 (Unreinforced masonry with RC-floors) [Lagomarsino and Giovinazzi, 2006].

Table 19: Computation of the vulnerability index Benchmark YVR14

Building type:	**Unreinforced masonry with RC-floors (M6) [Lagomarsino and Giovinazzi, 2006]**	
V_I^*:		+0.62
ΔV_m :	Good maintenance	-0.04
	Number of floors	+0.02
	Good connection of walls	-0.02
$\bar{V}_I$:		+0.58

V_I^*: Most probable value of the vulnerability index

ΔV_m : Behavior modifier

$\bar{V}_I$: Total vulnerability index

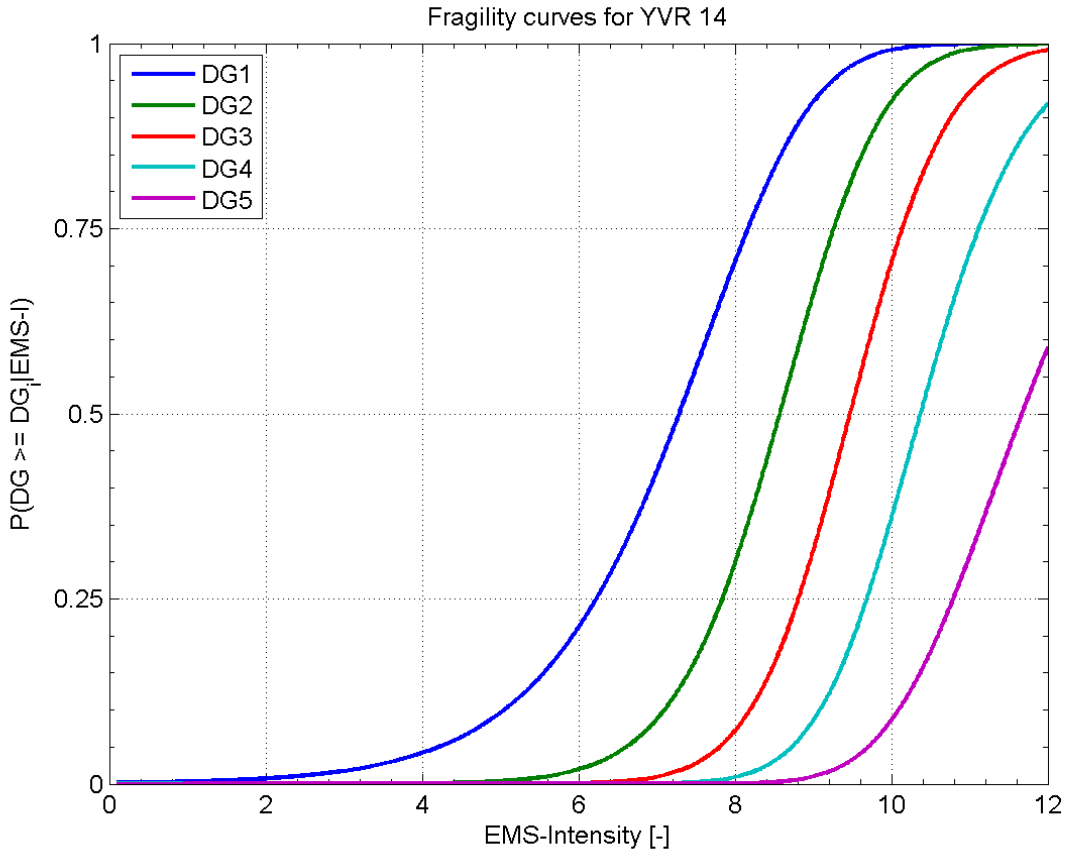

Figure 34: Benchmark YVR14 fragility curves of DG1 to DG5 (best estimate curves)

3.6.2 Benchmark CHB30

Structural characteristics of the benchmark CHB30 are already documented in Table 7. The benchmark can be best categorized in in class M6 (Unreinforced masonry with RC-floors) [Lagomarsino and Giovinazzi, 2006].

Table 20: Computation of the vulnerability index Benchmark CHB30

Building type:	**Unreinforced masonry with RC-floors (M6) [Lagomarsino and Giovinazzi, 2006]**	
V_I^*:		+0.62
ΔV_m :	Good maintenance	-0.04
	Number of floors	+0.06
	Thick walls	-0.02
$\bar{V}_I$:		+0.62

V_I^*: Most probable value of the vulnerability index

ΔV_m : Behavior modifier

$\bar{V}_I$: Total vulnerability index

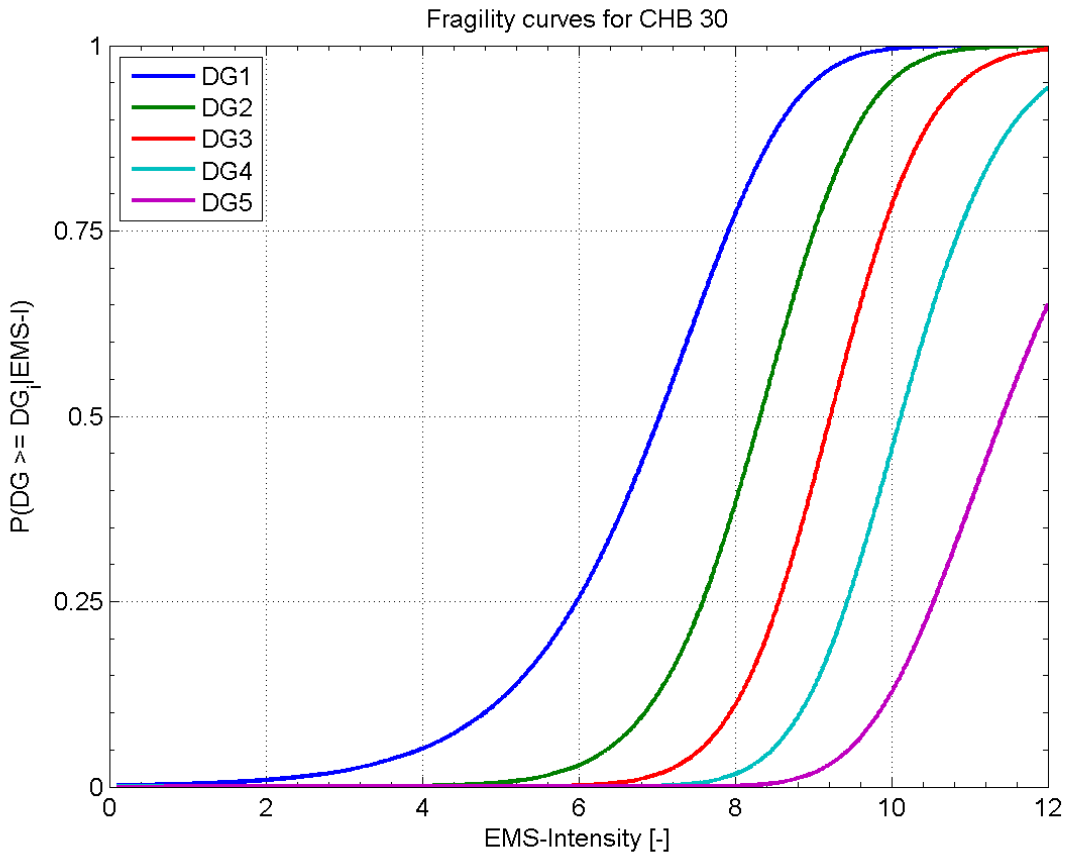

Figure 35: Benchmark CHB30 fragility curves of DG1 to DG5 (best estimate curves)

3.6.3 Benchmark CHB30 ORG

Structural characteristics of the benchmark CHB30 ORG are already documented in Table 9. The benchmark can be best categorized in in class M5 (Unreinforced masonry with old bricks) [Lagomarsino and Giovinazzi, 2006].

Table 21: Computation of the vulnerability index Benchmark CHB30 ORG

Building type:	**Simple stone (M3) [Lagomarsino and Giovinazzi, 2006]**	
V_I^*:		+0.74
ΔV_m :	Number of floors	+0.06
	Thick walls	-0.02
$\overline{V}_I$:		+0.78

V_I^*: Most probable value of the vulnerability index

ΔV_m : Behavior modifier

$\overline{V}_I$: Total vulnerability index

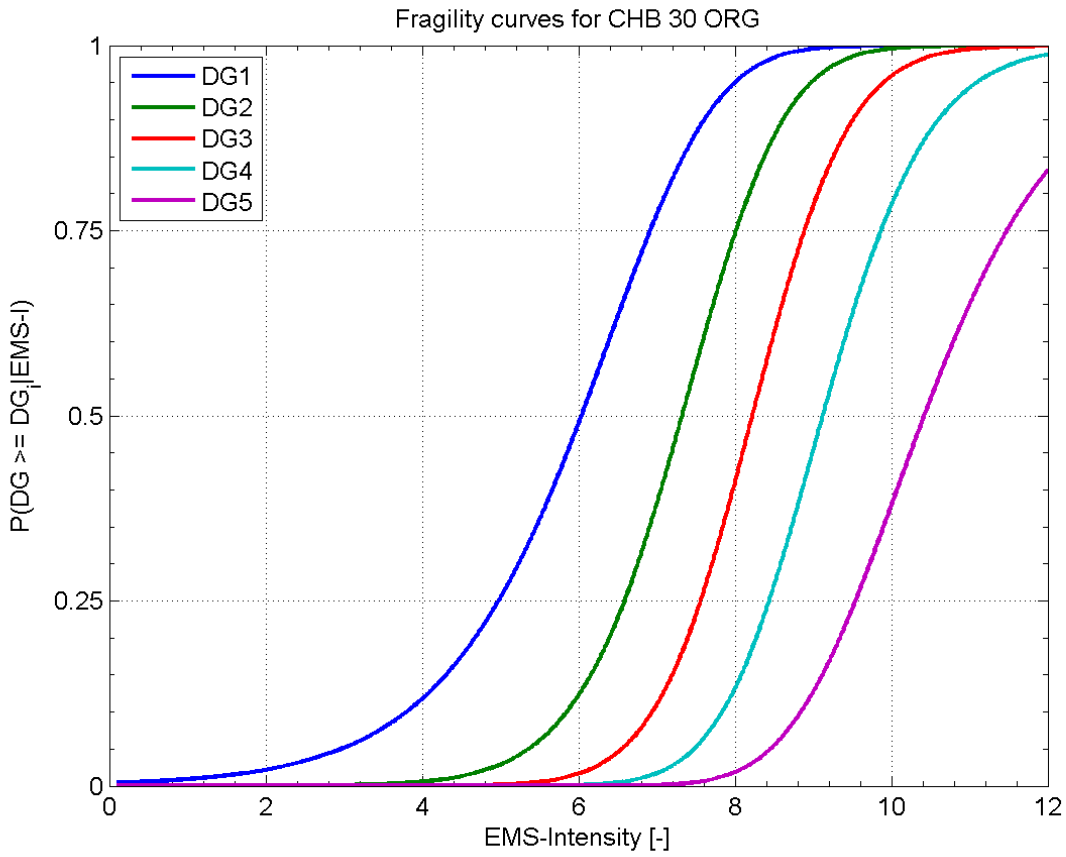

Figure 36: Benchmark CHB30 ORG fragility curves of DG1 to DG5 (best estimate curves)

3.6.4 Benchmark SECH7

Structural characteristics of the benchmark SECH7 are already documented in Table 11. The benchmark can be best categorized in in class M6 (Unreinforced masonry with RC-floors) [Lagomarsino and Giovinazzi, 2006].

Table 22: Computation of the vulnerability index Benchmark SECH7

Building type:	**Unreinforced masonry with RC-floors (M6) [Lagomarsino and Giovinazzi, 2006]**	
V_I^*:		+0.62
ΔV_m :	Number of floors	+0.06
$\overline{V}_I$:		+0.68

V_I^*: Most probable value of the vulnerability index

ΔV_m : Behavior modifier

$\overline{V}_I$: Total vulnerability index

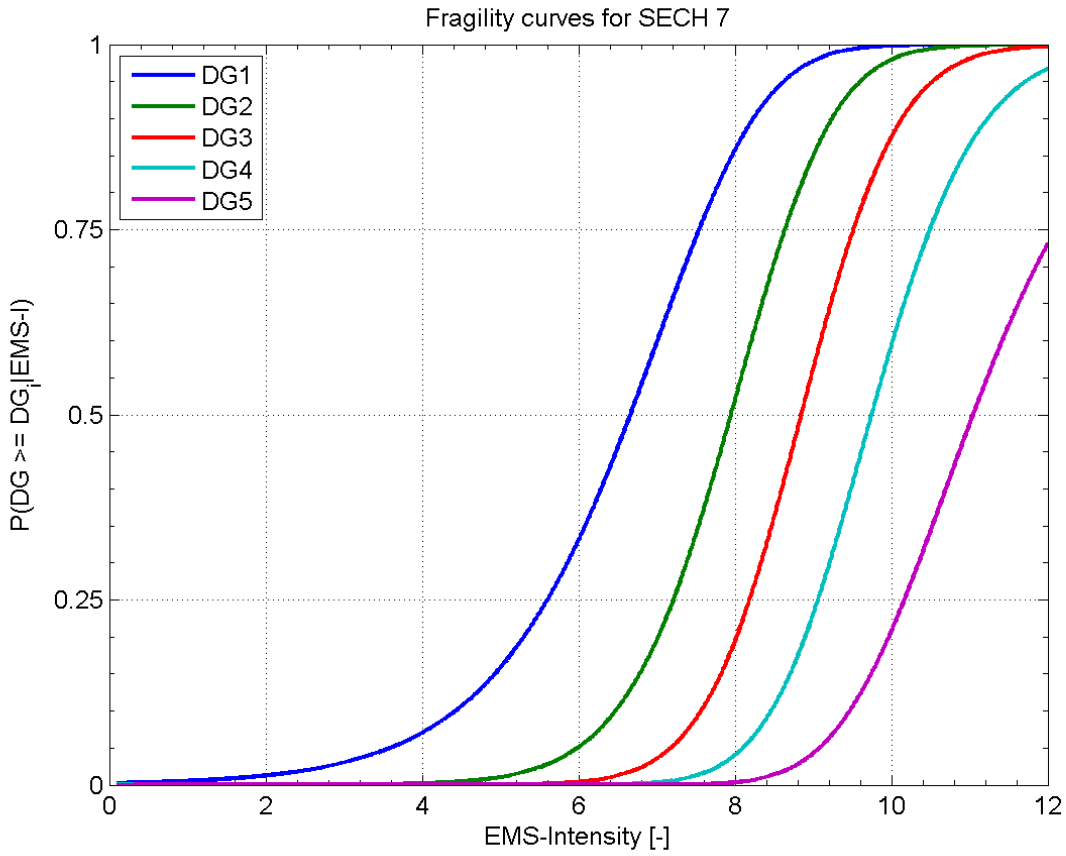

Figure 37: Benchmark SECH7 fragility curves of DG1 to DG5 (best estimate curves)

3.6.5 Benchmark SUVA

Structural characteristics of the benchmark SUVA are already documented in Table 13. The benchmark can be best categorized in in class RC2 (shear walls without Engineering Resistant Design) [Lagomarsino and Giovinazzi, 2006].

Table 23: Computation of the vulnerability index Benchmark SUVA

Building type:	**Shear walls without ERD (RC2) [Lagomarsino and Giovinazzi, 2006]**	
V_I^*:		+0.55
ΔV_m :	Number of floors	+0.10
	Vertical irregularity + Soft story	+0.10
$\overline{V}_I$:		+0.75

V_I^*: Most probable value of the vulnerability index

ΔV_m : Behavior modifier

$\overline{V}_I$: Total vulnerability index

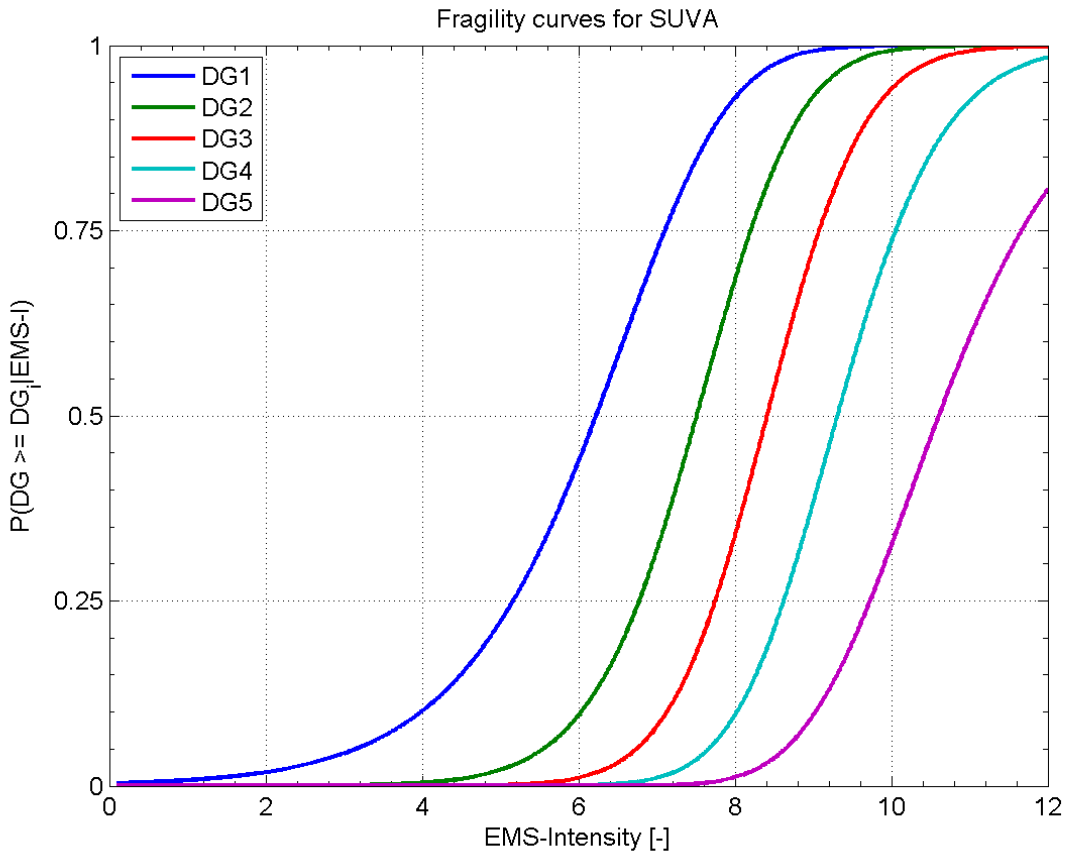

Figure 38: Benchmark SUVA fragility curves of DG1 to DG5 (best estimate curves)

3.6.6 Benchmark STD40 ORG

Structural characteristics of the benchmark STD40 ORG are already documented in Table 15. The benchmark can be best categorized in class M6 (Unreinforced masonry with RC-floors) [Lagomarsino and Giovinazzi, 2006].

Table 24: Computation of the vulnerability index Benchmark STD40 ORG

Building type:	**Unreinforced masonry with RC-floors (M6) [Lagomarsino and Giovinazzi, 2006]**	
V_I^*:		+0.62
ΔV_m :	Number of floors	+0.06
	Vertical irregularity + Soft story	+0.10
$\overline{V}_I$:		+0.78

V_I^*: Most probable value of the vulnerability index

ΔV_m : Behavior modifier

$\overline{V}_I$: Total vulnerability index

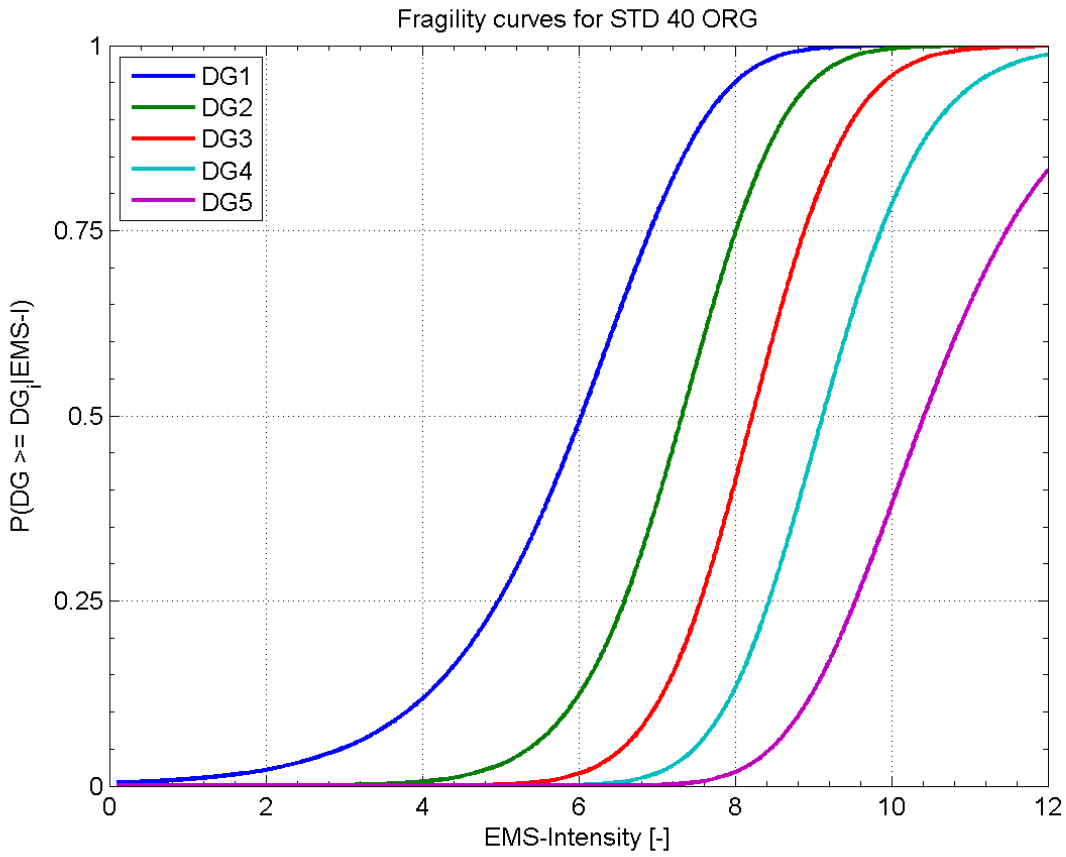

Figure 39: Benchmark STD40 ORG fragility curves of DG1 to DG5 (best estimate curves)

3.6.7 Benchmark STD40

Structural characteristics of the benchmark STD40 ORG are already documented in Table 17. The benchmark can be best categorized in class M6 (Unreinforced masonry with RC-floors) [Lagomarsino and Giovinazzi, 2006].

Table 25: Computation of the vulnerability index Benchmark STD40

Building type:	**Unreinforced masonry with RC-floors (M6) [Lagomarsino and Giovinazzi, 2006]**	
V_I^*:		+0.62
ΔV_m :	Number of floors	+0.06
$\bar{V}_I$:		+0.68

V_I^*: Most probable value of the vulnerability index

ΔV_m : Behavior modifier

$\bar{V}_I$: Total vulnerability index

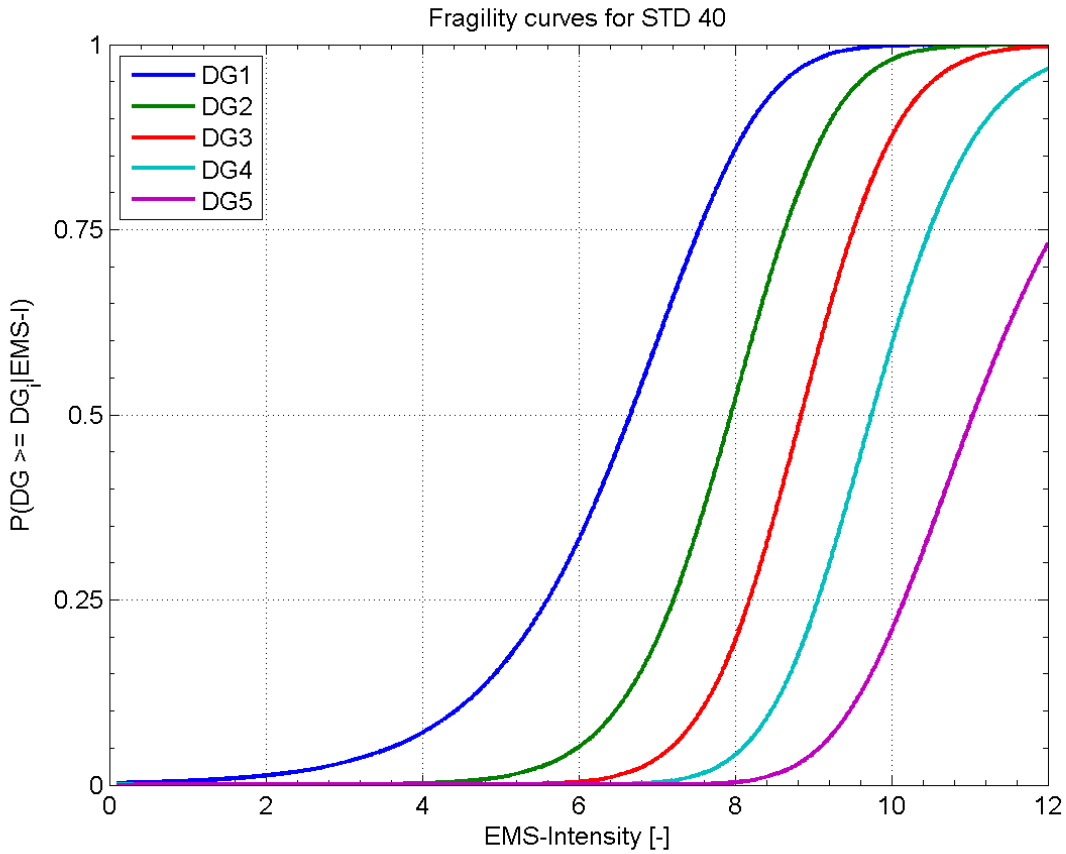

Figure 40: Benchmark STD40 fragility curves of DG1 to DG5 (best estimate curves)

4 Consequences

4.1 Introduction

In this project unit casualty risk and unit property risk directly caused by structural damage are considered. Collateral or indirect damages, as for example damages because of fire, ground failure, or due to the loss of function, are not covered.

Consequences are linked to vulnerability by the help of damage grades (Table 4) as they are defined in [EMS, 1998].

No variability has been considered for the damage grade dependant consequences. The given ratios are considered to be expected values. Such variability could be easily introduced for the damage grade dependent consequences. Because these consequences are modelled as ratios, they could be modelled as uncertain quantities by the help of discrete or continuous probability distribution with arguments in the range between zero and one. In case of the casualty rate the results are more or less linear proportional to the adopted values for the casualty rate.

4.2 Casualties

Numerous factors govern the casualty rate in an earthquake. In this study the focus is laid on the direct casualty risk related to the structural failure and neglect secondary hazards as for example tsunamis, earthquake-related fires and landslides. Besides, other factors affecting death toll as slowness of search, treatment and rescue program are not covered here.

From the structural point of view there are several parameters that may affect the casualty rate in a building, e.g.:

– Building type
– Detailing
– Construction method
– Workmanship

The major primary cause of death in an earthquake is total or partial building collapse. Because of this, damage grades 4 and 5 are considered to contribute to the casualty risk. Given a certain earthquake, the probability of extensive structural damage and collapse is a function of the structural behaviour, which can roughly be associated to certain building types [Jaiswal et al., 2011; Spence, 2011]. In Table 26 casualty rates of different building types are given. They can be compared with those given in Hazus (Table 27).

Table 26: Casualty rate as a function of the building type [Jaiswal et al., 2011]

Building type	Casualty rate
Brick masonry with lime/cement mortar	0.06
Rubble or field stone masonry	0.06
Block or dressed stone masonry	0.08
Adobe building	0.06
Mud wall building	0.06
Non-ductile concrete moment frame	0.15
Steel moment frame with concrete infill wall	0.14

Table 27: Casualty matrix pertinent to vulnerability classes A and B based on HAZUS casualty rates for unreinforced masonry building type [Hazus, 2003]

Damage state	Casualty rate
Complete structural damage with collapse (URMM and URML)	0.10

Studies done by Jaiswal et al. seem to be more consistent with EMS definition of damage grades. A casualty rate of 2% for DG4 (extensive structural damage) and 10% for DG5 (collapse) will be applied:

$$P(CR|DG4) = 0.02 \quad (4.1)$$

$$P(CR|DG5) = 0.10 \quad (4.2)$$

However, it must be noted that generally proposing reasonable values of casualty rates (CR) conditioned on damage grade is a very challenging task. Particularly for damage grade 4 there are very few references to CR in the literature.

4.3 Direct property loss

To investigate the direct property loss rate of a structure in this study the expected monetary loss is related to the structural damage with empirical relationships. With this aim the damage ratio is defined as a function of damage grade as:

$$Damage\ Ratio = f(DG_{EMS}) = \frac{Cost\ of\ repair}{Replacement\ cost} \quad (4.3)$$

Ranges of damage ratios for all damage grades are given in Table 28 [ATC 13, 1985; Tyagunov, 2004]. For each range a mean damage ratio representing the range is also given.

Table 28: Mean damage ratio [Tyagunov, 2004]

Classification of damage	Damage ratio [%]	Mean damage ratio [%]
Damage grade 0: No damage	0	0
Damage grade 1: Negligible to slight damage (no structural damage, slight non-structural damage)	0 – 1	0.5
Damage grade 2: Moderate damage (slight structural damage, moderate non-structural damage)	1 – 20	10
Damage grade 3: Substantial to heavy damage (moderate structural damage, heavy non-structural damage)	20 – 60	40
Damage grade 4: Very heavy damage (heavy structural damage, very heavy non-structural damage)	60 – 100	80
Damage grade 5: Destruction (very heavy structural damage)	100	100

Actually, the mean damage ratio is not only a function of damage grade, but also of several other parameters as for example economic condition of the studied region or country. In a country with a stronger economy, the social acceptance to repair a badly damaged structure is much lower in comparison to another country, where there are considerably fewer resources available for the replacement of damaged structures. Because of this, the SIA 269/8 working group preliminarily defined the values given in Table 29 for Switzerland:

Table 29: Mean damage ratio (as suggested by working group SIA 269/8)

Classification of damage	**Mean damage ratio [%]**
Damage grade 0: No damage	0
Damage grade 1: Negligible to slight damage (no structural damage, slight non-structural damage)	1
Damage grade 2: Moderate damage (slight structural damage, moderate non-structural damage)	40
Damage grade 3: Substantial to heavy damage (moderate structural damage, heavy non-structural damage)	80
Damage grade 4: Very heavy damage (heavy structural damage, very heavy non-structural damage)	100
Damage grade 5: Destruction (very heavy structural damage)	100

5 Risk Computation Framework

5.1 Spectral-acceleration-based Risk assessment model

The total risk of casualty and damage caused by earthquakes is a function of the seismic hazard (including site effects), vulnerability of the affected buildings and assets (fragility) and the consequences of their failure or destruction (loss of life and financial loss).

$$Risk = Hazard\ x\ Vulnerability\ x\ Consequences \quad (5.1)$$

All these components have been already introduced in former chapters. The same framework for risk assessment is applied for both spectral-acceleration (Sa-based) and intensity-based risk assessments. In section 5.1 relations for the Sa-based framework are given. Relations for Intensity-based framework are given in section 5.3.

For simplicity the whole range of the possible seismic actions has been discretized into several events. Each event represents a specific return period. The total seismic risk can be computed as:

$$R = \sum_{i=1}^{n} R_i \quad (5.2)$$

in which R_i is the seismic risk related to the seismic event *i* with a return period T_i. R_i can be computed as:

$$R_i = P_i C_i \quad (5.3)$$

in which P_i is the probability that event *i* happens and C_i is the consequence of this event (including vulnerability). P_i and C_i are computed as follows:

$$P_i = P(Sa|T_i) = \Delta H(Sa) = H(sa_i) - H(sa_{i+1}) = PDF(sa_i)(sa_{i+1} - sa_i) \quad \textit{(Figure 41)} \quad (5.4)$$

$$C_i = \sum_{dg=0}^{dg=5} P(DG = dg|Sa(T_i))\, c(DG = dg) \quad (5.5)$$

in which *c(DG)* is the loss ratio (casualty rate and damage ratio, see chapter 4). To compute C_i deterministic and probabilistic approaches have been used. In the deterministic approach for each event *i* single values for hazard and fragility have been used, e.g. mean, median or any other percentile of the variables. In probabilistic approach, however, a range of data considering the uncertainty of the variables has been used. For example in Figure 42 for the event *i* one may see the range of data (hazard and fragility) considered for the convolution.

Hence, the total loss is:

$$R = \sum_{i=1}^{n} P(Sa|T_i) \sum_{dg=0}^{dg=5} P(DG = dg|Sa(T_i))\, C(DG = dg) \quad (5.6)$$

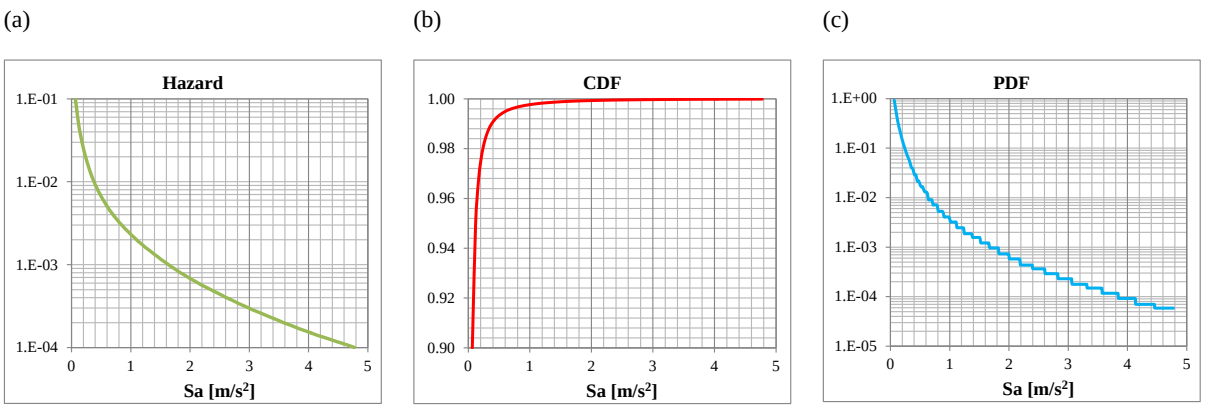

Figure 41: (a) Hazard, (b) cumulative distribution function and (c) probability density function of the seismic hazard for a site

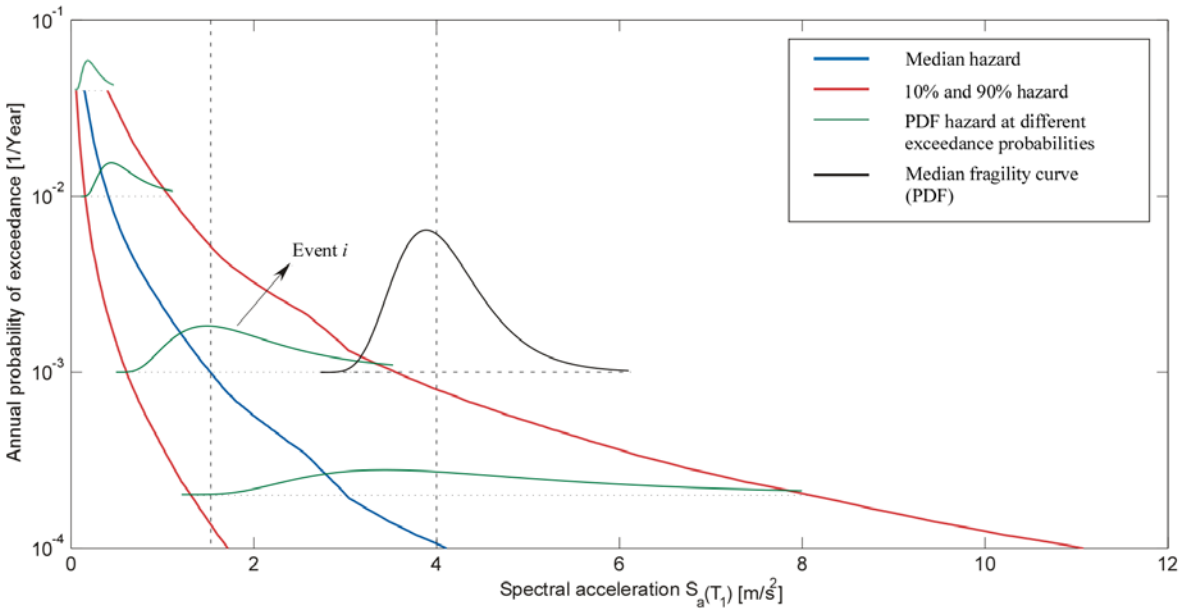

Figure 42: Median seismic hazard and its 10th and 90th percentiles of a site in combination with a fragility curve

5.2 Numerical application of the Sa-based framework

To show how the model works, the seismic risk value is computed for a benchmark. The studied benchmark is similar to the benchmark STD40 ORG (introduced in section 3.5.6). Note that there are some minor differences to the benchmark STD40 ORG. Both deterministic and probabilistic approaches are used to compute the casualty risk. In deterministic approach the median hazard and fragility curves will be used. In probabilistic approach the seismic hazard is considered on the whole range and truncated at 90th percentile value. For fragility, however, only the median curves are used.

Risk assessment is done in the following steps:

– The whole range of the possible seismic actions has been discretized into 400 events with return periods from 25 years to 10'000 years. Percentile hazard curves for Sion OT at surface at 1 Hz (1st mode of the building) are demonstrated in Figure 43. Median Hazard, CDF and PDF are demonstrated in Figure 44. Probability of occurrence (P_i) of events is demonstrated in Figure 45. For example the P_i for the event with a return period of 475 years is 1x10^{-4} (1/475 - 1/500).

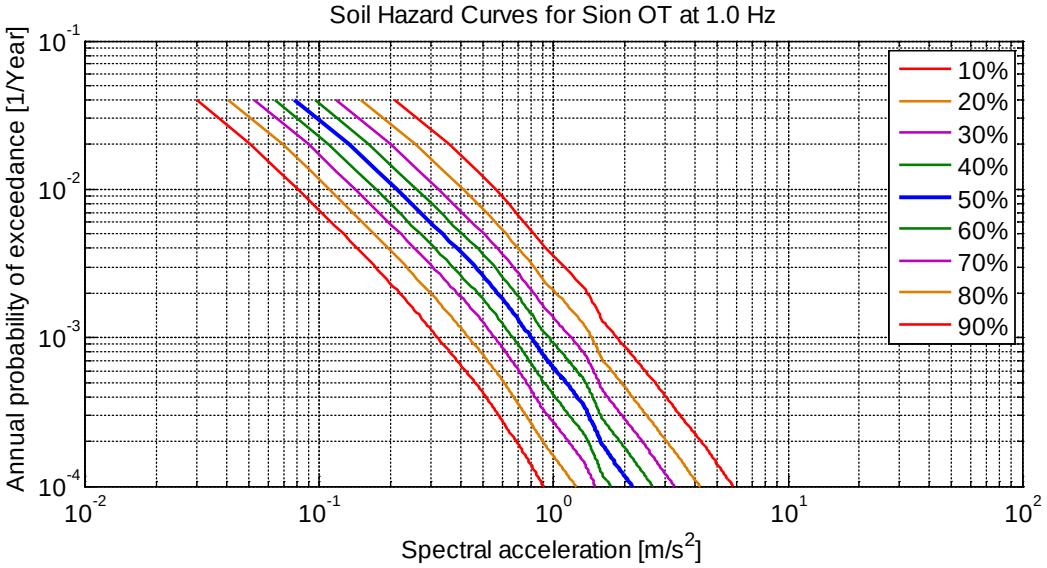

Figure 43: Hazard curve for Sion OT at surface at 1 Hz

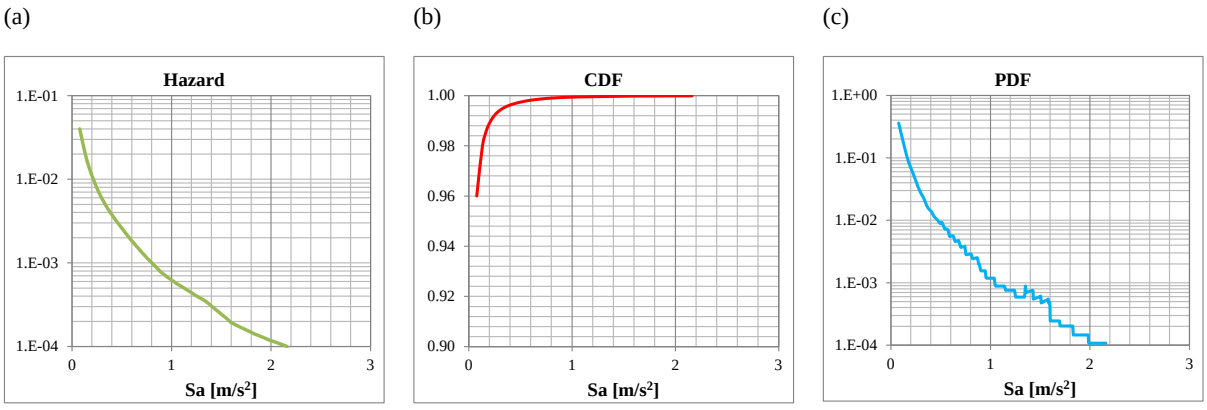

Figure 44: (a) Hazard, (b) cumulative distribution function and (c) probability density function of the seismic hazard at surface for Sion OT at 1 Hz

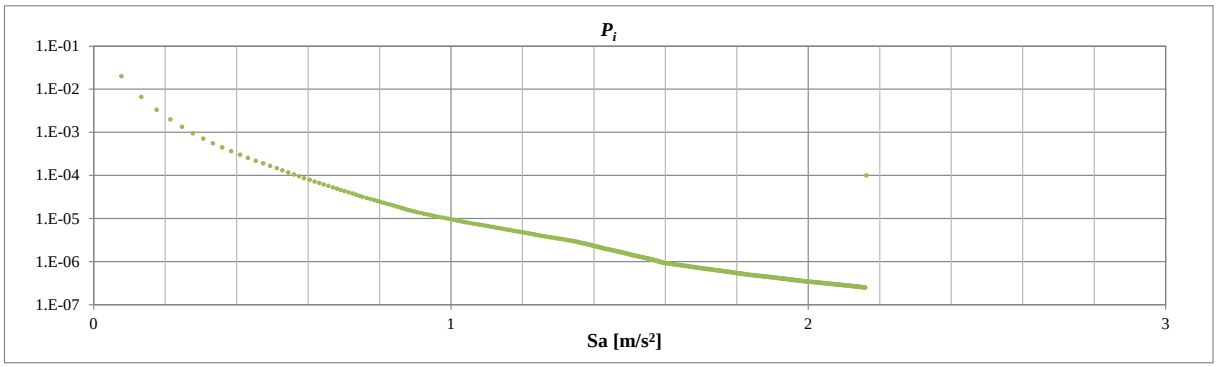

Figure 45: Probability of occurrence (P_i) of events

– To compute the consequences in deterministic approach for each event the median value of the spectral acceleration of the event is read. Then the fragilities (probabilities) of relevant damage grades at this spectral acceleration are read. For example for the event with a return period of 475 years the median spectral acceleration at surface is about 0.6 m/s^2. For loss of life only damage grades 4 and 5 are relevant. Probabilities that at spectral acceleration 0.6 m/s^2 damage grades 4 and 5 happen are $2x10^{-18}$ and $4x10^{-23}$, respectively. Noting that loss ratios (in this case casualty rates) are 0.02 and 0.10 for damage grades 4 and 5, respectively, C_i will be $4x10^{-20}$. Multiplying this with the probability of occurrence of this event the casualty risk for this event will be $4 x10^{-24}$. R_i values are given in Figure 46a.
– To compute the consequences in probabilistic approach for each event a distribution function is fitted for the hazard curve. At 90% probability the distribution function is truncated. Distribution functions for two events with return periods 475 and 2500 years are given in Figure 47. Performing a convolution of hazard and fragility for both damage grades 4 and 5, $P(DG = dg \mid Sa(T_i))$ are $4x10^{-8}$ and $2x10^{-11}$, respectively. Multiplying these values with loss ratios and summing them, the consequence C_i of this event will be $8x10^{-10}$ (several orders of magnitude larger than the value computed with the median hazard). Multiplying this with the probability of occurrence of this event the casualty risk for this event will be $8x10^{-14}$. R_i values are given in Figure 46b. Comparing Figure 46a with b, it is clear that in this case considering only median hazard value (ignoring uncertainty of hazard data) has led to underestimation of the total casualty risk.
– In both last two steps only median fragility curves have been used to compute the casualty risk. To demonstrate how model uncertainty affects the risk value, 16th and 84th percentile fragility curves have been used to compute again the casualty risk (only with probabilistic approach). R_i values are illustrated in Figure 48.

(a)

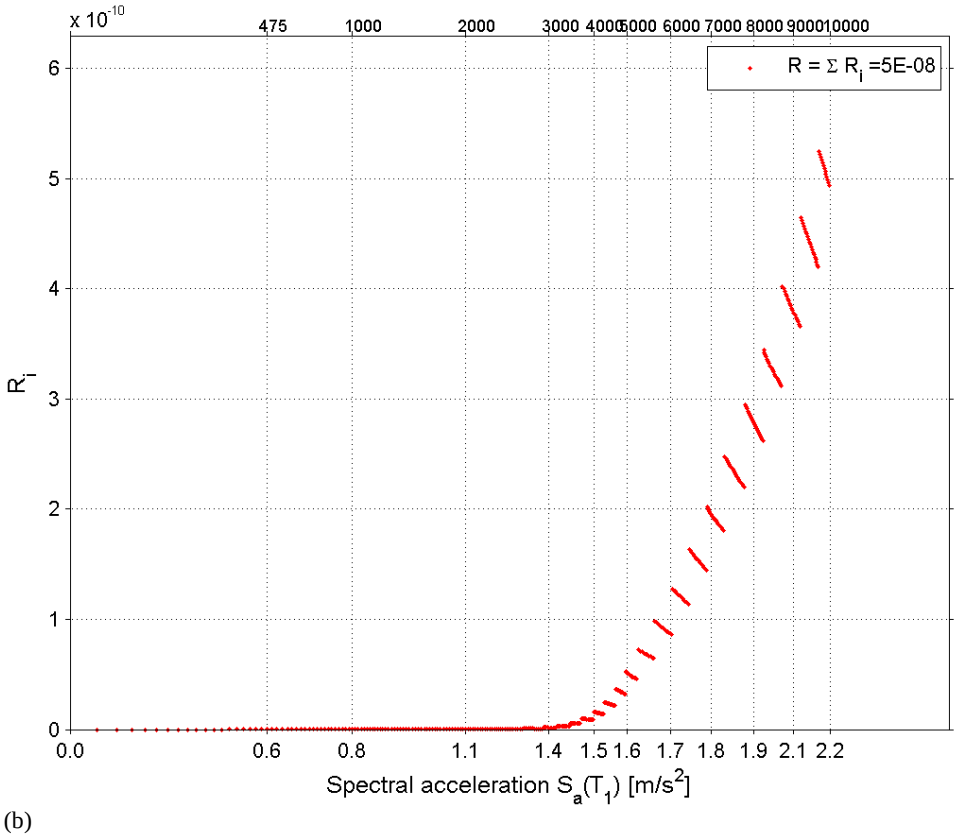

(b)

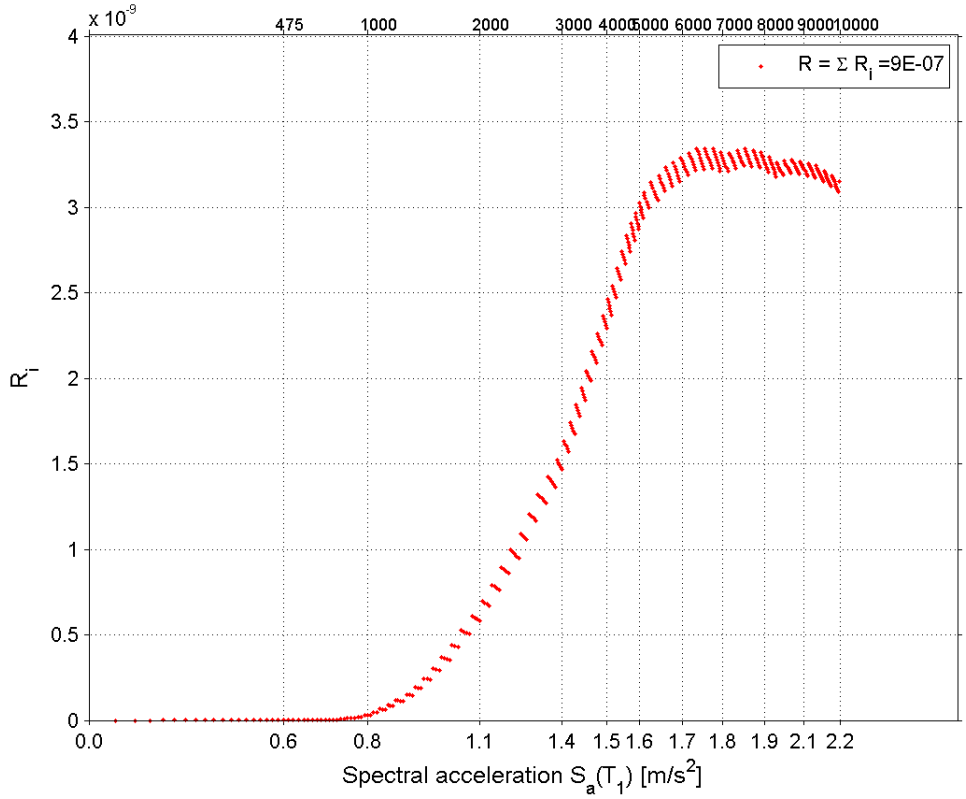

Figure 46: R_i values (a) using median hazard values only, (b) considering hazard distribution truncation at 90th percentile for the studied benchmark in Sion OT

(a)

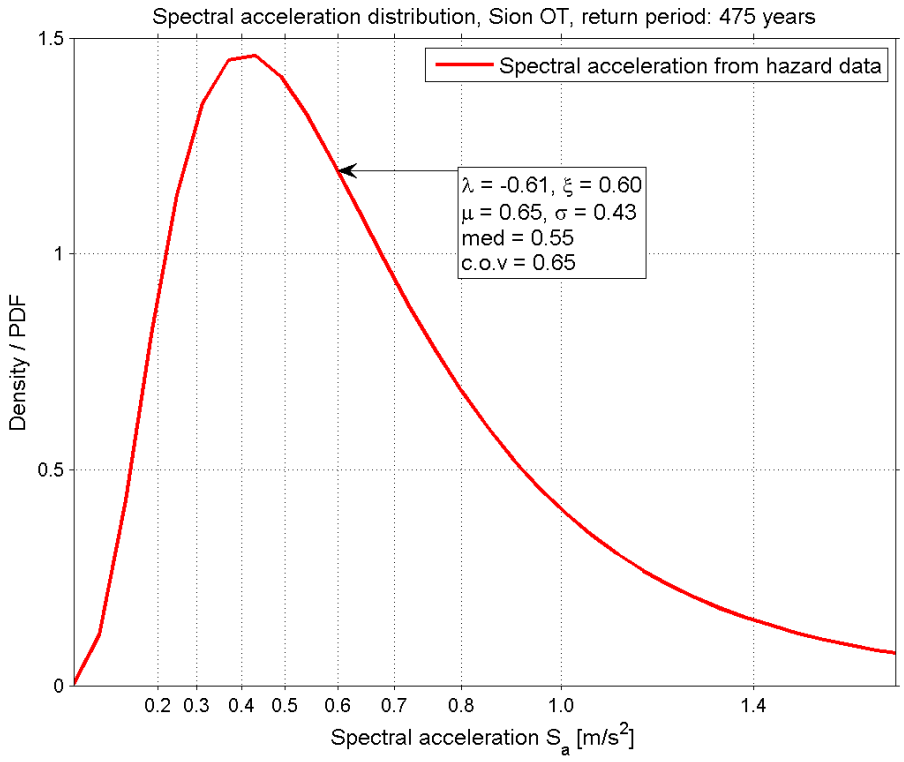

(b)

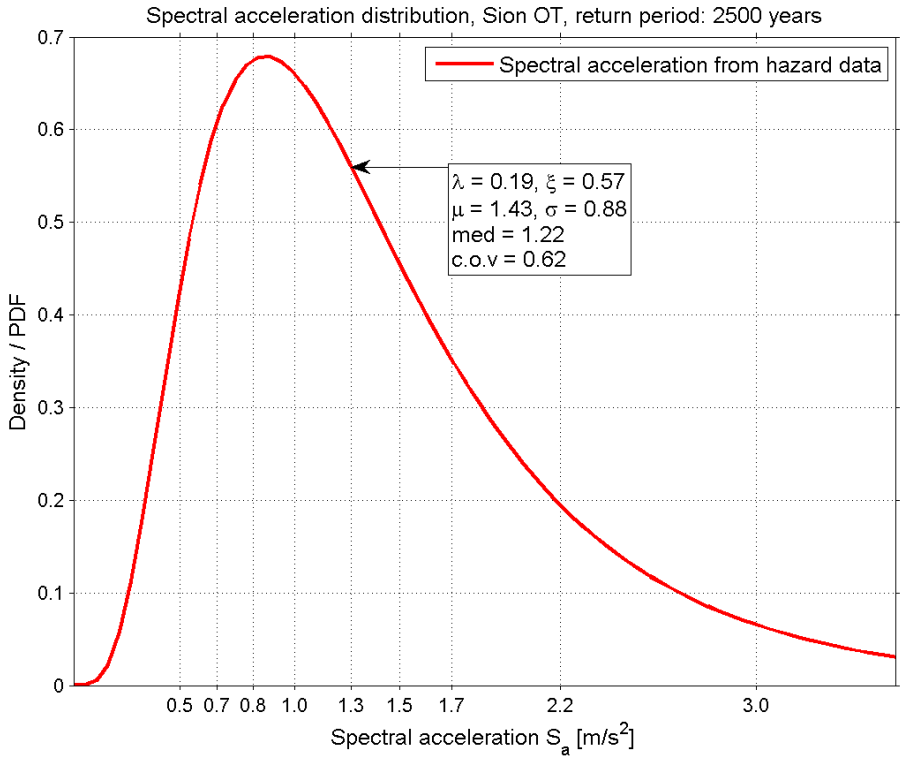

Figure 47: Probability distributions of events with return periods of (a) 475 years and (b) 2'500 years in terms of spectral acceleration for Sion OT at f = 1 Hz (Ticks on X-axis are giving 10^{th} to 90^{th} percentiles according to SED model).

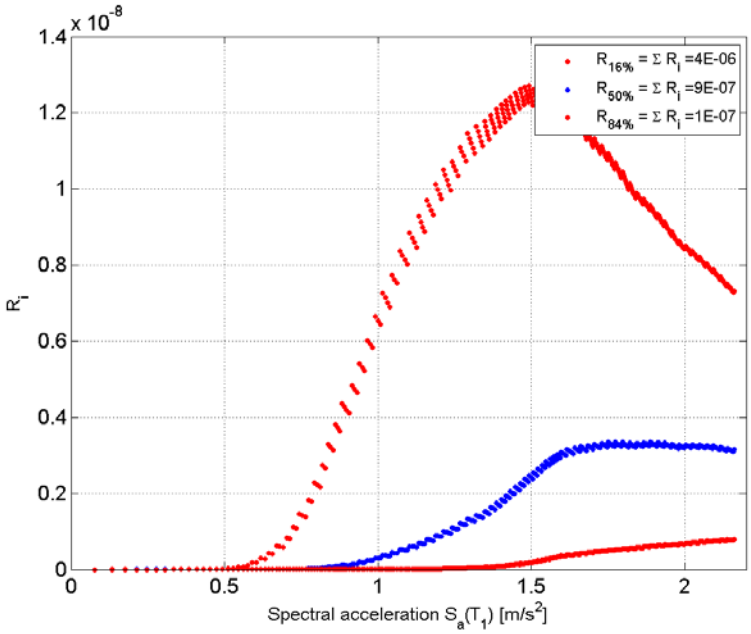

Figure 48: R_i values using 16th, 50th (median) and 84th percentile fragility curves for the studied benchmark in Sion OT

5.3 EMS-based risk assessment

The same framework introduced in 5.1 has been applied for EMS-based approach. In EMS-based approach hazard and fragility curves are given as a function of EMS-Intensity. In equations 5.4 to 5.6 spectral acceleration (Sa) is substituted with EMS-Intensity (I):

$$P_i = P(I|T_i) = \Delta H(I) = H(I_i) - H(I_{i+1}) = PDF(I_i)(I_{i+1} - I_i) \quad 5.7$$

$$C_i = \sum_{dg=0}^{dg=5} P(DG = dg|I(T_i))\, c(DG = dg) \quad 5.8$$

$$R = \sum_{i=1}^{n} P(I|T_i) \sum_{dg=0}^{dg=5} P(DG = dg|I(T_i))\, C(DG = dg) \quad 5.9$$

5.4 Numerical application of the EMS-based framework

Benchmark STD40 ORG (introduced in section 3.6.6) located in the site Sion OT is selected to show how the model works. Only deterministic approach is used to compute the casualty risk.

Risk assessment is done in the following steps:

– The whole range of the possible seismic actions has been discretized into 400 events with return periods from 25 years to 10'000 years. Percentile hazard curves for Sion OT are demonstrated in Figure 49. Median Hazard, CDF and PDF are demonstrated in Figure 50. Probability of occurrence (P_i) of events is demonstrated in Figure 51. For example the P_i for the event with a return period of 475 years is 1x10^{-4}.

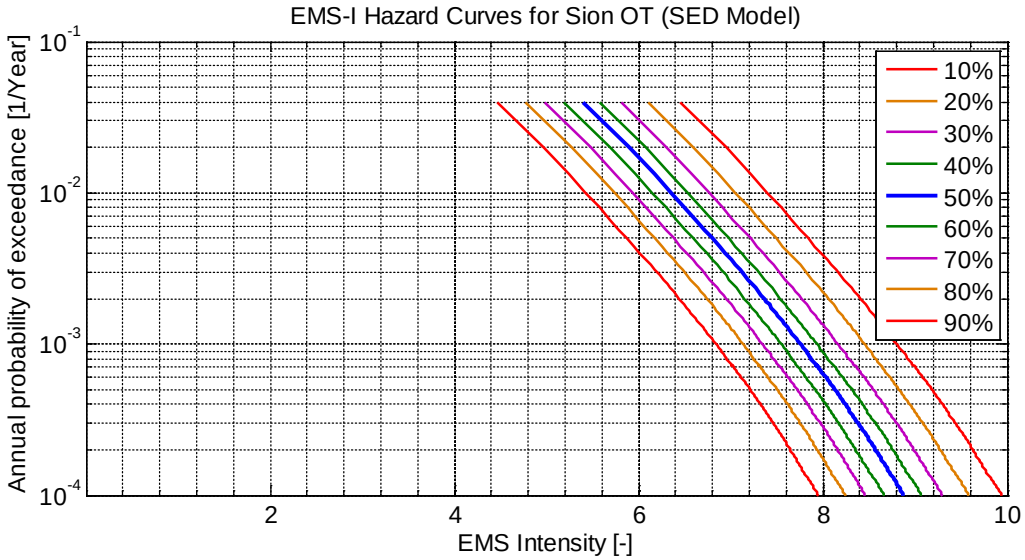

Figure 49: Hazard curve for Sion OT as a function of EMS-Intensity

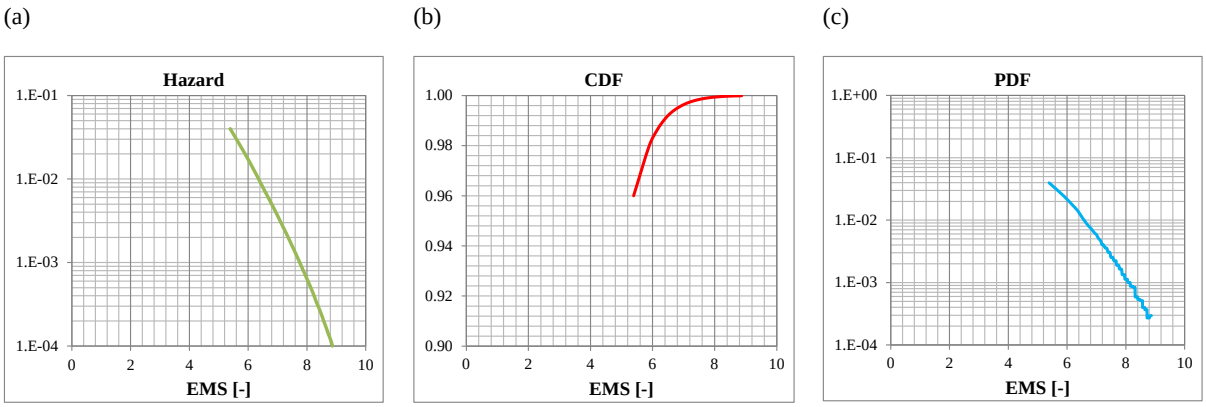

Figure 50: (a) Hazard, (b) cumulative distribution function and (c) probability density function of the seismic hazard for Sion OT

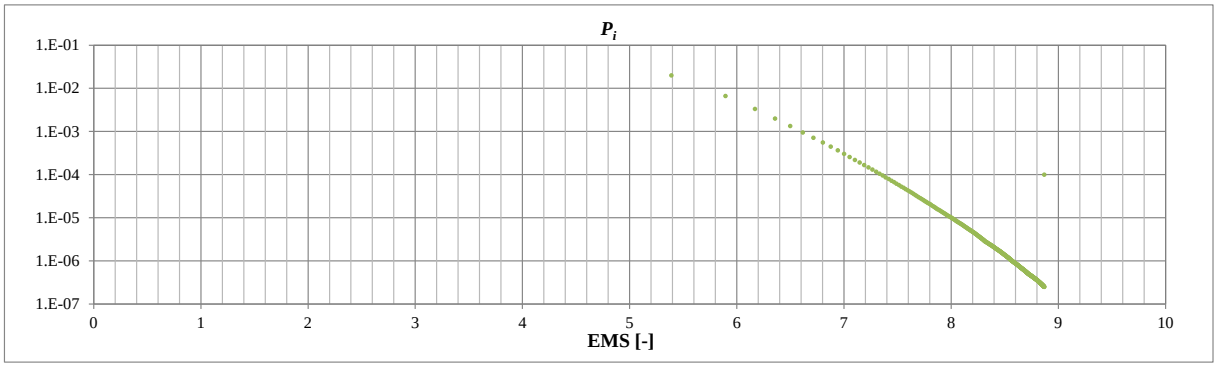

Figure 51: Probability of occurrence (P_i) of events

– To compute the consequence in deterministic approach for each event the median value of the EMS-Intensity of the event is read. Then the fragilities (probabilities) of relevant damage grades at

this EMS-Intensity are read. For example for the event with a return period of 475 years the median EMS-Intensity is about 7.3. For loss of life only damage grades 4 and 5 are relevant. Probabilities that at EMS-Intensity 7.3 damage grades 4 and 5 happen, are 0.034 and 0.003, respectively. Noting that loss ratios (in this case casualty rates) are 0.02 and 0.10 for damage grades 4 and 5, respectively, C_i will be 9.8×10^{-4}. Multiplying this with the probability of occurrence of this event the casualty risk for this event will be 9.8×10^{-8}. R_i values are given in Figure 52.

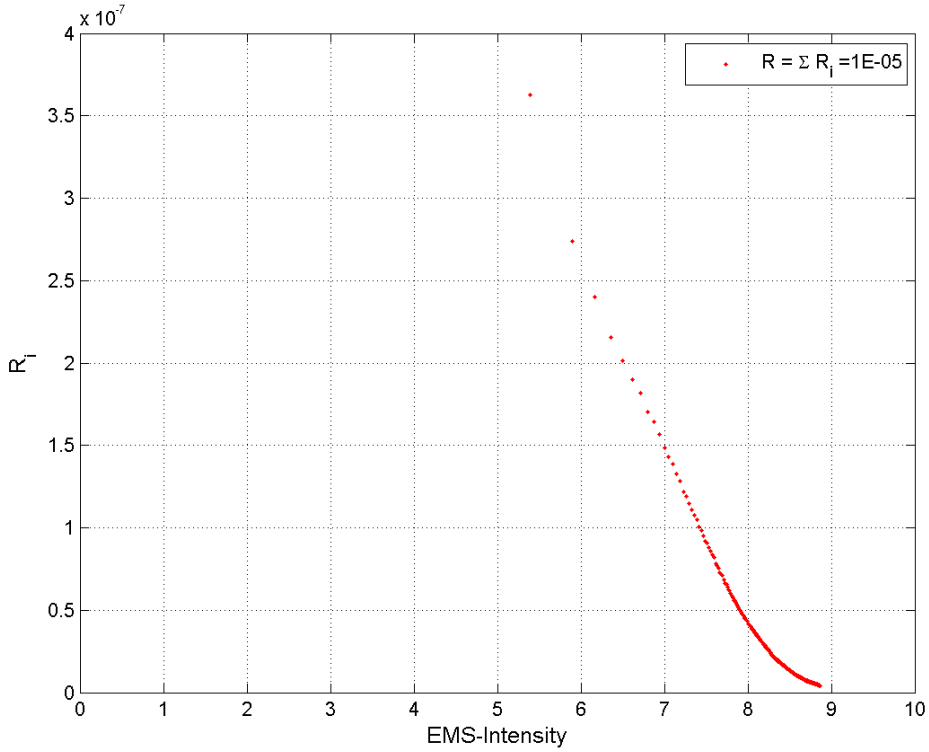

Figure 52: R_i values using median hazard values only for benchmark STD40 ORG in Sion OT

6 Results

6.1 Casualty risk

Based on the risk computation framework introduced in chapter 5, the casualty risk has been calculated for the 7 benchmarks described in chapter 3 and 4 sites described in chapter 2. Risk values are given for both spectral-acceleration-based and Intensity-based risk assessments.

6.1.1 Spectral-acceleration-based risk assessment

Table 30: Casualty risk values computed with median fragility curves ($V_{50\%}$) and different percentile hazard curves ($H_{10\%}$, $H_{50\%}$ and $H_{90\%}$). The case $H_{0\text{-}90\%}$-$V_{50\%}$ stands for the convolution of hazard curves truncated at the 90th percentile with median fragility curves

Benchmark	Site	$H_{10\%}$-$V_{50\%}$	$H_{50\%}$-$V_{50\%}$	$H_{90\%}$-$V_{50\%}$	$H_{0\text{-}90\%}$-$V_{50\%}$
CHB30	Basel	9E-08*	3E-06	2E-05	4E-06
	Sion OT	9E-09*	1E-06	1E-05	2E-06
	Sion TE	4E-08*	3E-06	2E-05	4E-06
	Zürich	2E-12*	5E-08*	3E-06	3E-07
CHB30 ORG	Basel	1E-08*	2E-06	2E-05	3E-06
	Sion OT	3E-09*	8E-07*	2E-05	2E-06
	Sion TE	2E-08*	3E-06	3E-05	5E-06
	Zürich	1E-14*	4E-09*	2E-06	1E-07*
YVR14	Basel	2E-19*	2E-10*	3E-06	1E-07*
	Sion OT	3E-13*	4E-07*	3E-05	3E-06
	Sion TE	6E-09*	1E-05	9E-05	2E-05
	Zürich	5E-32*	1E-16*	2E-08*	4E-10*
SECH7	Basel	1E-11*	6E-07*	3E-05	3E-06
	Sion OT	2E-16*	6E-10*	2E-06*	1E-07*
	Sion TE	4E-09*	6E-06	6E-05	1E-05
	Zürich	6E-24*	3E-14*	5E-08*	1E-09*
SUVA	Basel	9E-09*	3E-06	4E-05	7E-06
	Sion OT	1E-11*	6E-08*	6E-06	5E-07*
	Sion TE	1E-07*	1E-05	8E-05	2E-05
	Zürich	7E-17*	1E-10*	4E-07*	2E-08*
STD40 ORG	Basel	5E-10*	3E-06	5E-05	8E-06
	Sion OT	1E-15*	2E-08*	7E-06	5E-07*
	Sion TE	3E-08*	1E-05	8E-05	2E-05
	Zürich	7E-27*	2E-13*	3E-07*	1E-08*
STD40	Basel	2E-08*	4E-06	4E-05	8E-06
	Sion OT	8E-12*	1E-07*	8E-06	8E-07
	Sion TE	1E-07*	1E-05	7E-05	1E-05
	Zürich	3E-18*	8E-11*	7E-07*	3E-08*

* Risk estimation is not exhaustive (risk value is underestimated, for more details see 7.1.5)

Table 31: Casualty risk values computed with median hazard curves ($H_{50\%}$) and different percentile fragility curves ($V_{10\%}$, $V_{50\%}$ and $V_{90\%}$)

Benchmark	**Site**	**$H_{50\%}$-$V_{10\%}$**	**$H_{50\%}$-$V_{50\%}$**	**$H_{50\%}$-$V_{90\%}$**
CHB30	Basel	1E-05	3E-06	5E-07*
	Sion OT	4E-06	1E-06	1E-07*
	Sion TE	1E-05	3E-06	6E-07*
	Zürich	5E-07*	5E-08*	1E-09*
CHB30 ORG	Basel	9E-06	2E-06	2E-07*
	Sion OT	5E-06	8E-07*	7E-08*
	Sion TE	1E-05	3E-06	4E-07*
	Zürich	1E-07*	4E-09*	3E-11*
YVR14	Basel	8E-08*	2E-10*	2E-14*
	Sion OT	7E-06	4E-07*	2E-09*
	Sion TE	4E-05	1E-05	1E-06*
	Zürich	4E-12*	1E-16*	8E-23*
SECH7	Basel	7E-06	6E-07*	9E-09*
	Sion OT	1E-07*	6E-10*	5E-13*
	Sion TE	2E-05	6E-06	5E-07*
	Zürich	6E-11*	3E-14*	3E-18*
SUVA	Basel	2E-05	3E-06	3E-07*
	Sion OT	1E-06*	6E-08*	1E-09*
	Sion TE	3E-05	1E-05	2E-06*
	Zürich	1E-08*	1E-10*	3E-13*
STD40 ORG	Basel	2E-05	3E-06	2E-07*
	Sion OT	8E-07*	2E-08*	2E-11*
	Sion TE	4E-05	1E-05	2E-06*
	Zürich	8E-10*	2E-13*	8E-19*
STD40	Basel	2E-05	4E-06	5E-07*
	Sion OT	2E-06*	1E-07*	2E-09*
	Sion TE	3E-05	1E-05	2E-06*
	Zürich	2E-08*	8E-11*	6E-14*

* Risk estimation is not exhaustive (risk value is underestimated, for more details see 7.1.5)

Table 32: Maximum and minimum values of the computed casualty risk. For comparison the casualty risk values computed with median hazard and median fragility curves are also given ($H_{50\%}$-$V_{50\%}$)

Nr.	Benchmark	Site	$H_{90\%}$-$V_{10\%}$	$H_{50\%}$-$V_{50\%}$	$H_{10\%}$-$V_{90\%}$
1	CHB30	Basel	7E-05	3E-06	2E-09*
2		Sion OT	3E-05	1E-06	1E-10*
3		Sion TE	7E-05	3E-06	9E-10*
4		Zürich	1E-05	5E-08*	2E-15*
5	CHB30 ORG	Basel	7E-05	2E-06	9E-11*
6		Sion OT	5E-05	8E-07*	2E-11*
7		Sion TE	8E-05	3E-06	2E-10*
8		Zürich	8E-06	4E-09*	3E-18*
9	YVR14	Basel	2E-05	2E-10*	2E-26*
10		Sion OT	7E-05	4E-07*	2E-18*
11		Sion TE	2E-04	1E-05	4E-12*
12		Zürich	1E-06*	1E-16*	1E-41*
13	SECH7	Basel	7E-05	6E-07*	4E-15*
14		Sion OT	1E-05	6E-10*	4E-21*
15		Sion TE	1E-04	6E-06	6E-12*
16		Zürich	2E-06*	3E-14*	6E-30*
17	SUVA	Basel	1E-04	3E-06	8E-11*
18		Sion OT	2E-05	6E-08*	1E-14*
19		Sion TE	2E-04	1E-05	2E-09*
20		Zürich	4E-06	1E-10*	9E-21*
21	STD40 ORG	Basel	1E-04	3E-06	6E-14*
22		Sion OT	3E-05	2E-08*	1E-21*
23		Sion TE	2E-04	1E-05	6E-11*
24		Zürich	4E-06	2E-13*	8E-36*
25	STD40	Basel	1E-04	4E-06	6E-11*
26		Sion OT	3E-05	1E-07*	3E-15*
27		Sion TE	2E-04	1E-05	2E-09*
28		Zürich	5E-06	8E-11*	4E-23*

* Risk estimation is not exhaustive (risk value is underestimated, for more details see 7.1.5)

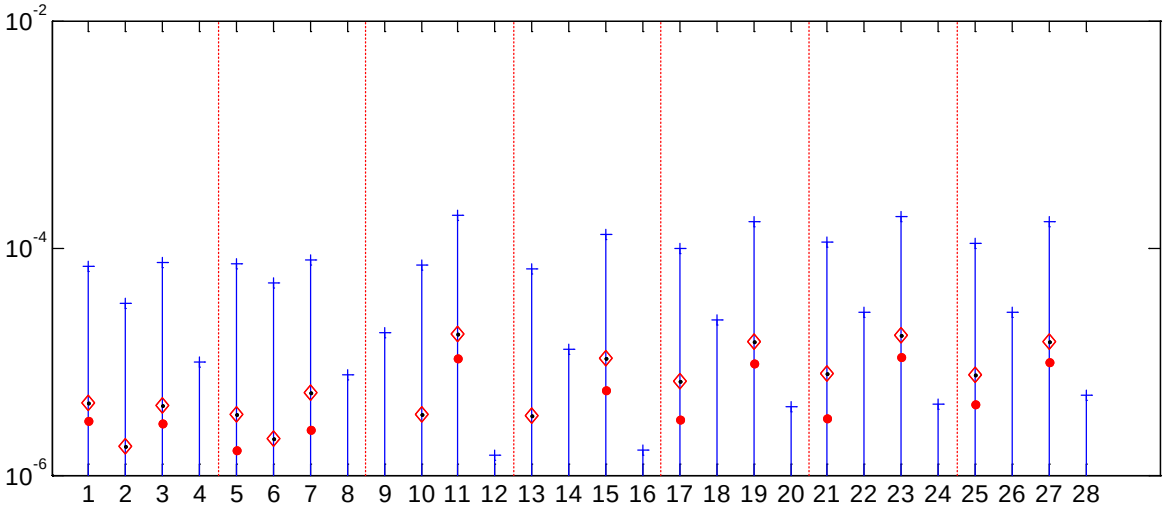

Figure 53: Extreme values of casualty risk; • for $H_{50\%}$-$V_{50\%}$, ◊ for $H_{0\text{-}90\%}$-$V_{50\%}$ and + for $H_{10\%}$-$V_{90\%}$ and $H_{90\%}$-$V_{10\%}$ values

6.1.2 Intensity-based risk assessment

Note that for Intensity-based risk assessment only median fragility curves are available.

Table 33: Casualty risk values computed with median fragility curves ($V_{50\%}$) and different percentile hazard curves ($H_{10\%}$, $H_{50\%}$ and $H_{90\%}$). The case $H_{0\text{-}90\%}$-$V_{50\%}$ stands for the convolution of hazard curves truncated at the 90th percentile with median fragility curves

Benchmark	Site	Hazard model	$H_{10\%}$-$V_{50\%}$	$H_{50\%}$-$V_{50\%}$	$H_{90\%}$-$V_{50\%}$	$H_{0\text{-}90\%}$-$V_{50\%}$
CHB30	Basel	SED	7E-08	6E-07	5E-06	9E-07
	Sion OT	SED	1E-07	1E-06	8E-06	2E-06
	Sion TE	SED	2E-06	1E-05	5E-05	1E-05
	Sion TE	Faenza	3E-07	2E-06	1E-05	2E-06
	Zürich	SED	2E-08	2E-07	2E-06	3E-07
	Zürich	Faenza	2E-09	3E-08	5E-07	6E-08
CHB30 ORG	Basel	SED	1E-06	6E-06	4E-05	8E-06
	Sion OT	SED	2E-06	1E-05	5E-05	1E-05
	Sion TE	SED	2E-05	7E-05	3E-04	8E-05
	Sion TE	Faenza	4E-06	2E-05	7E-05	2E-05
	Zürich	SED	3E-07	2E-06	2E-05	4E-06
	Zürich	Faenza	6E-08	6E-07	6E-06	1E-06
YVR14	Basel	SED	3E-08	3E-07	3E-06	5E-07
	Sion OT	SED	6E-08	5E-07	4E-06	8E-07
	Sion TE	SED	1E-06	6E-06	3E-05	8E-06
	Sion TE	Faenza	1E-07	1E-06	6E-06	1E-06
	Zürich	SED	7E-09	8E-08	9E-07	1E-07
	Zürich	Faenza	1E-09	1E-08	2E-07	3E-08
SECH7	Basel	SED	2E-07	2E-06	1E-05	2E-06
	Sion OT	SED	4E-07	3E-06	2E-05	4E-06
	Sion TE	SED	4E-06	2E-05	1E-04	3E-05
	Sion TE	Faenza	8E-07	5E-06	2E-05	6E-06
	Zürich	SED	5E-08	5E-07	4E-06	8E-07
	Zürich	Faenza	8E-09	1E-07	1E-06	2E-07
SUVA	Basel	SED	7E-07	4E-06	2E-05	6E-06
	Sion OT	SED	1E-06	7E-06	4E-05	9E-06
	Sion TE	SED	1E-05	5E-05	2E-04	6E-05
	Sion TE	Faenza	3E-06	1E-05	5E-05	1E-05
	Zürich	SED	2E-07	1E-06	1E-05	2E-06
	Zürich	Faenza	3E-08	3E-07	4E-06	6E-07
STD40 ORG	Basel	SED	1E-06	6E-06	4E-05	8E-06
	Sion OT	SED	2E-06	1E-05	5E-05	1E-05
	Sion TE	SED	2E-05	7E-05	3E-04	8E-05
	Sion TE	Faenza	4E-06	2E-05	7E-05	2E-05
	Zürich	SED	3E-07	2E-06	2E-05	4E-06
	Zürich	Faenza	6E-08	6E-07	6E-06	1E-06
STD40	Basel	SED	2E-07	2E-06	1E-05	2E-06
	Sion OT	SED	4E-07	3E-06	2E-05	4E-06
	Sion TE	SED	4E-06	2E-05	1E-04	3E-05
	Sion TE	Faenza	8E-07	5E-06	2E-05	6E-06
	Zürich	SED	5E-08	5E-07	4E-06	8E-07
	Zürich	Faenza	8E-09	1E-07	1E-06	2E-07

* Risk estimation is not exhaustive (risk value is underestimated, for more details see 7.1.5)

6.2 Property loss risk

Based on the risk computation framework introduced in chapter 5, the property loss risk has been calculated for the 7 benchmarks described in chapter 3 and the 4 sites described in chapter 2.

6.2.1 Spectral-acceleration-based risk assessment

Table 34: Property loss risk values computed with median fragility curves ($V_{50\%}$) and different percentile hazard curves ($H_{10\%}$, $H_{50\%}$ and $H_{90\%}$). The case $H_{0\text{-}90\%}$-$V_{50\%}$ stands for the convolution of hazard curves truncated at the 90th percentile with median fragility curves

Benchmark	Site	$H_{10\%}$-$V_{50\%}$	$H_{50\%}$-$V_{50\%}$	$H_{90\%}$-$V_{50\%}$	$H_{0\text{-}90\%}$-$V_{50\%}$
CHB30	Basel	5E-05	4E-04	2E-03	5E-04
	Sion OT	1E-05	2E-04	1E-03	2E-04
	Sion TE	6E-05	5E-04	3E-03	6E-04
	Zürich	5E-07*	3E-05	4E-04	6E-05
CHB30 ORG	Basel	2E-04	1E-03	6E-03	1E-03
	Sion OT	1E-04	6E-04	3E-03	8E-04
	Sion TE	5E-04	2E-03	8E-03	2E-03
	Zürich	6E-06	1E-04	1E-03	2E-04
YVR14	Basel	4E-06	1E-04	8E-04	2E-04
	Sion OT	3E-05	3E-04	2E-03	4E-04
	Sion TE	1E-04	1E-03	4E-03	1E-03
	Zürich	4E-08*	7E-06	2E-04	2E-05
SECH7	Basel	2E-04	1E-03	5E-03	1E-03
	Sion OT	2E-05	2E-04	1E-03	2E-04
	Sion TE	3E-04	2E-03	7E-03	2E-03
	Zürich	1E-06*	5E-05	7E-04	9E-05
SUVA	Basel	4E-04	2E-03	8E-03	2E-03
	Sion OT	6E-05	4E-04	2E-03	4E-04
	Sion TE	6E-04	3E-03	1E-02	3E-03
	Zürich	6E-06	1E-04	1E-03	2E-04
STD40 ORG	Basel	2E-04	1E-03	5E-03	1E-03
	Sion OT	2E-05	2E-04	1E-03	2E-04
	Sion TE	3E-04	2E-03	7E-03	2E-03
	Zürich	1E-06	4E-05	6E-04	7E-05
STD40	Basel	6E-05	5E-04	3E-03	6E-04
	Sion OT	4E-06	8E-05	6E-04	1E-04
	Sion TE	1E-04	8E-04	4E-03	9E-04
	Zürich	3E-08*	7E-06	2E-04	2E-05

* Risk estimation is not exhaustive (risk value is underestimated, for more details see 7.1.5)

Table 35: Property loss risk values computed with median hazard curves ($H_{50\%}$) and different percentile fragility curves ($V_{10\%}$, $V_{50\%}$ and $V_{90\%}$)

Benchmark	**Site**	**$H_{50\%}$-$V_{10\%}$**	**$H_{50\%}$-$V_{50\%}$**	**$H_{50\%}$-$V_{90\%}$**
CHB30	Basel	1E-03	4E-04	1E-04
	Sion OT	5E-04	2E-04	4E-05
	Sion TE	2E-03	5E-04	1E-04
	Zürich	1E-04	3E-05	5E-06
CHB30 ORG	Basel	3E-03	1E-03	5E-04
	Sion OT	1E-03	6E-04	3E-04
	Sion TE	5E-03	2E-03	7E-04
	Zürich	4E-04	1E-04	3E-05
YVR14	Basel	4E-04	1E-04	2E-05
	Sion OT	9E-04	3E-04	1E-04
	Sion TE	2E-03	1E-03	4E-04
	Zürich	4E-05	7E-06	7E-07*
SECH7	Basel	3E-03	1E-03	4E-04
	Sion OT	5E-04	2E-04	7E-05
	Sion TE	4E-03	2E-03	7E-04
	Zürich	2E-04	5E-05	1E-05
SUVA	Basel	5E-03	2E-03	8E-04
	Sion OT	9E-04	4E-04	1E-04
	Sion TE	6E-03	3E-03	1E-03
	Zürich	4E-04	1E-04	3E-05
STD40 ORG	Basel	3E-03	1E-03	4E-04
	Sion OT	5E-04	2E-04	6E-05
	Sion TE	4E-03	2E-03	6E-04
	Zürich	2E-04	4E-05	7E-06
STD40	Basel	1E-03	5E-04	2E-04
	Sion OT	3E-04	8E-05	2E-05
	Sion TE	2E-03	8E-04	3E-04
	Zürich	4E-05	7E-06	8E-07*

* Risk estimation is not exhaustive (risk value is underestimated, for more details see 7.1.5)

Table 36: Maximum and minimum values of the computed property loss risk. For comparison the casualty risk values computed with median hazard and fragility curves are also given ($H_{50\%}$-$V_{50\%}$)

Nr.	Benchmark	Site	$H_{90\%}$-$V_{10\%}$	$H_{50\%}$-$V_{50\%}$	$H_{10\%}$-$V_{90\%}$
1	CHB30	Basel	6E-03	4E-04	1E-05
2		Sion OT	2E-03	2E-04	2E-06
3		Sion TE	7E-03	5E-04	1E-05
4		Zürich	1E-03	3E-05	5E-08*
5	CHB30 ORG	Basel	1E-02	1E-03	7E-05
6		Sion OT	6E-03	6E-04	3E-05
7		Sion TE	2E-02	2E-03	1E-04
8		Zürich	3E-03	1E-04	1E-06*
9	YVR14	Basel	2E-03	1E-04	4E-07*
10		Sion OT	4E-03	3E-04	4E-06
11		Sion TE	8E-03	1E-03	3E-05
12		Zürich	5E-04	7E-06	2E-09*
13	SECH7	Basel	1E-02	1E-03	5E-05
14		Sion OT	3E-03	2E-04	4E-06
15		Sion TE	1E-02	2E-03	1E-04
16		Zürich	2E-03	5E-05	2E-07*
17	SUVA	Basel	1E-02	2E-03	1E-04
18		Sion OT	4E-03	4E-04	2E-05
19		Sion TE	2E-02	3E-03	2E-04
20		Zürich	3E-03	1E-04	9E-07*
21	STD40 ORG	Basel	1E-02	1E-03	4E-05
22		Sion OT	3E-03	2E-04	3E-06
23		Sion TE	1E-02	2E-03	8E-05
24		Zürich	2E-03	4E-05	1E-07*
25	STD40	Basel	7E-03	5E-04	9E-06
26		Sion OT	1E-03	8E-05	3E-07*
27		Sion TE	8E-03	8E-04	2E-05
28		Zürich	7E-04	7E-06	7E-10*

* Risk estimation is not exhaustive (risk value is underestimated, for more details see 7.1.5)

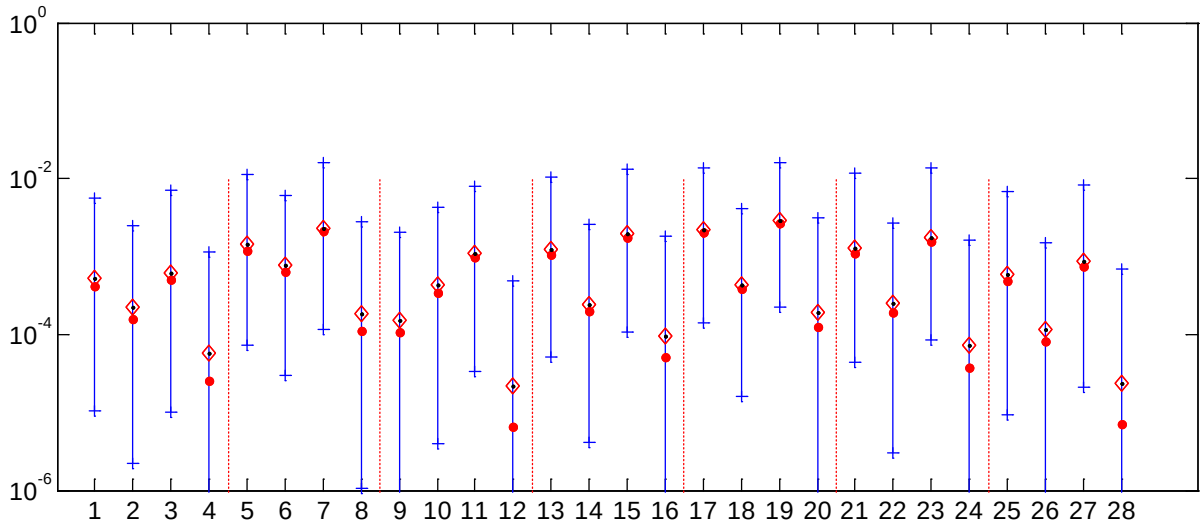

Figure 54: Extreme values of property loss risk; • for $H_{50\%}$-$V_{50\%}$, ◊ for $H_{0\text{-}90\%}$-$V_{50\%}$ and + for $H_{10\%}$-$V_{90\%}$ and $H_{90\%}$-$V_{10\%}$

6.2.2 Intensity-based risk assessment

Table 37: Property loss risk values computed with median fragility curves ($V_{50\%}$) and different percentile hazard curves ($H_{10\%}$, $H_{50\%}$ and $H_{90\%}$). The case $H_{0\text{-}90\%}$-$V_{50\%}$ stands for the convolution of hazard curves truncated at the 90th percentile with median fragility curves

Benchmark	Site	Hazard model	$H_{10\%}$-$V_{50\%}$	$H_{50\%}$-$V_{50\%}$	$H_{90\%}$-$V_{50\%}$	$H_{0\text{-}90\%}$-$V_{50\%}$
CHB30	Basel	SED	3E-04	9E-04	3E-03	9E-04
	Sion OT	SED	4E-04	1E-03	3E-03	1E-03
	Sion TE	SED	2E-03	4E-03	1E-02	4E-03
	Sion TE	Faenza	9E-04	2E-03	4E-03	2E-03
	Zürich	SED	2E-04	5E-04	2E-03	6E-04
	Zürich	Faenza	1E-04	3E-04	1E-03	3E-04
CHB30 ORG	Basel	SED	1E-03	3E-03	8E-03	3E-03
	Sion OT	SED	2E-03	4E-03	1E-02	4E-03
	Sion TE	SED	5E-03	1E-02	2E-02	1E-02
	Sion TE	Faenza	3E-03	7E-03	1E-02	6E-03
	Zürich	SED	8E-04	2E-03	6E-03	2E-03
	Zürich	Faenza	4E-04	1E-03	4E-03	1E-03
YVR14	Basel	SED	2E-04	6E-04	2E-03	7E-04
	Sion OT	SED	3E-04	8E-04	3E-03	9E-04
	Sion TE	SED	1E-03	3E-03	8E-03	3E-03
	Sion TE	Faenza	6E-04	1E-03	3E-03	1E-03
	Zürich	SED	1E-04	4E-04	1E-03	4E-04
	Zürich	Faenza	7E-05	2E-04	8E-04	2E-04
SECH7	Basel	SED	5E-04	1E-03	4E-03	1E-03
	Sion OT	SED	7E-04	2E-03	5E-03	2E-03
	Sion TE	SED	3E-03	6E-03	1E-02	6E-03
	Sion TE	Faenza	2E-03	3E-03	7E-03	3E-03
	Zürich	SED	3E-04	9E-04	3E-03	1E-03
	Zürich	Faenza	2E-04	5E-04	2E-03	6E-04
SUVA	Basel	SED	9E-04	2E-03	6E-03	3E-03
	Sion OT	SED	1E-03	3E-03	8E-03	3E-03
	Sion TE	SED	4E-03	9E-03	2E-02	9E-03
	Sion TE	Faenza	3E-03	5E-03	1E-02	5E-03
	Zürich	SED	6E-04	2E-03	5E-03	2E-03
	Zürich	Faenza	3E-04	9E-04	3E-03	1E-03
STD40 ORG	Basel	SED	1E-03	3E-03	8E-03	3E-03
	Sion OT	SED	2E-03	4E-03	1E-02	4E-03
	Sion TE	SED	5E-03	1E-02	2E-02	1E-02
	Sion TE	Faenza	3E-03	7E-03	1E-02	6E-03
	Zürich	SED	8E-04	2E-03	6E-03	2E-03
	Zürich	Faenza	4E-04	1E-03	4E-03	1E-03
STD40	Basel	SED	5E-04	1E-03	4E-03	1E-03
	Sion OT	SED	7E-04	2E-03	5E-03	2E-03
	Sion TE	SED	3E-03	6E-03	1E-02	6E-03
	Sion TE	Faenza	2E-03	3E-03	7E-03	3E-03
	Zürich	SED	3E-04	9E-04	3E-03	1E-03
	Zürich	Faenza	2E-04	5E-04	2E-03	6E-04

* Risk estimation is not exhaustive (risk value is underestimated, for more details see 7.1.5)

6.3 Compliance factor vs. risk

Compliance factors of benchmark buildings have been calculated based on force- and displacement-based methods (see Table 2). Computed risk values (casualty risk and Property loss risk) are demonstrated in the following figures as a function of compliance factors. This has been done for compliance factors computed with spectral accelerations according to SIA 261 at periods of vibration according to engineering models. In force-based method, the forces are distributed according to the moment of inertia of bearing walls (SIA 261). As displacement-based method the Eurocode approach has been applied (EC8). Only risk values larger than 10^{-6} and compliance factors lower than 1.0 are depicted. Following risk values are used: $H_{50\%}$-$V_{50\%}$ and $H_{0\text{-}90\%}$-$V_{50\%}$ for Sa-based risk values and $H_{50\%}$-$V_{50\%}$ for EMS-based risk values (See sections 6.1 and 6.2).

(a)

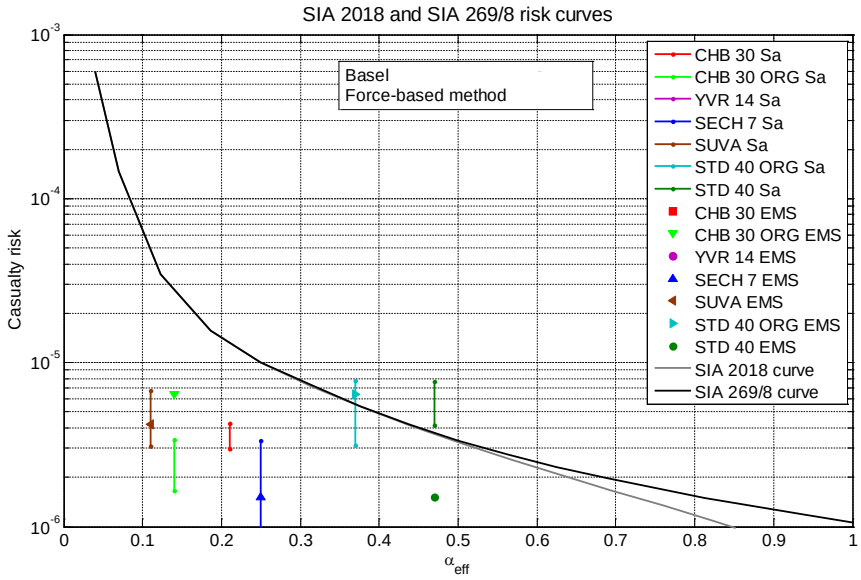

(b)

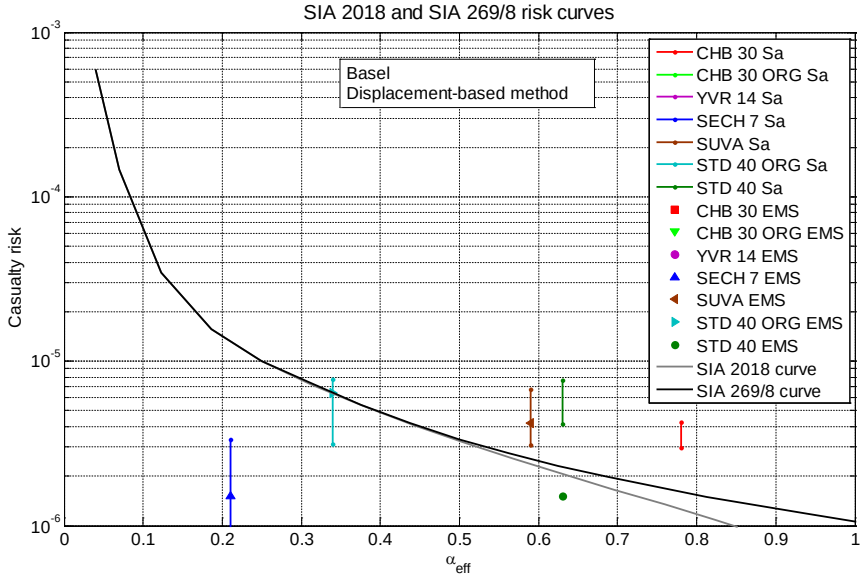

Figure 55: Demonstration of the casualty risk values on the Prestandard 2018 and SIA 269/8 risk curves for all benchmarks in Basel for compliance factors computed with (a) force-based method, (b) displacement-based method

(a)

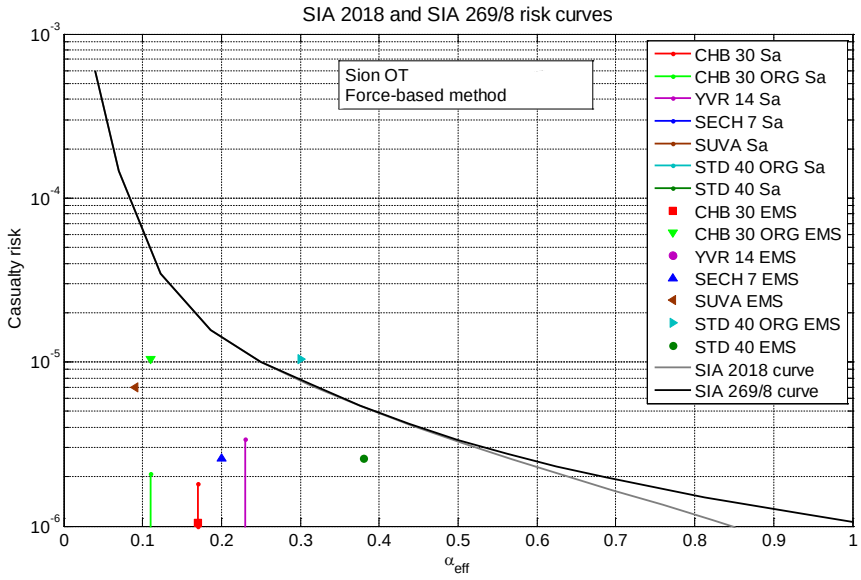

(b)

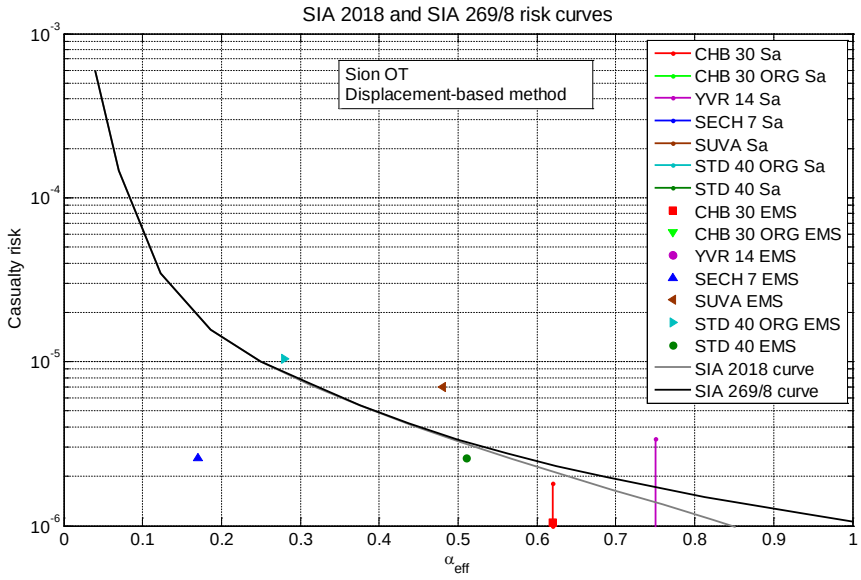

Figure 56: Demonstration of the casualty risk values on the Prestandard 2018 and SIA 269/8 risk curves for all benchmarks in Sion OT for compliance factors computed with (a) force-based method, (b) displacement-based method

(a)

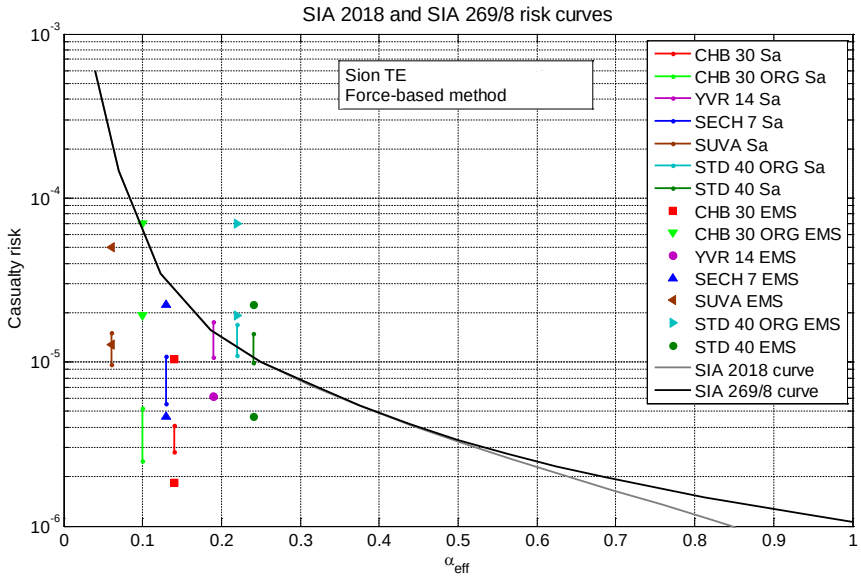

(b)

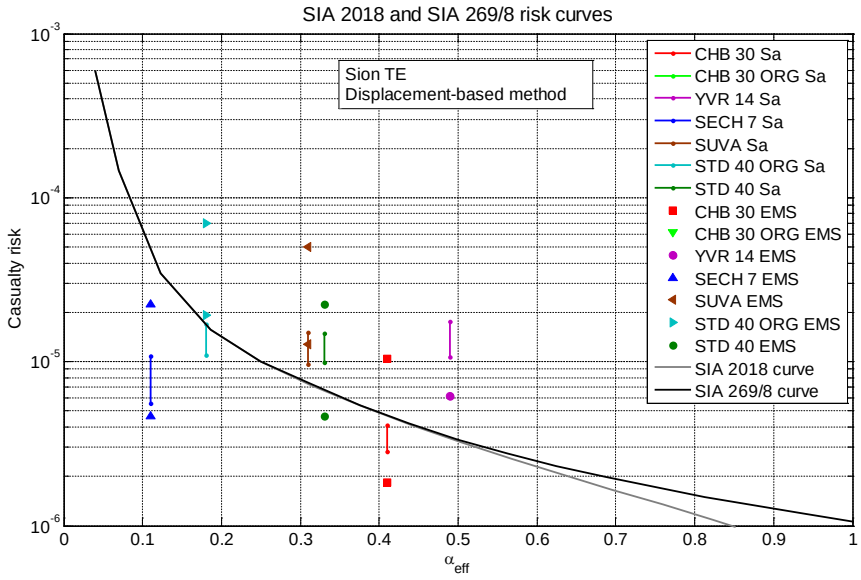

Figure 57: Demonstration of the casualty risk values on the Prestandard 2018 and SIA 269/8 risk curves for all benchmarks in Sion TE for compliance factors computed with (a) force-based method, (b) displacement-based method

Casualty risk values of benchmarks in Zurich are not depicted on risk curves as either the computed compliance factors are too high or the computed risk values are not exhaustive (for more details see section 7.1.5).

(a)

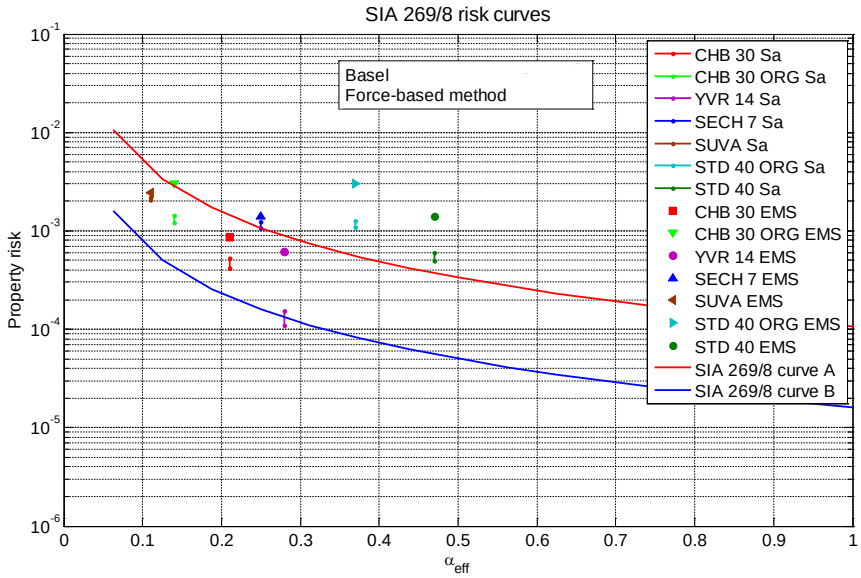

(b)

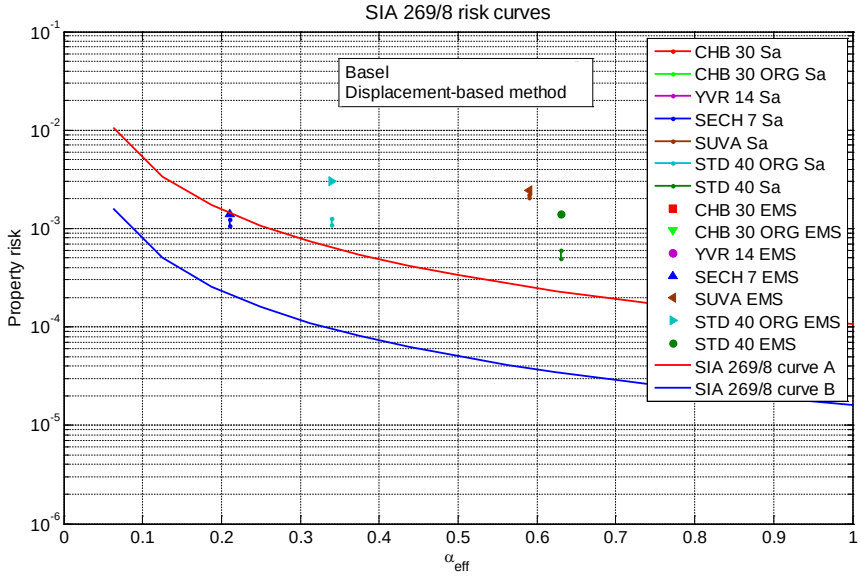

Figure 58: Demonstration of the property loss risk values on the SIA 269/8 risk curves for all benchmarks in Zurich for compliance factors computed with (a) force-based method, (b) displacement-based method

(a)

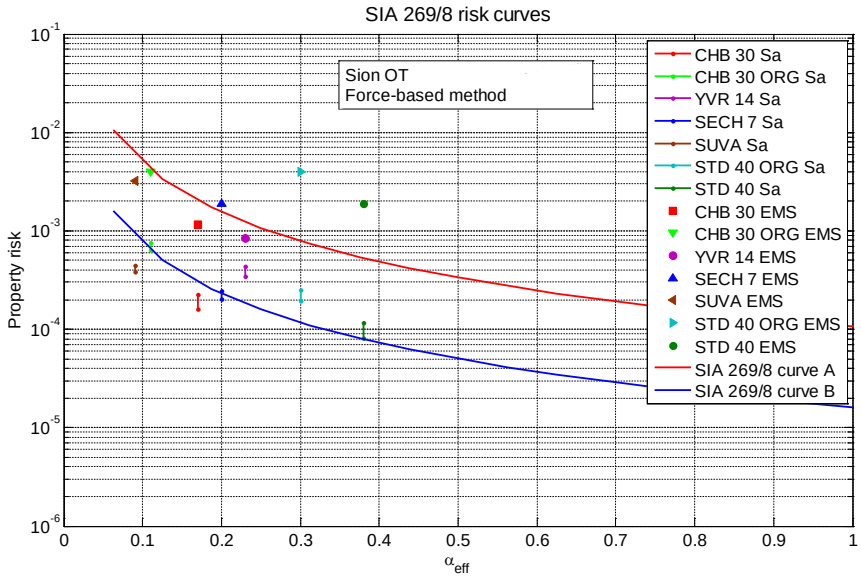

(b)

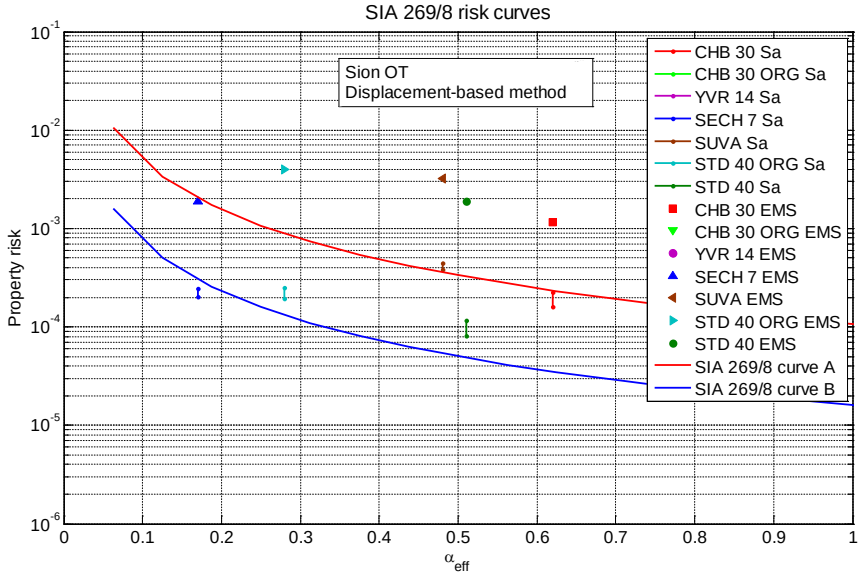

Figure 59: Demonstration of the property loss risk values on the SIA 269/8 risk curves for all benchmarks in Zurich for compliance factors computed with (a) force-based method, (b) displacement-based method

(a)

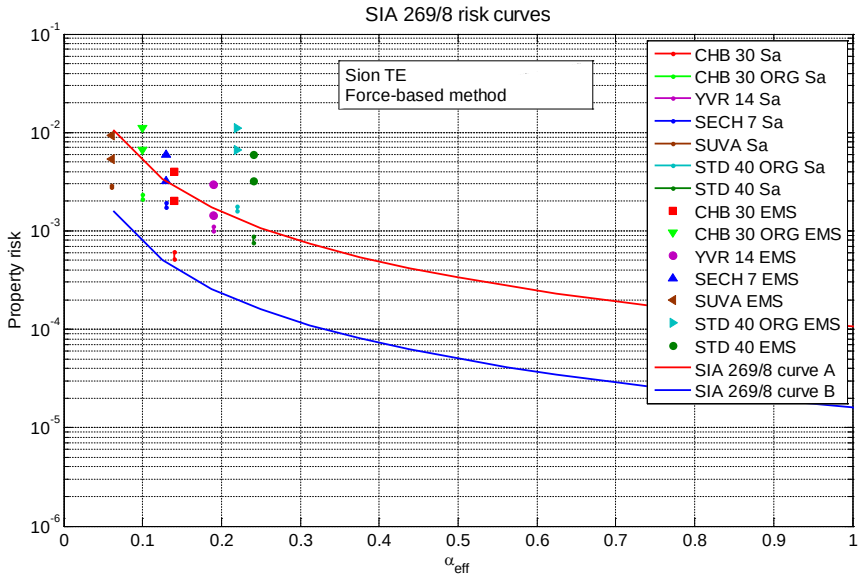

(b)

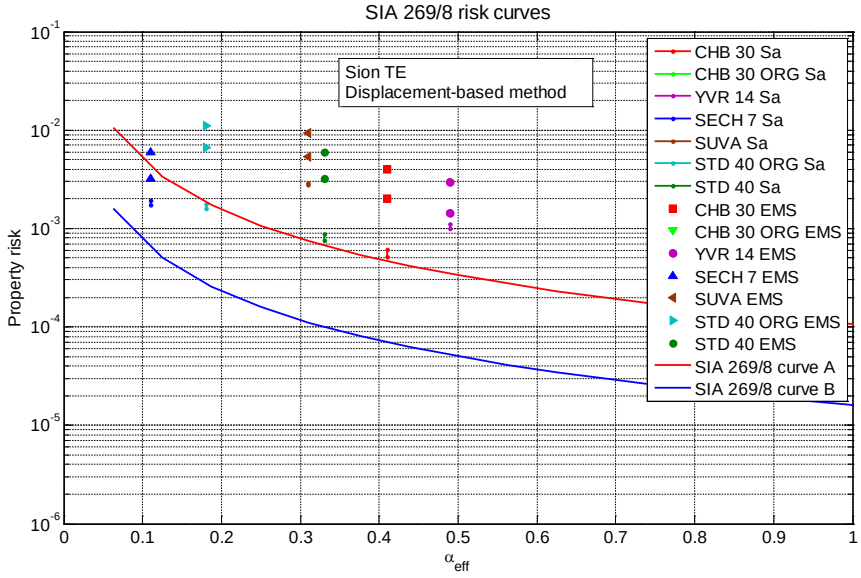

Figure 60: Demonstration of the property loss risk values on the SIA 269/8 risk curves for all benchmarks in Zurich for compliance factors computed with (a) force-based method, (b) displacement-based method

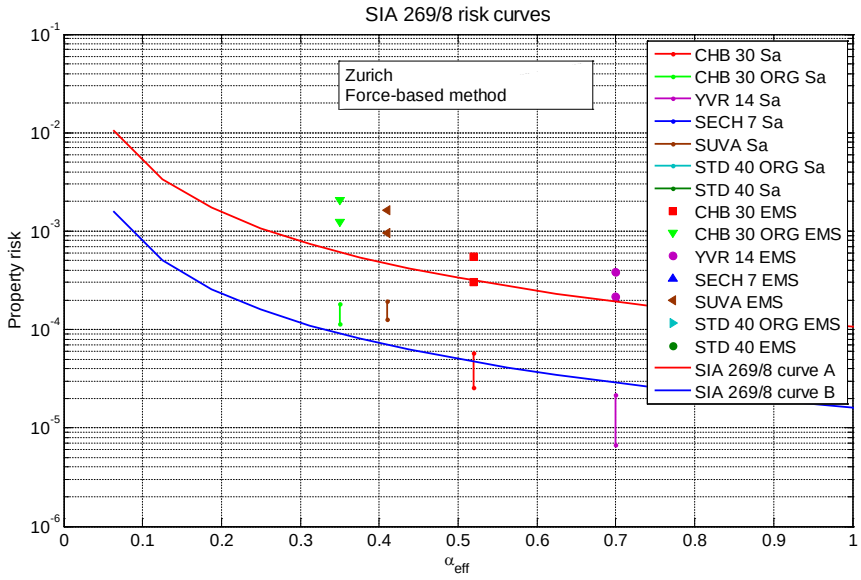

Figure 61: Demonstration of the property loss risk values on the SIA 269/8 risk curves for all benchmarks in Zurich for compliance factors computed with force-based method

7 Discussion

7.1 Risk estimation

7.1.1 Hazard

Table 30 shows for median fragility curves the casualty risk calculated for the 10^{th}, the 50^{th}, and the 90^{th} percentile of the hazard. The results show that the uncertainty associated with hazard plays a predominant role in the estimation of risk. For example in the case of the casualty risk where probabilities of about 10^{-4} for damage grade 5 are very relevant it is obvious that even the 90^{th} percentile of the 1'000-years event has a large impact on the probability for damage grade 5. For all of the considered sites, the 90^{th} percentile is associated with Sa-values of the same magnitude as the median values for the 10'000-year event. It can be summarised, that the higher percentiles are very important, whereas the lower percentiles can almost be neglected because they only contribute little to the risk. Percentiles higher than the 90^{th} percentile have not been given by SED. It is for this reason, that in the evaluation of risk no arbitrary values beyond the 90^{th} percentile have been defined and that the lognormal distribution by which the uncertainty was modelled, had been truncated at the 90^{th} percentile.

Another important issue associated to the estimation of the risk is the consideration of site-effects (nonlinear soil response, see chapter 2.4). Ignoring de-amplification as a result of nonlinear behaviour of soil layers, the estimated risks would be considerably higher. De-amplification is important for higher percentiles of events with smaller return periods as well as for events with higher return periods. Whereas the de-amplification seems to be justified for physical reasons, it is not clear how far the amount of de-amplification is in coincidence with reality, because no data for comparison was available within the project.

7.1.2 Vulnerability

In the case of the vulnerability the quite opposite characteristic in comparison to the hazard can be observed. If uncertainty in the fragility curves is taken into account, then the lower percentiles contribute disproportionately high to the risk. This characteristic can be observed for example for the 10^{th} percentile shown by Table 31. It is for this reason that the adopted model uncertainty highly influences the risk. In the current project the influence of the model uncertainty has been demonstrated by the help of lognormal distribution which can be considered as a standard to represent this type of uncertainty. Whereas in the construction of the fragility curves only little data was available a relatively large scatter had been assumed to represent model uncertainty. Furthermore it has been assumed, that the fragility curves developed by IMAC represent median fragility curves. This means that the fragility curves would have no bias. As has been already mentioned for the material properties median values have been considered in the mechanical model which produced the fragility curves. Besides this, only little information is available to support the assumption that the produced fragility curves are median curves. A model building (dual system with masonry and concrete walls) tested on a shaking table in Pavia (CoMa walls project) is also simulated by IMAC with the same software used in this project. In this specific case the test building performed better than the modelled building. But this was only one specific comparison and it is not clear, whether this conservatism holds in general.

Another important aspect is the dependency of the fragility curves on the used earthquake records. For the elaboration of the fragility curves earthquake records have been used from the European strong motion database, Italian database and several registered records from the Christchurch earthquake. In some cases the amplitudes of these earthquake records have been changed in a manner that the mechanical model was able to produce data points for the required damage grades. The hazard given by SED consists of values for acceleration to be observed with certain probabilities. The statistics behind

are covered by a variety of earthquakes with different return periods, strengths and distances to the considered site. Each of these earthquakes contributes to the site hazard. Therefore in order to evaluate the vulnerability of a building the earthquake records should be chosen in a manner that they are representative for the site specific hazard. This means, that earthquake records should be chosen in proportion to their contribution to the hazard. In order to do this a hazard disaggregation would be necessary and earthquake records should be defined which are representative for the hazard in Switzerland.

The model uncertainty and the dependency on the used earthquake records are two important fields which deserved further investigations.

7.1.3 Consequences

The adopted casualty rates were 10 % for damage grade 5 and 2 % for damage grade 4. In the literature some values for casualty rates associated with collapses could be found for different building types, which lie between 6 % and 15 %. With respect to these values the 10 % casualty rate can be considered to be a mean value. For lower damage grades no data could be found.

For some of the benchmarks it could be observed that the casualty risk is dominated by damage grade 4. Whereas the adopted casualty rates are 10 % for damage grade 5 and 2 % for damage grade 4, it is obvious that in situations where the probability for damage grade 4 is more than five times higher than that for damage grade 5, damage grade 4 contributes more to the risk than damage grade 5.

In the case of the property risk specific damage ratios have been adopted, which should be valid. The choice of these damage ratios pays tribute to the assumption, that in Switzerland the willingness to repair a heavily damaged structure is less than elsewhere. This assumption might not be true under certain conditions. For example, if in the case of a strong earthquake many structures will be damaged, than the reparation of structures could be the better option, when the resources of the construction industry are limited. Another example could be associated with the loss of function. If there is a strong urge to re-establish the functionality as soon as possible, than repair will in many cases be the faster option compared to demolishing a structure and to rebuild it.

7.1.4 Calculus

For the risk assessment a numerical approach is applied. The whole range of all possible seismic actions is discretized into several events, each representing a specific return period. The probability that an event happens, in this approach, depends not only on the return period of that event but also on the fineness of the discretization (time steps). For the computation of the probability of happening of events (P_i, see 5.1), only the median hazard curve is used.

7.1.5 Saturation of calculated risk

The calculated risk depends on the intersection between hazard and vulnerability. The larger the intersection between hazard and vulnerability is for a given return period, the larger is the contribution to the overall risk from this return period. If a considerable intersection is already given for short return periods like 500 years, then the overall risk will be high and the uncertainty does not have a predominant meaning. If in the opposite a weak intersection can only be observed for long return periods like 2'000 years then the resulting risk will be governed by the uncertainty associated to hazard and vulnerability.

For structures which are less vulnerable with respect to the site specific hazard, important contributions to the risk stem from the 10'000-year event and more important contributions could be expected from events with return periods which are even higher. Because no higher return periods have been

considered, the risk estimation for these structures is not exhaustive and in these cases the risk is underestimated. As an example the results of the risk assessment (casualty risk) for benchmark STD40 ORG in Sion OT and Sion TE in Figure 62 are considered. Partial risk values (R_i) from DG5 are illustrated in red and those from DG4 in blue. Risk values are computed with the median hazard and the median fragility curves ($H_{50\%}$-$V_{50\%}$, see 6.1.1). Spectral acceleration corresponding to return periods of 500 and 2'500 years are marked.

(a)

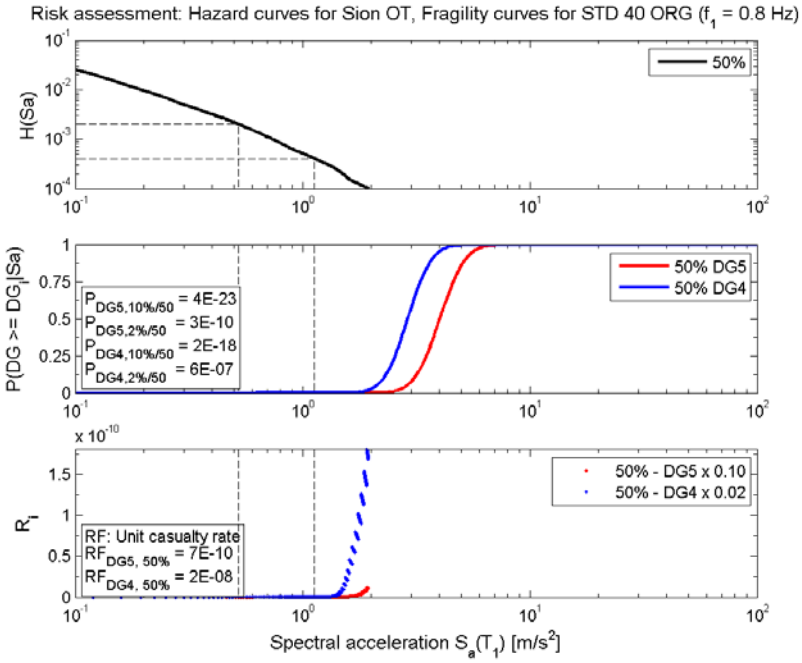

(b)

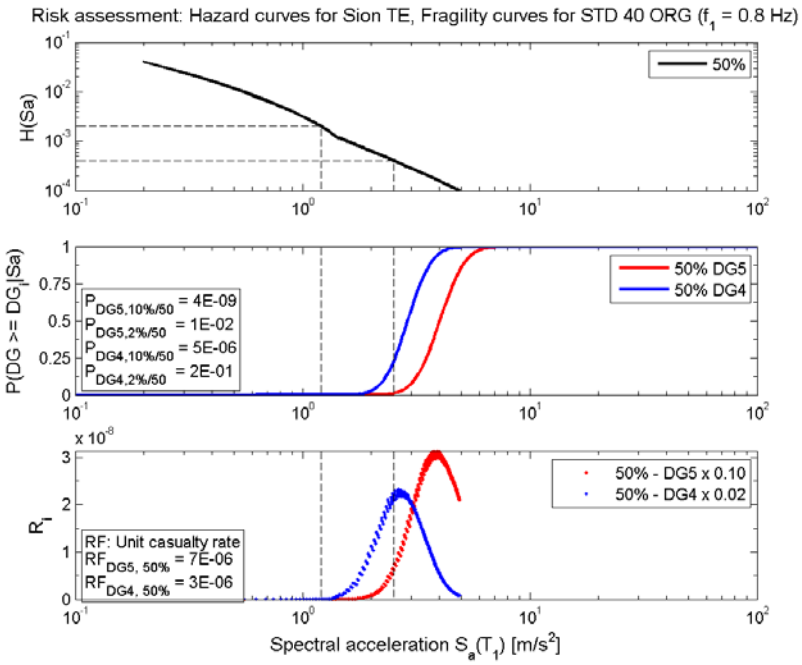

Figure 62: Casualty risk for benchmark STD40 ORG in (a) Sion OT and (b) Sion TE

Taking into account, that the earthquakes, which have not explicitly been considered in the estimation of risk are associated to return periods larger than 10'000 years, that the probability of DG5 is less than 1 and that the casualty ratio is taken to be 0.1, then the maximum omitted risk will definitely be smaller than 10^{-5} per year. It seems to be reasonable to assume a threshold in the order of 10^{-6} per year for the omitted unit casualty risk.

Risk values computed with the empirical method (based on EMS intensity) are almost always saturated. This is mainly because of the fact that the share of lower seismic events, i.e. more frequent events, on the whole risk value is considerably larger than the share of larger seismic events, i.e. less frequent events or events with larger return periods. Because of this, even in cases, where the risk value is in the order of 10^{-6} to 10^{-8}, taking events with a return period up to 10'000 years is enough for the saturation of the risk value.

In one case (benchmark CHB30) the share in casualty risk of DG4 is two orders of magnitude larger than the share of DG5 (Figure 63). In this case, in contrast to other benchmarks, there is considerable shift between the fragility curves of DG4 and DG5 with respect to the acceleration-axis. For such a case, the casualty risk is governed mainly by DG4. This effect is even more pronounced, when the risk calculation for DG5 is not exhaustive.

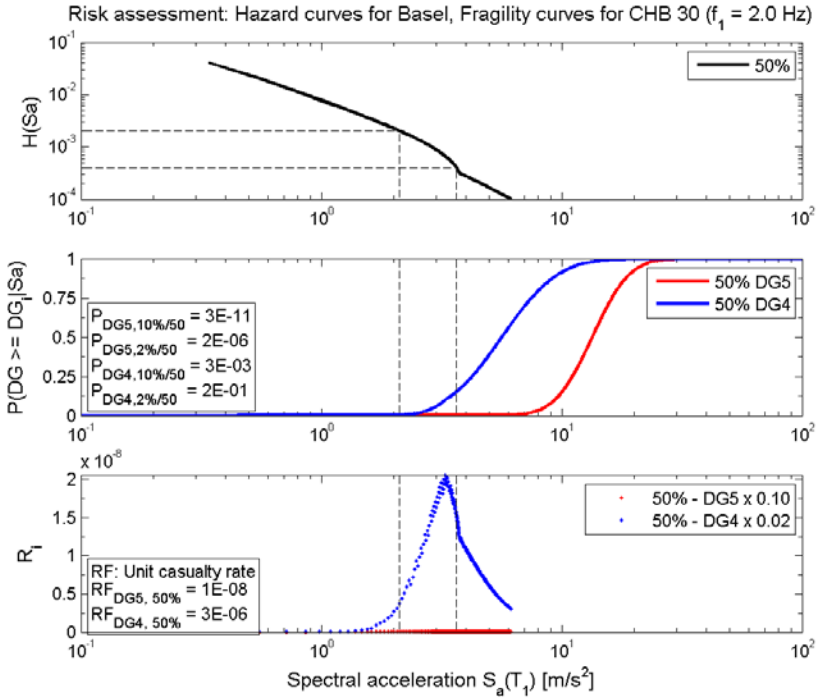

Figure 63: Casualty risk for benchmark CHB30 in Basel

7.1.6 Influence of nonlinearity of soil on the results

To avoid unrealistic ground motions, the nonlinear response of the sites has been considered. To show the influence of considering this nonlinearity on the risk values, a case study has been done. For benchmark STD40 in Sion TE the casualty risk values are computed with (NL) and without considering de-amplification (L) of seismic hazard as a result of soil nonlinear behaviour (Table 38 and Figure 64). Except the first case ($H_{10\%}$-$V_{50\%}$), in which the risk calculation was not exhaustive, the risk values for analyses without considering nonlinearities are 2 to 3 times larger than those with considering de-amplification.

Table 38: Casualty risk values computed with median fragility curves (V50%) and different percentile hazard curves (H10%, H50% and H90%) for benchmark STD40 ORG in Sion TE

Benchmark	Site	Case	$H_{10\%}$-$V_{50\%}$	$H_{50\%}$-$V_{50\%}$	$H_{90\%}$-$V_{50\%}$	$H_{0\text{-}90\%}$-$V_{50\%}$
STD40 ORG	Sion TE	NL	3E-8*	1E-5	8E-5	2E-5
STD40 ORG	Sion TE	L	9E-7*	3E-5	2E-4	4E-5
		Ratio	30	3	2.5	2

* Risk estimation is not exhaustive

(a)

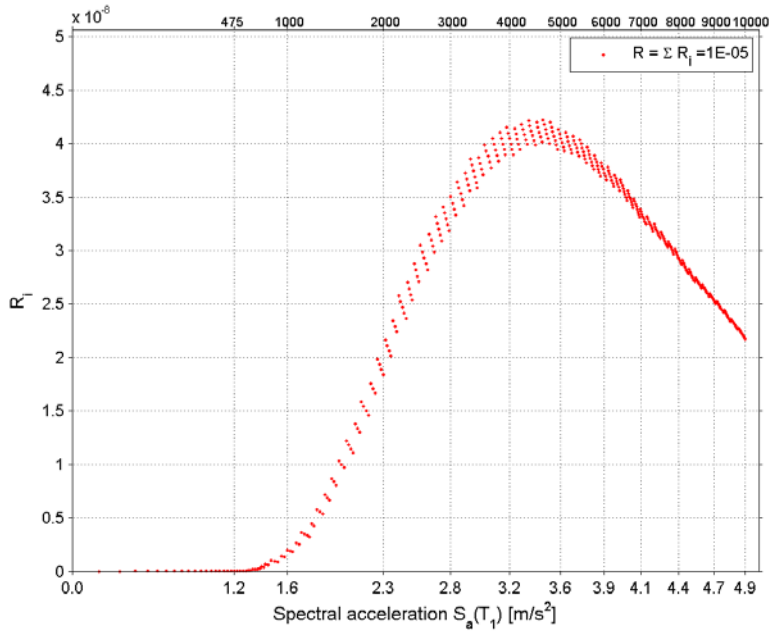

(b)

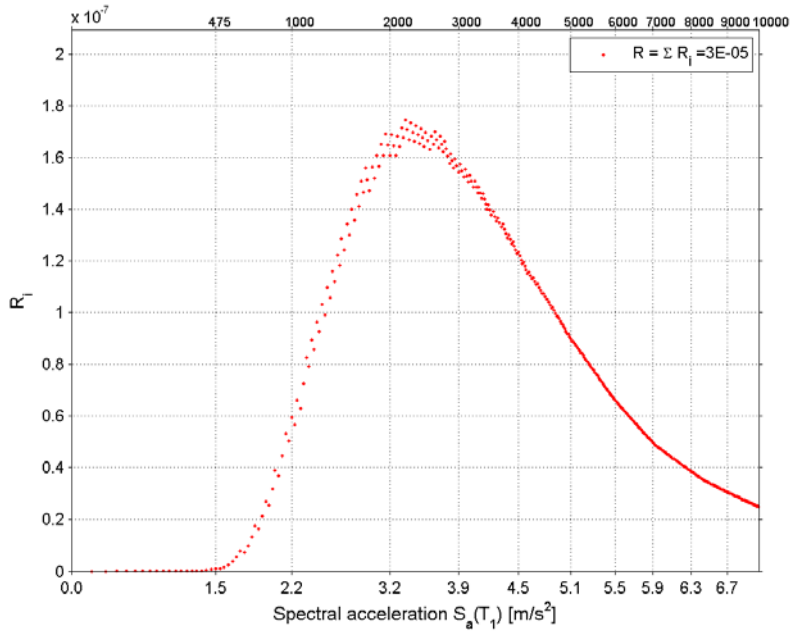

Figure 64: Casualty risk values ($H_{50\%}$-$V_{50\%}$) computed for STD40 ORG in Sion TE (a) considering nonlinear soil response (NL), (b) without considering nonlinear soil response (L)

7.1.7 Comparison EMS / Sa

When the casualty risk based on Sa-values (Table 30) is compared to the casualty risk based on EMS-values (Table 33), it can be stated that some values differ in one order of magnitude, whereas others differ only slightly. Both, the hazard and the vulnerability are responsible for the differences.

The hazard for Sa and EMS values is assessed by the help of different approaches. The Sa-hazard for a specific site is assessed by the help of a model for earthquake sources producing different magnitudes with different recurrence rates and by the help of so-called ground motion prediction equations. The EMS-Intensities are produced by the help of earthquake catalogues which are built up by exploiting the description of historical earthquake events.

For the estimation of the Sa-site-specific hazard a de-amplification has been used for the Sa-hazard, whereas the EMS-Intensities have been considered to represent directly the hazard on the surface (only for the site Sion TE to consider site effects, hazard curves are shifted one intensity degree).

The other important factor is the representation of vulnerability for both models. The Sa-fragility curves are specific for the considered buildings, except the assumption that the curves are modelled by lognormal distribution functions. The curves for the different damage grades may have different distance to each other, they may be differently inclined and they may even coincide. The EMS-based fragility curves all refer to families of fragility curves, which are adopted somehow by the help of modifiers to better correspond to the considered building. Nevertheless, these curves are almost parallel to each other and the distance between these curves is almost constant. In this project it cannot be ruled out, that the choice of the modifiers was influenced by knowledge on the Sa-based fragility curves. In conjunction with the hazard, the EMS-approach leads to probabilities of damage grades which in general differ about one order of magnitude from one damage grade to the other.

Besides, in some cases the choice of modifiers is affected because of the expectations of the engineer. For example in case of benchmark STD40 ORG based only on architectural plans without further investigation the engineer expected to deal with a building with a possible soft story mechanism. However, the computed compliance factor and the comparison of Sa-based with EMS-based risk values show that the selected modifier to consider the vertical irregularity and the soft story mechanism is overestimated.

The observed differences in the results of the casualty risk are not straightforward. On one hand for a given site half of the risk values calculated by the help of the Sa-approach can be lower, whereas the other half can be higher compared to the values calculated by the help of EMS-Intensities. On the other hand for a given building, the risk values for the different sites are partly higher and partly lower. This means that hazard and vulnerability interact with each other in a way that no clear tendency can be identified. A deeper investigation would be necessary to improve the knowledge in this field.

In the EMS-approach only one fragility curve was considered. When the epistemic uncertainty of the hazard is taken into account it can be determined that in the case of the EMS-approach the risk associated to the 10^{th} percentile and the 90^{th} percentile of the hazard differs by two orders of magnitude, which is similar with the Sa-approach.

In case of the property risk, the results based on EMS lie systematically above the values produced by the Sa-approach. This can be traced back to the higher vulnerability of the lower intensities in conjunction with the definition of the intensity hazard compared to the Sa-vulnerability in conjunction with the definition of the Sa-hazard.

The advantage of the Sa-approach is given, when the structure has specific deficiencies which can only be revealed by the help of a finite element analysis. The EMS-approach is very simple to be applied and is not time consuming.

7.2 Compliance factor

The compliance factor is not a deterministic parameter, although in this study it is considered like one. In the opposite, the compliance factor is an uncertain quantity. The uncertainty associated with the compliance factor stems from all the parameters which may be influenced by the engineer during the seismic verification. Therefore the uncertainty is associated with the choice of the verification method, models, stiffness, strength and so on.

7.2.1 Analysis methods

Benchmarks are analysed with force-based and displacement-based methods. In force-based method the seismic forces are distributed according to the moment of inertia of bearing walls. For benchmark YVR14 in an alternative approach, the forces are distributed according to the strength of the bearing walls, too (Table 6). Comparison of compliance factors shows that the classic method of distribution forces according to the moment of inertia is much more conservative than the alternative method with the distribution according to the strength of the bearing walls (with a factor of 2 to 3).

Displacement-based method has been done according to Eurocode 8 approach. For benchmark YVR14 this has been done according to SIA D0237, too (Table 6). Comparison of compliance factors shows that compliance factors according to Eurocode 8 approach are smaller than those according to SIA D0237 approach.

7.2.2 Correlation with vulnerability

For the seismic assessment of structural systems (i.e. the determination of the compliance factor) the computation of the structural period of vibration plays a very important role. To be consistent with the fragility curves developed, the period of vibration is determined based on numerical models. For some benchmarks, however, the period according to the numerical model and the engineering model are very different (see section 3.5).

Besides the before-mentioned variation in the determination of the compliance factor, some contradictory results have been observed associated to benchmarks STD40 ORG and STD40. For both benchmarks the mechanical models indicate a relatively high vulnerability compared with the expected vulnerability based on the computed compliance factors. In case of benchmark STD40 ORG this may be because of following issues:

– The compliance factor is computed for the longitudinal direction. In the numerical model, however, the transverse direction is more critical.
– The first period of vibration of the numerical and engineering models are very different (see chapter 3.5.6).
– For both, the force-based and the displacement-based analyses the height of shear span (h_0) is assumed to be equal to the height of the first floor. For the force-based analysis this assumption seems to be optimistic. As no strong coupling of walls exists (no framing action), the height of the shear span is expected to be 2 to 3 times of the story height. Taking this into account, the compliance factors could be halved.

In case of the benchmark STD40 (retrofitted) the mechanical model indicates a relatively high vulnerability (no influence of the retrofit), whereas the compliance factor is also relatively high (large influence of the retrofit). Note that the retrofitting measure considered for the benchmark STD40, i.e. continuation of concrete and masonry walls in first floor, is a fictive retrofitting measure. Comparing fragility curves of STD40 ORG with STD40, it can be observed that they are more or less the same. Compliance factors computed, however, are in case of STD40 larger. One reason could be that for the benchmark STD40 the mechanical model revealed a structural deficiency and or a new failure mecha-

nism, which has not been discovered by the seismic verification or that the structural deficiency becomes more important for earthquakes with longer return periods.

7.3 Comparison with Pre-standard SIA 2018 risk curve

In Figure 55 to Figure 61 for each of the considered sites the casualty risks for the benchmarks and the compliance factors associated to them are shown together with the pre-standard SIA 2018 curve and the suggestion for the SIA 269/8 curve. The upper diagrams (a) contain the force-based compliance factors, whereas the lower diagrams (b) contain the displacement-based compliance factors.

Generally risk values demonstrated as a function of force-based compliance factors are below the curves given by SIA. Risk values computed for two benchmarks STD40 and STD40 ORG are in some cases larger than those predicted by SIA curves. Some possible reasons are discussed in section 7.2.2.

For risk values demonstrated as a function of the displacement-based compliance factor, however, there are several cases, in which the computed risk value lies above the SIA curves. Generally the compliance factors computed with the displacement-based method are two to three times larger than those computed with force-based method. This is mainly because of the conservatism inherent in the force-based method. In other words, by reaching the nominal failure anticipated with the force-based method, it is believed that in general there are more structural reserves available before the structural system actually fails.

A question arises here, whether it can be accepted, that some of the risk values lie above the SIA curves. To answer this question two aspects should be considered: (a) For the seismic verification of existing buildings the engineers are dealing with a large amount of uncertainty i.e. a large scatter of results. The verification method should be robust enough to cover the existing sources of uncertainty. (b) There are always some outliers and special cases, which cannot be covered with classical methods. If the verification method is calibrated so that such cases could be covered as well as “normal” cases, then the method would be for many other cases too conservative.

SIA risk curves are intended to link “realistically” the compliance factor with the risk value. They were not intended to be too conservative. If so, there would be so many structures that should be reinforced although it is not really necessary. Because of this, one should be aware that there exist situations for which the risk values are larger than those predicted by the curves. It is the task of the engineer to identify and handle such cases based on his/her “engineering judgment” with respect to the vulnerability of a structure and the possible seismic demand.

In this study it is observed that for the site Zurich and in some cases for the site Sion OT the casualty risk values lie far below the SIA curves. For these sites the risk calculation is not exhaustive if only median values are considered. This means, that in these cases earthquakes with return periods larger than 10'000 years should be considered and the respective risks could be up to an order of 10^{-6} (see 7.1.5) higher. For the property loss is the exhaustiveness to a lesser extent relevant, as for the computation of the property loss lower damage grades are dominant. Because of this, the saturation of results occurs sooner than the saturation of the casualty loss in general.

Whereas in the figures only casualty risk calculated by the help of median hazard and median vulnerability are considered, the consideration of uncertainty would lead to higher risk values. Even if uncertainty is taken into account, the force-based compliance factors seem to confirm the SIA curves. For the displacement-based compliance factors the consideration of uncertainty is more critical. A higher safety factor with respect to the Eurocode 8 definitions seems to be justified.

7.4 Loss of Function

The possible loss of function can be a very important issue, when the commensurability of a seismic upgrade has to be assessed. The loss of function has not been considered in the risk assessment framework. Nevertheless, the damage grade related fragility functions can be used to qualify the probability for functional losses, which are directly related to the state of the structure. Which damage grade could have an impact on the function depends on the type of function.

When the loss of function is considered, one has to keep in mind, that it is also related to the behaviour of non-structural elements, installations, machines and the availability of the necessary people. Furthermore the ability to supply a specific function depends on several external factors. Many functions depend on electricity, communication, water and so on.

7.5 Non-structural elements

Non-structural elements have not been particularly considered in this research project. When dealing with non-structural elements one has to distinguish between such elements, which can be expected to fail, because the structure fails and such elements, which can fail independently from the structure because of their individual response to the earthquake which is highly influenced by the dynamic behaviour of the structure (amplification of accelerations, deformations).

With respect to the consequences for the estimation of the casualties it cannot be distinguished whether these losses stem from the failure of the structure or the damage to non-structural elements, which is caused by the behaviour of the structure. In spite of this, one can imagine that non-structural elements like e.g. heavy cladding or non-bearing walls can increase the casualty contribution to the risk. If the failure of such elements is possible for damage grades below damage grade 4, then these kinds of failures can have a considerable impact to casualty risk. Therefore, for structures with high load bearing capacities, but weak non-structural elements, the calculated risk can be underestimated.

With respect to the property risk it cannot either be distinguished, whether these losses stem from the failure of or the damage to non-structural elements. In spite of this, it can be assumed that such damages are covered by the given damage ratios.

8 Conclusions

A computational model for earthquake risk assessment based on Sa-accelerations (mechanical approach) has been developed. Another computational model for earthquake risk assessment has been developed based on EMS-Intensities (empirical approach). Applying these models the risk to people and the risk to property for seven (two of them retrofitted) typical Swiss buildings at 4 different Swiss sites have been calculated. The resulting risk to people was demonstrated on the hazard curve of pre-standard SIA 2018 and of SIA 269/8 as a function of the compliance factor calculated according to force-based method and where compared to compliance factors which have been calculated based on displacement-based methods.

The following conclusions can be drawn from this research project:

– Probabilistic seismic hazard assessment (PSHA) has been done to compute rock hazard curves (SED-rock). To consider local site effects constant amplification factors given for different locations have been used. De-amplification because of nonlinear behaviour of soil has been considered according to ASCE 41-06 approach. Ignoring this factor would result in an overestimation of the seismic risk. It should be noted that consideration of site effects is actually a part of PSHA. The approach applied here does not consider any uncertainty in the calculation of site effects.
– The hazard has been considered up to return periods of 10'000 years. For some of the benchmarks even higher return periods should be taken into consideration, because the risk calculation is not exhaustive otherwise. This is in particular the case for buildings with low vulnerability at sites with low hazard.
– The definition and interpretation of damage grades are an important factor, because the damage grades link the fragility curves to the consequences.
– The computed risks depend very much on the sources and the amount of uncertainty which is taken into account. In this case there is a lack of knowledge with respect to vulnerability. Uncertainty of consequences was not considered at all.
– The results of risk assessment based on the mechanical approach are reasonably comparable with those calculated according to empirical approach.
– Force-based and displacement-based verification methods have been applied in the assessment of the compliance factor. In several cases, the displacement-based compliance factor is about three times higher than the force-based compliance factor. In one case, the displacement-based compliance factor is almost 8 times higher than the force-based compliance factor. In one exceptional case the compliance factor according to displacement-based method is lower than the one according to the force-based method.
– Generally, it is shown, that risk values demonstrated as a function of force-based compliance factors are located below the curves given by SIA. Some exceptions are observed. They are discussed in detail in section 7.2.2.
– For risk values demonstrated as a function of the displacement-based compliance factor, however, there are several cases, in which the computed risk value lies above the SIA curves. Generally the compliance factors computed with the displacement-based method are two to three times larger than those computed with force-based method.
– Moreover, for the results gained with the displacement-based method, the displacement demand associated with the design earthquake (475 years return period) is too small to achieve that a structure could survive earthquakes associated with considerably higher return periods (1’000 or several 1’000 years) with a sufficient reliability. The ability to survive such stronger earthquakes would be necessary to keep the risk even of newly build structures below acceptable thresholds.
– The results of risk assessment with different models and assumptions show a large amount of scatter in risk values. The most important sources for this scatter are uncertainty associated with

the seismic hazard, seismic fragility of the studied benchmarks and consequences of structural failure and/or damage.

– SIA risk curves are intended to link “realistically” the compliance factor with the risk value. They are not intended to be too conservative. Because of this, it should be accepted that there may be some real cases with risk values larger than those predicted by the curves. It is the task of the engineer to identify and handle such cases based on his/her “engineering judgment” with respect to the structural vulnerability and the possible seismic demand.
– The computed property risks which were based on the suggestion for SIA 269/8 seem to be relatively high. On one side this risk is strongly affected by assumptions made in relation between damage grade and mean damage ratio (the ratio of cost of repair to the replacement cost). On the other side there is only some information available for the calibration of such relationships, especially for countries with low to medium risk of seismicity.
– The risk reduction for the two retrofitted buildings was almost negligible and even the compliance factors were only slightly improved.
– It must be taken into account, that only a small number of benchmarks could be investigated. But, these benchmarks were chosen in way, so that they are quite representative for Switzerland.

The following aspect should be investigated in more detail:

– Amplification functions for higher acceleration levels should be established under consideration of the effect of non-linearity.
– The model bias and uncertainty associated to fragility curves should be explored. The validity of the lognormal representation of fragility curves should be examined.
– The uncertainty associated to consequences should be taken into account.
– The uncertainty associated to the computation of the compliance factors should be taken into account.

9 References

[ASCE 41-06, 2007]: Seismic Rehabilitation of Existing Buildings, American Society of Civil Engineers, 2007.

[ATC 13, 1985]: Applied Technology Council, Earthquake Damage Evaluation Data for California, 1985.

[Spence, 2002]: Spence (Ed.), R., So, E., Scawthorn, C., Human Casualties in Earthquakes, Progress in Modelling and Mitigation, Springer, 2011.

[EMS-98]: Grünthal (ed.), G., European Macroseismic Scale, 1998.

[Fäh et al., 2003]: Fäh, D., Giardini, D., Kästli, P., Deichmann, N., Gisler, M., Schwarz-Zanetti, G., Alvarez-Rubio, S., Sellami, S., Edwards, B., Allmann, B., Bethmann, F., Wössner, J., Gassner-Stamm, G., Fritsche, S., Eberhard, D.,, Earthquake Catalogue Of Switzerland (ECOS) and the related Macroseismic database, Eclogae Geol. Helv., 96(2), 219-236, 2003.

[Faenza and Michelini, 2010]: Faenza, L. and Michelini, A., Regression Analysis of MCS Intensity and ground motion spectral accelerations, SA, in Italy, unpublished report, 2010.

[Faenza and Michelini, 2010]: Faenza, L. and Michelini, A., Regression analysis of MCS intensity and ground motion parameters in Italy and its application in ShakeMap, Geophys. J. Int. 180, 1138-1152, 2010.

[Field]: Probabilistic Seismic Hazard Analysis (PSHA), A Primer, http://www.relm.org/tutorial_ materials

[Giardini et al., 2004]: Giardini, D., Wiemer, S., Fäh, D. and Deichmann, N., Seismic hazard assessment of Switzerland, Swiss Seismological Service, ETH Zurich, 2004.

[Hadjian, 2004]: Hadjian, A., Earthquake reliability of structures, 13th World Conference on Earthquake Engineering, Vancouver, B.C., Canada, 2004.

[Hazus-MH, 2003]: Federal Emergency Management Agency (FEMA), Multi-hazard Loss Estimation Methodology Earthquake Model HAZUS-MH MR3, Technical Manual, 2003.

[IMAC, 2014]: Karbassi, A. and Lestuzzi, P., Seismic risk for existing buildings – Development of fragility curves using dynamic analysis – Application for masonry buildings in Switzerland, Swiss Federal Institute of Technology, Lausanne (EPFL) / Applied Computing and Mechanics Laboratory (IMAC), 2014.

[Jaiswal et al., 2011]: Jaiswal, K., Wald, D., Earle, P.S., Porter, K.A., and Hearne M., Earthquake Casualty Models within the USGS Prompt Assessment of Global Earthquakes for Response (PAGER) System, 2011.

[Kölz et al., 2006]: Kölz, E., Vogel, T. and Duvernay, B., risk-based safety evaluation of existing buildings – the concept of the swiss technical note sia 2018, 13th ECEE, Geneva, 2006.

[Kölz and Bürge, 2001]: Kölz, E. and Bürge, M., Priorities in Earthquake Upgrading of Existing Structures, Structural Engineering International, Vol. 11, No 3, 202-206, 2001.

[Kiureghian, 2007]: A. D. Kiureghian and O. Ditlevsen, Aleatory or epistemic? Does it matter? Special Workshop on Risk Acceptance and Risk Communication, Stanford University, March 26-27 2007.

[Lagomarsino and Giovinazzi, 2006]: Lagomarsino, S. and Giovinazzi, S., Macroseimic and mechanical models for the vulnerability and damage assessment of current buildings, Bulletin of earthquake engineering 4:415-443, 2006.

[Risk-UE, 2003]: Milutinovic, Z.V. and Trendafiloski, G.S., RISK-UE: An advanced approach to earthquake risk scenarios with applications to different European towns, WP4 Vulnerability of current buildings, 2003.

[SIA 269/8, 2014]: Existing structures – Earthquakes (in discussion), Swiss Society of Engineers and Architects, 2014.

[Spence et al., 2011]: Spence, R., So, E. and Scawthorn, C., Human casualties in earthquakes: Progress in modeling and mitigation, Springer, 2011.

[Tyagunov, 2004]: Tyagunov, S.; Stempniewski, L.; Grünthal, G.; Wahlström, R.; Zschau, J., Vulnerability and risk assessment for earthquake prone cities, Paper No. 868, 13th World Conference on earthquake engineering, Vancouver, 2004.

[Wiemer et al., 2011]: Wiemer, S., SED hazard input to the BAFU project, May 2011.

[Wiemer et al., 2009]: Wiemer, S., Giardini, D., Fäh, D., Deichmann, N., and Sellami, S., Probabilistic seismic hazard assessment of Switzerland: best estimates and uncertainties, Journal of Seismology 13:449-478, 2009.

A A short report on hazard input

ETH
Eidgenössische Technische Hochschule Zürich
Swiss Federal Institute of Technology Zurich

SED
Schweizerischer Erdbebendienst
Swiss Seismological Service

Schweizerischer Erdbebendienst
Sonneggstr. 5 (NO), H57
CH-8092 Zürich, Schweiz
Prof. Stefan Wiemer

Tel.: + 41 44 633 38 57 / 2179 (Sekr).
Fax: + 41 44 633 10 65
wiemerr@sed.ethz.ch
www.earthquake.ethz.ch

Zürich, Mai 18, 2011

SED hazard Input to the BAFU project *« risque sismique pour les bâtiments existants »*

Dear Blaise, dear Jamali

Along with this letter, I am submitting the hazard input files as required for the project on the seismic risk of existing buildings in Switzerland. Below follows a short description of the format of the data and the assumptions made in the calculations.

1. Location of the calculations

I performed calculations for three sites, Sion, Zurich and Basel. The coordinates of the sites are given below. Note that the rock hazard computed here generally varies only smoothly, so hazard in nearby ('few km') location will be similar.

Sion:	*lat = 46.233*	*lon = 7.360*
Zurich (ETHZ):	*lat = 47.376*	*lon = 8.548*
Basel (Munster)	*lat = 47.554*	*lon = 7.590*

2. Method and results: Spectral hazard

The method applied to compute the rock hazard is the same as described in given in [*Giardini et al.*, 2004; *Wiemer et al.*, 2009]. Calculations are based on a Monte-Carlo approach, using a synthetic earthquake catalog as input. Note that because aleatory uncertainties are represented through randomly drawn distributions, repeated hazard calculations at the same sites can lead to slightly different results, particular for low probabilities. The only change with respect to the 2004 hazard model is the computation of fractiles (also called percentiles) at 10%, 20%, …, 90% probability of exceedance. The 50 percentile is identical to the mean hazard provided in the 2004 hazard model. Spectral values are provided at 0.5, 1, 2, 3, 5, 10 and 12 Hz. An example of the resulting hazard curves for the site Basel is show in Figure 1.

The Swiss Hazard models is based on the ground motion prediction equations (GMPE) by Bay et al., [*Bay et al.*, 2003; *Bay et al.*, 2005], derived largely from short period weak motion data recorded on seismographs of the Swiss network. The site condition for which the GMPE is valid is describes as 'hard rock' (Vs about 1500m/s), however, because no

measurements of shear wave velocities at the sites were available at the time, the reference site condition is somewhat uncertain.

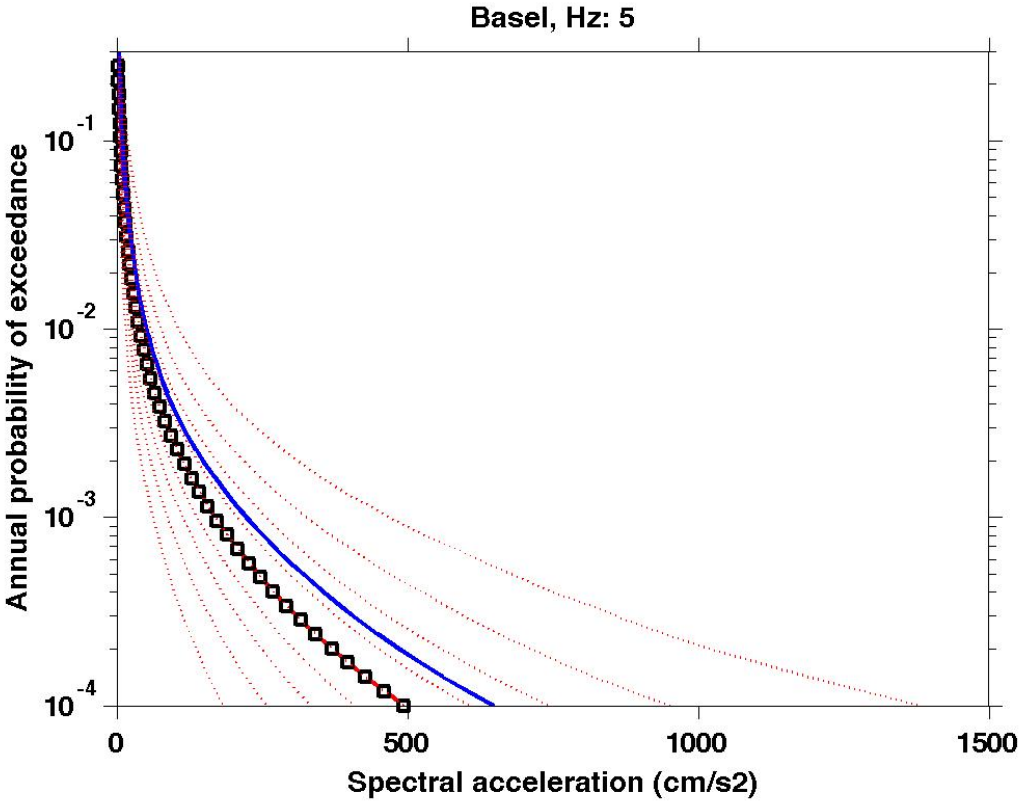

***Figure 1**. Example oft he hazard curves for the site Basel. Shown is the annual probability of exceedance in units of 5% damped acceleration response spectrum at 5 Hz. Black squares: Median. Blue line: Mean. Red dashed line: Fractiles (10%, 20% …, 90%).*

Results are illustrated as plots oft he hazard curves for each site and each frequency. Results are provided in a Matlab .mat file, one file for each hazard curve and frequency. Where the values are stored in the matrix *'Res'*, with the annual exceedance probability in column 1, and then the ground motions at the 10, 20, 30, 40, 50, 60, 70, 80 and 90 percentile in subsequent columns.

3. Method and Results: Intensity

The SED has not computed Intensity based hazard curves as part of the 2004 Swiss hazard. However, macroseismic intensity data continue to play an important role in the seismological, engineering, and loss modelling communities. Indeed, the advent of the ShakeMap system [*Wald et al.*, 1999a] and related systems like the Prompt Assessment of Global Earthquakes for Response [PAGER, *Earle et al.*, 2009; *Wald et al.*, 2008] have increased the visibility of macroseismic intensity not only in these arenas, but also in the view of the public, the media and educational realms, as well as earthquake response and planning communities. Critically, macroseismic observations can provide valuable constraints for reconstructing shaking distributions for historical events; often they are abundant whereas strong-motion recordings are sparse for such events (citation from Cua et al., 2010).

Two approaches to deriving Intensity based ground motion prediction equations are

available: direct intensity prediction (IPEs), and ground motion to intensity conversion equations (GMICEs). *Cua et al.* [2010] provide a comprehensive overview of the state of the art, comparisons between different existing equations, and the need for regional differences. They also evaluate the residual of IPEs and GMICE against a (partially) independent dataset and give recommendations to the GEM1 project for suitable IPE's for global risk calculations.

For this project we attempt to represent the epistemic uncertainty in intensity calculations by implementing three different IPE'S, two direct ones and one GMICE. The choice of these three equations is based largely on a review of *Cua et al.* [2010] and on discussions with G. Cua. To compute the intensity hazard curves, we used the some seismogenic source model used for the Swiss hazard and for this project in the spectral domain, but replaced the GMPE by the respective IPE and its uncertainty. We again compute the fractiles in 10% increments. Results for all three sites are shown in Figure 2.

A) Swiss ECOS IPE

For Switzerland, a dedicated IPE based on intercept intensity was developed as part of the ECOS catalog creation [*Fah et al., 2003*]. The main purpose of this IPE was to determine an Mw magnitude to historical earthquakes; however, the equations given below are well suited as an IPE.

For points in the 0-70 km distance range:

Shallow : *Mm = [Iobs – 0.096 + 0.043 D] / 1.27*
Deep : *Mm = [Iobs + 1.73 + 0.030 D] / 1.44*

For points in the 70-200 km distance range we obtain:

Shallow-Foreland: *Mm = [Iobs + 1.65 + 0.0115 D] / 1.27*
Shallow-Alpine : *Mm = [Iobs + 1.93 + 0.0064 D] / 1.27*
Deep-Foreland : *Mm = [Iobs + 2.76 + 0.0115 D] / 1.44*
Deep-Alpine : *Mm = [Iobs + 3.04 + 0.0064 D] / 1.44*

B) Global active crust IPE by Allen and Wald (2010)

Allen and Wald [2010], derived for Global active crust and valid in the range 4.9 ≤ Mw ≤ 7.9 for distances < 300km, is the most recent IPE. It was developed with arguably a more comprehensive macroseismic intensity dataset of moderate-to-large magnitude earthquake data than any of the regional models available so far. It performs the most consistently across the full magnitude range in the evaluation of *Cua et al.* [2010], which is not a fair comparison since it was developed against the same data set that is was tested against. The functional form is shown below:

$$I = 3.15 + 1.03M - 1.11\ln\sqrt{R_{rup}^2 + \left[1 + 0.72\,\mathrm{e}^{(M-5)}\right]^2}$$
$$\sigma(R_{rup}) = 0.73, \quad \text{for } R_{rup} = 100 \text{ km} \tag{3.14}$$

C) GMICE by Faenza and Michelini

In a recent study, *Faenza and Michelini* [2010a,b] performed an Orthogonal Distance Regression (ODR) on PGA and PGV and Spectral Acceleration with IMCS for Italy. This GMICE is also the one used in the Swiss ShakeMap system. It is valid for 3.0 ≤ M ≤ 6.9 and distances < 200 km. They used the following dataset as input for their regression:

- PGM and intensity data from 66 Italian earthquakes with $3.9 \leq M_w \leq 7.9$, and $2 \leq I_{MCS} \leq 8$
- ITACA strong motion database (http://itaca.mi.ingv.it)
- DBMI intensity database (http://emidius.mi.ingv.it/DMI04/)
- Mercalli-Cancani-Sieberg (MCS) scale with assignments at 0.5 increments
- PGM is defined as the larger of two horizontal components
- Geometric mean and σ of PGM data at each intensity level (at 0.5 intervals)
- 266 intensity-PGM pairs

The following functional form is adopted in *Faenza and Michelini* [2010]:

Iobs=1.01+2.56 log(PSA(0.3s))
Iobs=3.02+2.10 log(PSA(1.0s))
Iobs=4.22+2.05 log(PSA(2.0s))

In a first step, we applied the *Faenza and Michelini* [2010a, b] GMICE conversion on top of the 0.5, 1 and 3 Hz hazard curves; the results of these three frequencies are then averaged.

Generally, we observe in Figure 2 that the intensity hazard curves based on Faenza and Michelini are for return periods of more than 100 year quite similar to *Allen and Wald* [2010], whereas the ones based on *Faeh et al.* [2003] are about half an Intensity unit higher for return periods of 475 years, and not quite one intensity unit higher for return periods of 10'000 years. However, this difference is well within the uncertainty distribution of each hazard curve.

I am providing the intensity-based results in terms of figures and data in the same format described above, separate for each of the three IPE's. In the subsequent risk calculations, it can be informative to compute loss curves based on different IPE's; however, it is also feasible to combine all three IPE's into one 'average' intensity hazard curve. This approach would be equivalent to the three GMPE's used in the spectral domain as an expression of epistemic uncertainty. Note that the applicable site condition for IPEs and GMICE is generally poorly referred, and in the context of this study possibly best referred to as 'average'.

Please let me know if there are remaining question or issues where my input is needed. Looking forward to seeing the results from the loss modeling!

With best wishes

Stefan Wiemer

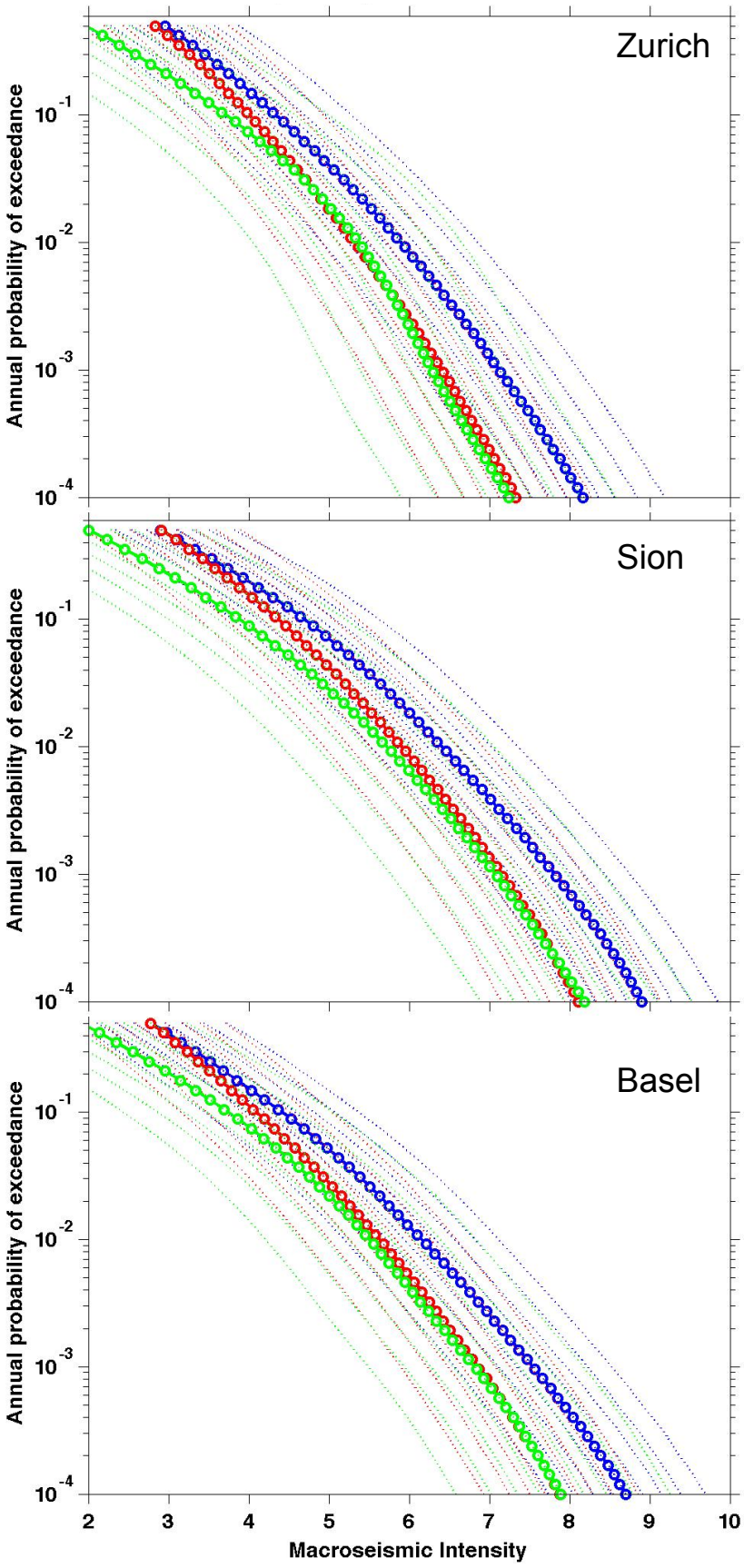

***Figure 2**. Example oft the intensity-based hazard curves for the sites Zurich, Sion and Basel. Shown is the annual probability of exceedance of a given Macroseismic Intensity. Red: Hazard curve based on the IPE by Allen and Wald [2010], Blue: Based on Faeh et al. [2003]. Green: Based in GMICE conversion of Faenza and Michelini [2010].*

References

Allen, T. I., and D. J. Wald (2010). Prediction of macroseismic intensities for global active crustal earthquakes, J. Seismol. in prep.

Bay, F., D. Fah, L. Malagnini, and D. Giardini (2003), Spectral shear-wave ground-motion scaling in Switzerland, *Bull. Seismol. Soc. Am.*, *93*(1), 414-429.

Bay, F., S. Wiemer, D. Fah, and D. Giardini (2005), Predictive ground motion scaling in Switzerland: Best estimates and uncertainties, *J. Seismol.*, *9*(2), 223-240.

Cua, G., Wald, D. J., Allen, T. I, Garcia, D., Worden, C.B., Gerstenberger, M., Lin, K., and Marano, K., Best Practices" for Using Macroseismic Intensity and Ground Motion-Intensity Conversion Equations for Hazard and Loss Models in GEM1. Report available at www.globalquakemodel,org.

Earle, P. S., D. J. Wald, K. S. Jaiswal, T. I. Allen, M. G. Hearne, K. D. Marano, A. J. Hotovec, and J. M. Fee (2009), Prompt Assessment of Global Earthquakes for Response (PAGER): A system for rapidly determining the impact of earthquakes worldwide, *Rep.*, 15 pp, Golden.

Faenza and Michelini, (2010a). Regression Analysis of MCS Intensity and ground motion spectral accelerations, SA, in Italy, unpublished report.

Faenza, L., and A. Michelini (2010). Regression analysis of MCS intensity and ground motion parameters in Italy and its application in ShakeMap, *Geophys. J. Int.* 180, 1138-1152.

Fah, D., et al. (2003), Earthquake Catalogue Of Switzerland (ECOS) and the related macroseismic database, *Eclogae Geol. Helv.*, *96*(2), 219-236.

Giardini, D., S. Wiemer, D. Faeh, and N. Deichmann (2004), Seismic hazard assessment of Switzerland, 2004, *SED internal report*.

Wald, D. J., V. Quitoriano, T. H. Heaton, H. Kanamori, C. W. Scrivner, and B. C. Worden (1999a), TriNet "ShakeMaps": Rapid generation of peak ground-motion and intensity maps for earthquakes in southern California, *Earthq. Spectra*, *15*(3), 537-556.

Wald, D. J., P. S. Earle, T. I. Allen, K. Jaiswal, K. Porter, and M. Hearne (2008), Development of the U.S. Geological Survey's PAGER system (Prompt Assessment of Global Earthquakes for Response), paper presented at 14th World Conf. Earthq. Eng., Beijing, China, October.

Wiemer, S., D. Giardini, D. Fah, N. Deichmann, and S. Sellami (2009), Probabilistic seismic hazard assessment of Switzerland: best estimates and uncertainties, *J. Seismol.*, *13*(4), 449-478.

B Annual probabilities of damage grades

Table 39: Annual probabilities of damage grades P(DG ≥ dg | Sa) calculated with $H_{50\%}$ and $V_{50\%}$

Benchmark	Site	DG1	DG2	DG3	DG4	DG5
CHB30	Basel	2.6E-03	5.3E-04	4.1E-05	1.5E-04	8.2E-08*
	Sion OT	1.1E-03	2.3E-04	1.2E-05	5.0E-05	5.1E-09*
	Sion TE	5.0E-03	7.3E-04	3.8E-05	1.4E-04	1.6E-07*
	Zürich	3.8E-04	4.8E-05	0.0E+0*	2.4E-06*	6.8E-13*
CHB30 ORG	Basel	1.0E-02	1.6E-03	4.7E-04	8.0E-05	6.5E-07*
	Sion OT	4.8E-03	8.7E-04	2.6E-04	4.0E-05	1.9E-07*
	Sion TE	1.7E-02	3.2E-03	6.6E-04	1.1E-04	3.0E-06*
	Zürich	2.2E-03	1.7E-04	2.7E-05	1.9E-07*	9.8E-13*
YVR14	Basel	9.8E-04	2.3E-04	6.5E-06*	8.7E-09*	3.3E-11*
	Sion OT	1.7E-03	5.7E-04	1.1E-04	7.3E-06*	2.2E-06*
	Sion TE	5.5E-03	1.3E-03	3.4E-04	4.3E-05	9.8E-05
	Zürich	1.5E-04	1.3E-05	2.2E-09*	5.5E-15*	7.6E-21*
SECH7	Basel	3.2E-03	1.9E-03	3.0E-04	1.1E-05*	4.2E-06*
	Sion OT	6.6E-04	4.1E-04	3.7E-05	6.4E-10*	5.5E-09*
	Sion TE	4.1E-03	2.9E-03	5.4E-04	6.9E-05	4.2E-05
	Zürich	3.5E-04	1.1E-04	2.5E-06*	4.3E-13*	4.3E-13*
SUVA	Basel	9.5E-03	4.0E-03	3.5E-04	5.7E-05	1.9E-05
	Sion OT	2.1E-03	8.2E-04	4.0E-05	1.9E-06*	1.9E-07*
	Sion TE	9.8E-03	5.0E-03	5.5E-04	1.2E-04	7.2E-05
	Zürich	1.5E-03	2.8E-04	5.1E-07*	4.8E-09*	1.4E-10*
STD40 ORG	Basel	9.4E-03	1.8E-03	2.0E-04	8.7E-05	1.4E-05*
	Sion OT	1.8E-03	4.0E-04	2.3E-05	7.7E-07*	6.8E-09*
	Sion TE	9.6E-03	2.5E-03	3.0E-04	1.7E-04	7.5E-05
	Zürich	1.1E-03	6.6E-05	1.7E-07*	8.0E-12*	3.4E-15*
STD40	Basel	4.2E-03	8.8E-04	3.7E-05	3.8E-05	3.4E-05
	Sion OT	8.6E-04	1.7E-04	2.4E-06*	3.5E-07*	1.2E-06*
	Sion TE	4.9E-03	1.2E-03	5.8E-05	8.6E-05	8.2E-05
	Zürich	2.3E-04	1.2E-05	5.1E-09*	0.0E+00*	7.6E-10*

* Risk estimation is not exhaustive (risk value is underestimated, for more details see 7.1.5)

Table 40: Annual probabilities of damage grades P(DG ≥ dg | EMS-I) calculated with $H_{50\%}$ and $V_{50\%}$

Benchmark	Site	Hazard model	DG1	DG2	DG3	DG4	DG5
CHB30	Basel	SED	1.1E-02	1.7E-03	2.2E-04	2.3E-05	1.5E-06
	Sion OT	SED	1.3E-02	2.3E-03	3.4E-04	4.1E-05	2.8E-06
	Sion TE	SED	2.2E-02	7.6E-03	1.9E-03	3.6E-04	4.2E-05
	Sion TE	Faenza	1.7E-02	4.0E-03	6.3E-04	7.2E-05	4.9E-06
	Zürich	SED	8.8E-03	1.1E-03	9.9E-05	7.1E-06	2.9E-07
	Zürich	Faenza	6.7E-03	5.7E-04	3.3E-05	1.4E-06	3.3E-08
CHB30 ORG	Basel	SED	2.0E-02	5.8E-03	1.3E-03	2.2E-04	2.4E-05
	Sion OT	SED	2.2E-02	7.6E-03	1.9E-03	3.6E-04	4.2E-05
	Sion TE	SED	3.2E-02	1.9E-02	7.4E-03	2.1E-03	3.5E-04
	Sion TE	Faenza	2.8E-02	1.2E-02	3.5E-03	6.7E-04	7.3E-05
	Zürich	SED	1.7E-02	4.1E-03	7.1E-04	9.2E-05	7.0E-06
	Zürich	Faenza	1.4E-02	2.5E-03	3.0E-04	2.5E-05	1.2E-06
YVR14	Basel	SED	9.0E-03	1.2E-03	1.3E-04	1.2E-05	6.6E-07
	Sion OT	SED	1.1E-02	1.7E-03	2.1E-04	2.2E-05	1.3E-06
	Sion TE	SED	2.0E-02	5.8E-03	1.3E-03	2.2E-04	2.3E-05
	Sion TE	Faenza	1.5E-02	2.9E-03	3.9E-04	3.9E-05	2.3E-06
	Zürich	SED	7.3E-03	7.4E-04	5.7E-05	3.5E-06	1.2E-07
	Zürich	Faenza	5.5E-03	3.9E-04	1.9E-05	6.5E-07	1.3E-08
SECH7	Basel	SED	1.4E-02	2.8E-03	4.4E-04	5.8E-05	4.5E-06
	Sion OT	SED	1.6E-02	3.7E-03	6.6E-04	9.7E-05	8.4E-06
	Sion TE	SED	2.6E-02	1.1E-02	3.3E-03	7.2E-04	9.8E-05
	Sion TE	Faenza	2.1E-02	6.3E-03	1.3E-03	1.7E-04	1.4E-05
	Zürich	SED	1.1E-02	1.8E-03	2.1E-04	2.0E-05	1.0E-06
	Zürich	Faenza	8.8E-03	1.0E-03	7.8E-05	4.3E-06	1.3E-07
SUVA	Basel	SED	1.8E-02	4.7E-03	9.4E-04	1.5E-04	1.5E-05
	Sion OT	SED	2.0E-02	6.2E-03	1.4E-03	2.4E-04	2.6E-05
	Sion TE	SED	3.1E-02	1.6E-02	5.9E-03	1.5E-03	2.4E-04
	Sion TE	Faenza	2.6E-02	1.0E-02	2.6E-03	4.5E-04	4.6E-05
	Zürich	SED	1.5E-02	3.3E-03	5.0E-04	5.9E-05	4.0E-06
	Zürich	Faenza	1.2E-02	1.9E-03	2.0E-04	1.5E-05	6.3E-07
STD40 ORG	Basel	SED	2.0E-02	5.8E-03	1.3E-03	2.2E-04	2.4E-05
	Sion OT	SED	2.2E-02	7.6E-03	1.9E-03	3.6E-04	4.2E-05
	Sion TE	SED	3.2E-02	1.9E-02	7.4E-03	2.1E-03	3.5E-04
	Sion TE	Faenza	2.8E-02	1.2E-02	3.5E-03	6.7E-04	7.3E-05
	Zürich	SED	1.7E-02	4.1E-03	7.1E-04	9.2E-05	7.0E-06
	Zürich	Faenza	1.4E-02	2.5E-03	3.0E-04	2.5E-05	1.2E-06
STD40	Basel	SED	1.4E-02	2.8E-03	4.4E-04	5.8E-05	4.5E-06
	Sion OT	SED	1.6E-02	3.7E-03	6.6E-04	9.7E-05	8.4E-06
	Sion TE	SED	2.6E-02	1.1E-02	3.3E-03	7.2E-04	9.8E-05
	Sion TE	Faenza	2.1E-02	6.3E-03	1.3E-03	1.7E-04	1.4E-05
	Zürich	SED	1.1E-02	1.8E-03	2.1E-04	2.0E-05	1.0E-06
	Zürich	Faenza	8.8E-03	1.0E-03	7.8E-05	4.3E-06	1.3E-07